

Generalized Finsler geometry and the anisotropic tearing of skin

J.D. Clayton¹

¹DEVCOM ARL, Aberdeen, MD 21005, USA

Abstract

A continuum mechanical theory with foundations in generalized Finsler geometry describes the complex anisotropic behavior of skin. A fiber bundle approach, encompassing total spaces with assigned linear and nonlinear connections, geometrically characterizes evolving configurations of a deformable body with microstructure. An internal state vector is introduced on each configuration, describing subscale physics. A generalized Finsler metric depends on position and the state vector, where the latter dependence allows for both direction (i.e., as in Finsler geometry) as well as magnitude. Equilibrium equations are derived using a variational method, extending concepts of finite-strain hyperelasticity coupled to phase-field mechanics to generalized Finsler space. For application to skin tearing, state vector components represent microscopic damage processes (e.g., fiber rearrangements and ruptures) in different directions with respect to intrinsic orientations (e.g., parallel or perpendicular to Langer’s lines). Non-linear potentials, motivated from soft-tissue mechanics and phase-field fracture theories, are assigned with orthotropic material symmetry pertinent to properties of skin. Governing equations are derived for one- and two-dimensional base manifolds. Analytical solutions capture experimental force-stretch data, toughness, and observations on evolving microstructure, in a more geometrically and physically descriptive way than prior phenomenological models.

Key Words: anisotropy; biological materials; continuum mechanics; Finsler geometry; nonlinear elasticity; orthotropic symmetry; skin; soft condensed matter

Mathematics Subject Classification (MSC) 2020: 53Z05 (primary), 53B40, 74B20

Contents

1	Introduction	3
1.1	Background	4
1.2	Prior work	5
1.3	Purpose and scope	6
1.3.1	Soft tissue and skin mechanics	6
1.3.2	Overview of the current work	8

2	Generalized Finsler space	8
2.1	Reference configuration	9
2.1.1	Basis vectors and nonlinear connections	9
2.1.2	Length, area, and volume	11
2.1.3	Covariant derivatives	11
2.1.4	A divergence theorem	13
2.1.5	Pseudo-Finsler and Finsler spaces	15
2.2	Spatial configuration	15
2.2.1	Basis vectors and nonlinear connections	16
2.2.2	Length, area, and volume	17
2.2.3	Covariant derivatives	17
2.2.4	A divergence theorem	18
3	Finsler-geometric continuum mechanics	18
3.1	Motion and deformation	18
3.2	Particular assumptions	20
3.2.1	Director fields	20
3.2.2	Connections and metrics	21
3.3	Energy and equilibrium	22
3.3.1	Variational principle	22
3.3.2	General energy density	23
3.3.3	Euler-Lagrange equations	23
3.3.4	Spatial invariance and material symmetry	25
4	One-dimensional base manifold	26
4.1	Geometry and kinematics	26
4.2	Governing equations	27
4.2.1	Energy density	28
4.2.2	Linear momentum	29
4.2.3	Micro-momentum	29
4.3	General solutions	30
4.3.1	Homogeneous fields	30
4.3.2	Stress-free states	30
4.4	Constitutive model	31
4.4.1	Metrics	32
4.4.2	Nonlinear elasticity	32
4.5	Specific solutions	33
4.5.1	Homogeneous fields	33
4.5.2	Stress-free states	34

5	Two-dimensional base manifold	38
5.1	Geometry and kinematics	38
5.2	Governing equations	39
5.2.1	Energy density	39
5.2.2	Linear momentum	40
5.2.3	Micro-momentum	41
5.3	General solutions	41
5.3.1	Homogeneous fields	41
5.3.2	Stress-free states	42
5.4	Constitutive model	42
5.4.1	Metrics	43
5.4.2	Nonlinear elasticity	44
5.5	Specific solutions	46
5.5.1	Uniaxial extension	47
5.5.2	Biaxial extension	48
5.5.3	Stress-free states	50
6	Conclusion	52
7	Appendix A: Variational derivatives	52
A.1	Deformation gradient and director gradient	52
A.2	Volume form	53
8	Appendix B: Toward residual stress and growth	54
B.1	Macroscopic momentum	54
B.2	Micro-momentum and growth	56

1 Introduction

Finsler geometry and its generalizations suggest the possibility of enriched descriptions of numerous phenomena in mathematical physics, albeit at the likely expense of greater complexity of analysis and calculations compared to Riemannian geometry. Fundamentals of Finsler geometry, aptly credited to Finsler [1], are discussed in the classic monograph of Rund and the more recent text of Bao et al. [2, 3]. See also the overview article by Eringen [4]. Extensions to pseudo- and generalized Finsler geometries are described in the monograph of Bejancu [5] and research cited therein [6–8], as well as several more recent works [9, 10].

Generalized Finsler geometry is predominantly used herein, since strict classical Finsler geometry is insufficient to describe all phenomena pertinent to the present class of materials physics. Applications of (generalized) Finsler geometry in the broad physical sciences are vast and diverse; a thorough review is outside the scope of the present article. Available books discuss applications in optics, thermodynamics, and biology [11] and spinor structures and other topics in modern physics

[12]. Finsler geometry and its generalizations have also been used for describing anisotropic space-time, general relativity, quantum fields, gravitation, electromagnetism, and diffusion [13–19]. The current work implements a continuum mechanical theory for the behavior of solid materials.

1.1 Background

Classical continuum mechanics, encompassing nonlinear elasticity and plasticity theories as example constitutive frameworks, is couched in the context of Riemannian-Cartan manifolds [20–22]. Non-vanishing torsion and/or curvature tensors may emerge depending on linear connections introduced to describe various incompatibilities and possible sources of residual stresses including dislocations and disclinations in crystals [21, 23–25], inhomogeneous temperature distributions [26, 27], or biological growth processes [28–30].

In the classical Riemannian context, a continuous material body is viewed as a differentiable manifold \mathcal{M} of dimension n , parameterized by coordinate chart(s) $\{X^A\}$ ($A = 1, \dots, n$). A Riemannian metric is introduced on \mathcal{M} : in components, $G_{AB} = G_{AB}(X)$ populate a symmetric and positive-definite $n \times n$ tensor field, where argument X implies functional dependence on the X^A [22]. A covariant derivative ∇ (i.e., the linear connection on \mathcal{M}) completes the geometric description. The corresponding linear connection coefficients most generally consist of n^3 independent field components $\Gamma_{BC}^A = \Gamma_{BC}^A(X)$. For usual solid bodies, $n = 3$, but other dimensions are permissible. Coordinate descriptions may be framed in terms of holonomic or anholonomic bases, where the latter do not correspond to continuous curves parameterizing the body [31, 32]; anholonomic coordinates emerge for a multiplicative decomposition of the deformation gradient [33, 34].

In Finsler geometry and its generalizations, a base manifold \mathcal{M} , parameterized by one or more charts $\{X^A\}$ ($A = 1, \dots, n$), is again introduced. A fiber bundle $(\mathcal{Z}, \mathcal{M}, \Pi, \mathcal{U})$ of total (generalized Finsler) space \mathcal{Z} of dimension $n+m$ is constructed. The total space in Finsler geometry is typically identified with the slit tangent bundle, i.e., $\mathcal{Z} \rightarrow T\mathcal{M} \setminus 0$ [3] with $m = n$, but this is not essential in more general formulations [5, 9, 10]. Auxiliary coordinates $\{D^K\}$ ($K = 1, \dots, m$) cover each fiber \mathcal{U} , such that \mathcal{Z} is parameterized by $\{X^A, D^K\}$. Particular transformation laws are assigned for changes of coordinates associated with X and D . Nonlinear connection coefficients define non-holonomic bases that transform conventionally on $T\mathcal{M}$ under X -coordinate changes. Furthermore, at least two, and up to four [5, 35], additional fields of connection coefficients are needed to enable horizontal and vertical covariant derivatives with respect to X and D on \mathcal{Z} [2, 5, 10].

The generalized pseudo-Finsler metric tensor is of the form $G_{AB} = G_{AB}(X, D)$, always symmetric. The metric is positive definite for Finsler geometry, but not always so for the pseudo-Finsler case [10]. For strict Finsler geometry (but not necessarily its generalizations [5, 6, 18, 36]), G_{AB} are second derivatives of a (squared) fundamental function $\frac{1}{2}\mathcal{F}^2$ with respect to D^A [2, 3]. In Finsler geometry, \mathcal{F} is positively homogeneous of degree one in D ; the resulting metric is homogeneous of degree zero in D [2, 3] and thus should not depend only on the magnitude of a vector comprised of components $\{D^A\}$. In (generalized) Finsler space, the (X, D) -coordinate dependencies of the metric and various linear and nonlinear connections enter other geometric objects and tensorial operations: torsion and curvature forms, volume and area forms, the divergence theorem [37], etc.

Motivation for Finsler geometry is description of detailed physics via the set of auxiliary coordinates $\{D^A\}$ attached to each position X in real physical space. In solid mechanics, the idea can

be interpreted as an extension of micropolar, micromorphic, or Cosserat-type theory [38–43] from Riemannian (and more often, Euclidean) space to generalized Finsler space. However, in classical micromorphic theories, a Riemannian, rather than Finsler, metric is used, the material domain with microstructure is fully parameterized by the $\{X^A\}$; basis vectors and coordinate transformation laws are those of classical continuum mechanics, as are integral theorems. The director triads of micromorphic theories enter the balance laws and constitutive functions, but they do not affect geometric objects and covariant derivatives in the same way as D of generalized Finsler space.

1.2 Prior work

The first application of Finsler geometry in the context of continuum mechanics of solids appears to be the treatment of ferromagnetic elastic-plastic crystals of Amari [44]. Conservation laws and field theories, with application to ferromagnetics, were further developed by Ikeda [45–48]. Bejancu [5] gives a generalized Finsler treatment of kinematics of deformable bodies. More contemporary theories includes those of Sączuk and Stumpf [49–51], with underpinnings in a monograph [52]. Different physical phenomena (e.g. different physical meanings of $\{D^K\}$ [51]) are encompassed by their models that include kinematics, balance laws, and thermodynamics, but their focus is most often on mechanics of elastic-plastic crystals and dislocations [49, 50, 52]. See also recent theory [53] that applies generalized Finsler geometry to topological defects and the comprehensive review [54] of prior works on generalized Finsler geometry in continuum physics.

A new theory of Finsler-geometric continuum mechanics was developed for nonlinear elastic solids with evolving microstructure, first published in the article [55] with a preliminary version in a technical report [56]. This variational theory was extended to allow for explicit inelastic deformation and applied to study phase transitions and shear localization in crystalline solids [55, 57]. The theory has also been broadened for dynamics and shock waves [58, 59], and most recently has been used to describe ferromagnetic solids [54], enriching the governing equations of Maugin and Eringen [60, 61] with pertinent aspects arising from Finsler geometry [44, 48].

Prior to this theory [54, 55], pragmatic solutions of boundary value problems using continuum mechanical models incorporating generalized Finsler geometry appeared intractable due to complexity of governing equations and unwieldy parameterizations (e.g., uncertain constitutive functions and material constants). Most aforementioned work [5, 44–49, 51, 53] presented purely theoretical constructions without attempt to formulate or solve physical boundary value problems. A material response was calculated by Sączuk and Stumpf [50, 52], but motion and internal state coordinates were prescribed a priori, without apparent solution of governing conservation laws for macroscopic and microscopic momentum and energy. In contrast, the present theory [55, 56] appears to be the first Finsler geometry-based continuum mechanics theory for which analytical and numerical solutions to the governing equations have been found, as evidenced by solutions to numerous problems for (non)linear elastic materials with evolving microstructure (e.g. fractures, twinning, phase transitions, dislocations), as evidenced in those and subsequent works [54–59, 62].

All prior applications considered stiff crystalline solids or generic materials. The current research newly applies the theory to soft biological tissues, specifically the skin. Furthermore, prior applications in fracture and cavitation [54, 55, 59, 62] were limited to either locally isotropic damage or to local material separation on a single cleavage plane. The current treatment advances the

description to anisotropic fractures or ruptures on multiple material surfaces at a single point X . Most cited prior applications invoked only a single non-trivial state vector component in D (an exception being a multi-component D for twinning and fracture [59]) and most often conformal Weyl-type rescaling of G_{AB} with canonically vanishing nonlinear connection (with a few exceptions studied [57, 62]). The current research incorporates an anisotropic generalized Finsler metric for multi-dimensional problems and non-trivial nonlinear connections to show utility by example.

1.3 Purpose and scope

The scope of this paper covers two primary purposes:

- Demonstration of utility of the generalized Finsler geometric theory for describing anisotropic elasticity and anisotropic structural rearrangements in soft biological tissue;
- Consolidation and refinement of the theory for the equilibrium (i.e., quasi-static) case.

The first item furnishes the first known application of Finsler geometry-based continuum theory to analyze finite-strain mechanics of soft biological tissue. Prior work of others [63, 64] used ideas from Finsler geometry to reproduce nonlinear stress-strain to failure responses of biologic solids, but that work used a discrete, rather than continuum, theory with material points represented as vertices linked by bonds; interaction potentials comprised bonding energies within a Hamiltonian. In that approach [65–67], a Finsler metric for bond stretch depends on orientation of local microstructure entities (e.g., molecular chains or collagen fibers) described by the Finsler director vector field D . Instead, the current continuum theory considers, in a novel way, effects of microstructure on anisotropy (elastic and damage-induced) in both a geometric and constitutive sense. The second item includes a renewed examination of Rund’s divergence theorem [37] in the context of an oscillating Riemannian metric. It is shown that certain choices of metric and connection coefficients, with possible addition of a source term to the energy conservation law, can recover governing equations for biologic tissue growth [30] in the quasi-static limit (Appendix B).

1.3.1 Soft tissue and skin mechanics

Most soft tissues have inherent directionality due to their collagen fiber-based and/or aligned cellular microstructures [68, 69], toward which tools of analysis from Finsler geometry might be anticipated to aptly apply. The mechanics of skin deformation [68, 70, 71], degradation [72, 73], and tearing [73, 74] are investigated herein. Like most biological materials, microstructure of skin is complex. The respective middle and outer layers of skin are the dermis and epidermis, with elastin and collagen fibers and cells embedded in a ground matrix. Underlying hypodermis (i.e., adipose) can be labeled an inner layer of the skin. The microstructure dictates nonlinear, anisotropic, viscoelastic, and tearing behaviors [74–76]. Mechanical behavior at small strains is primarily controlled by the elastin and ground substance, whereby the collagen fibers are coiled or slack [75]. Under increasing tensile stretch, the collagen fibers straighten and tighten, supporting most of the load, and compliance decreases. Under more severe stretching, fibers slide, delaminate, and rupture, leading to reduced stiffness, strain softening, and material failure [72–74, 77].

Experiments indicate that skin elasticity has orthotropic symmetry [68, 70, 71, 75]. Orthotropy arises from preferred arrangements of the collagen fibers, leading to greater stiffness along direc-

tions along which more fibers are aligned. In the plane of the dermis, fibers tend to be dispersed about a primary axis along which stiffness is greatest. In vivo, resting skin tension is greatest along this axis, parallel to Langer's lines [75]. In typical uniaxial and biaxial tests [68, 70, 71, 74], extracted skin is unstretched initially, but the greater stiffness along the primary direction persists, with differences in stiffness also emerging between orthogonal in-plane and out-of-plane directions [70, 75]. As might be expected, damage processes are also anisotropic due to fiber degradation that differs with respect to direction of loading relative to the microstructure [73, 74].

Skin, as is most biological tissue, is simultaneously nonlinear elastic, viscoelastic, and poroelastic [68, 76, 78, 79]; pertinence of mechanisms depends on the time scale of loading. The present application considers only monotonic loading at a constant rate (e.g. no cycling or rate fluctuations). Loading rates are assumed much slower or faster than viscous relaxation times. Thus, the pseudo elastic approach is justified to study these experiments [68], whereby hyperelastic models are deemed reasonable [71, 80–83], albeit noting that different elastic constants (e.g., static and dynamic moduli) are needed to fit data at vastly different limiting low and high loading rates [84, 85]. In future applications to problems with time dependence, internal state variables can be extended, leading to kinetic laws with explicit viscous dissipation [78, 86]. The current study is limited to relatively small samples, tested in vitro, under uniaxial or biaxial extension [68, 70, 74, 87]. The material is modeled as unstressed initially and homogeneous with regard to elastic properties. In the future, the current theory can be extended to study residual stress due to growth or heterogeneous material features, as well as heterogeneous elastic properties. Residual stresses can be addressed, in the context of Riemannian manifolds, using a material metric having a non-vanishing Riemann-Christoffel curvature of its Levi-Civita connection [27, 30] or an anholonomic multiplicative term in the deformation gradient [29, 88]. These ideas may be extended to generalized Finsler space (e.g., invoking the current fiber bundle approach) in future.

An early nonlinear elastic model described orthotropic symmetry using a phenomenological pseudo-strain energy potential [89]. Another early model delineated contributions of elastin and collagen fibers [79]. More recently, a class of nonlinear elastic models accounting for anisotropy from fiber arrangements using structure tensors has been successful for representing many soft tissues, including arterial walls [80, 90], myocardium [82, 91], and skin [71]. Polyconvex energy potentials can be incorporated for stability and to facilitate existence of (unique) solutions to nonlinear elastic problems [81, 90]. Fiber dispersion can be incorporated to modulate the degree of anisotropy [71, 92]. To date, most damage models accounting for softening and failure have been phenomenological, whether implemented at the macroscopic scale (either isotropic or along preferred fiber directions) or at the scale of individual fibers and their distributions [73, 77, 90, 93]. These damage models, with a basis in continuum damage mechanics [94], are thermodynamically consistent in the sense that damage is dissipative, but their particular kinetic laws and (often numerous) parameters are calibrated to experimental data without much physical meaning. In contrast, the phase-field approach has been recently implemented for soft-tissue fracture or rupture, incorporating relatively few parameters with physical origin (e.g., surface energy) and regularization facilitating unique solutions to problems involving material softening [95, 96]. The kinetic law or equilibrium equation for damage is derived from fundamental principles [97] and drives material to a local minimum-energy state, in contrast to ad hoc equations simply selected to match data.

1.3.2 Overview of the current work

Implementation of the present generalized Finsler theory consists of four key elements: definition of the internal state D , assignment of the metric tensor, assignment of the linear and nonlinear connections, and prescription of the local free energy potential. For soft tissue mechanics, the state vector represents the fiber rearrangements. Damage anisotropy is monitored via its direction, with different components of D reflecting fiber reorganization and rupture with respect to orientations of microstructure features [73, 74]; the magnitude of each component of D measures local intensity of damage in a given material direction. The metric tensor with components $G_{AB}(X, D)$ depends on position X as well as direction and magnitude of D in generalized Finsler space; novel D -dependence captures rescaling of the material manifold as damage entities open, close, or rearrange in different directions [54, 62]. The preferred linear connection is that of Chern and Rund [3], ensuring compatibility with the divergence theorem used to derive the Euler-Lagrange equations [54, 55]. The generalized Finslerian D -dependence of both the metric and linear connection explicitly affect the governing equations. Roles of nonlinear connections are newly examined; a non-trivial prescription is shown to influence the fracture energy and stress-strain response.

The free energy density consists of nonlinear elastic contribution and an internal structure contribution. The nonlinear elastic potential enriches the orthotropic theory of Holzapfel, Ogden, Gasser, and others [71, 80, 82, 83, 92] with implicit contributions from the generalized Finsler metric as well as anisotropic degradation from D . The structural contribution is motivated from phase-field mechanics [95, 98]. A previous model for arterial dissection [95] accounted for fiber-scale damage anisotropy using a scalar order parameter. The current theory invokes a more physically descriptive, vector-valued order parameter (i.e., normalized D) of generalized Finsler type. With regard to skin experiments, solutions obtained for the current model are shown to admirably match extension and failure data, including stress-strain behavior and fracture toughness [73, 74, 99] with parameters having physical or geometric origins. The general theory is thus potentially more physically realistic, and considered more descriptive from a geometric perspective, than past models based on phenomenological damage mechanics [90, 94, 100, 101].

This paper is organized as follows. Mathematical preliminaries (e.g., notation and definitions for objects in referential and spatial configurations) are provided in §2. The Finsler-geometric theory of continuum mechanics is presented in §3, including kinematics of finite deformation and equilibrium equations derived with a variational approach. The next two sections specialize the theory to model soft tissue, specifically skin. In §4, a one-dimensional (1-D) model for the base manifold \mathcal{M} is formulated. Analytical and semi-numerical solutions are obtained for uniaxial extension and compared to experimental data. In §5, a two-dimensional (2-D) model for \mathcal{M} is formulated, whereby the skin has orthotropic symmetry; solutions are obtained for biaxial extension with anisotropic damage in orthogonal material directions. Conclusions follow in §6.

2 Generalized Finsler space

Content of §2 consolidates a more thorough exposition given in a recent review [54], from which notation is adopted. Other extensive texts include those of Rund, Bejancu, and Bao et al. [2, 3, 5].

A new contribution in the present §2 is interpretation of the divergence theorem [37, 54] using an osculating Riemannian metric, whereby for the further simplifying assumption of vanishing nonlinear connection, a representation akin to that of classical Riemannian geometry is obtained.

2.1 Reference configuration

The very general fiber bundle approach of Bejancu [5] encompasses geometric fundamentals of the theory. The reference configuration is linked to a particular instant in time at which a deformable solid body is undeformed relative to some intrinsic state. A differential manifold \mathcal{M} of dimension n is physically identified with a body embedded in ambient Euclidean space of dimension $N \geq n$.

Remark 2.1.1. Such an embedding only applies to base manifold \mathcal{M} . Neither the total space of the fiber bundle \mathcal{Z} , to be introduced in what follows, nor its specialization to a Finsler space F_n discussed in §2.1.5, can generally be embedded in Euclidean space [2, 102, 103].

Let $X \in \mathcal{M}$ denote a material point or particle, and let $\{X^A\} (A = 1, 2, \dots, n)$ denote a coordinate chart that may partially or completely cover \mathcal{M} . Attached to each material point is a vector \mathbf{D} ; chart(s) of secondary coordinates $\{D^K\} (K = 1, 2, \dots, m)$ are assigned over \mathcal{M} . Fields $\{D^K\}$ are smooth over \mathcal{M} : \mathbf{D} is as many times continuously differentiable with respect to $\{X^A\}$ as needed.

Define $Z = (\mathcal{Z}, \Pi, \mathcal{M}, \mathcal{U})$ as a fiber bundle of total space \mathcal{Z} (dimension $n + m$), where $\Pi: \mathcal{Z} \rightarrow \mathcal{M}$ is the projection and $\mathcal{U} = \mathcal{Z}_X = \Pi^{-1}(X)$ is the fiber at X . A chart over a region of \mathcal{Z} is $\{X^A, D^K\}$. Each fiber is a vector space of dimension m ; $(\mathcal{Z}, \Pi, \mathcal{M})$ constitutes a vector bundle. Let $\mathcal{M}' \subset \mathcal{M}$ be an open neighborhood of any $X \in \mathcal{M}$, Φ an isomorphism of vector spaces, and P_1 a projection operator onto the first factor. Then the following diagram is commutative [5]:

$$\begin{array}{ccc} \Pi^{-1}(\mathcal{M}') & \xrightarrow{\Phi} & \mathcal{M}' \times \mathbb{R}^m \\ \downarrow \Pi & \swarrow P_1 & \\ \mathcal{M}' & & \end{array}$$

2.1.1 Basis vectors and nonlinear connections

Coordinate transformations from $\{X, D\}$ to another chart $\{\tilde{X}, \tilde{D}\}$ on \mathcal{Z} are of the form [5, 10]

$$\tilde{X}^A = \tilde{X}^A(X), \quad \tilde{D}^J(X, D) = Q_K^J(X) D^K, \quad (2.1)$$

where Q_K^J is non-singular and differentiable, with inverse obeying $\tilde{Q}_K^I Q_J^K = \delta_J^I$. As usual, $\delta_J^I = 1 \forall I = J, \delta_J^I = 0 \forall I \neq J$. The holonomic basis for the tangent bundle $T\mathcal{Z}$ is the field of frames $\{\frac{\partial}{\partial X^A}, \frac{\partial}{\partial D^K}\}$. The holonomic basis for the cotangent bundle $T^*\mathcal{Z}$ is $\{dX^A, dD^K\}$. Under a change of coordinates $(X, D) \rightarrow (\tilde{X}, \tilde{D})$ on \mathcal{Z} induced by $X \rightarrow \tilde{X}$ on \mathcal{M} , holonomic basis vectors on $T\mathcal{Z}$ transform from (2.1) as [5, 10]

$$\frac{\partial}{\partial \tilde{X}^A} = \frac{\partial X^B}{\partial \tilde{X}^A} \frac{\partial}{\partial X^B} + \frac{\partial D^K}{\partial \tilde{X}^A} \frac{\partial}{\partial D^K} = \frac{\partial X^B}{\partial \tilde{X}^A} \frac{\partial}{\partial X^B} + \frac{\partial \tilde{Q}_J^K}{\partial \tilde{X}^A} \tilde{D}^J \frac{\partial}{\partial D^K}, \quad (2.2)$$

$$\frac{\partial}{\partial \tilde{D}^J} = \frac{\partial X^B}{\partial \tilde{D}^J} \frac{\partial}{\partial X^B} + \frac{\partial D^K}{\partial \tilde{D}^J} \frac{\partial}{\partial D^K} = \tilde{Q}_J^K \frac{\partial}{\partial D^K}. \quad (2.3)$$

Similarly, for the holonomic basis on $T^*\mathcal{L}$,

$$d\tilde{X}^A = \frac{\partial \tilde{X}^A}{\partial X^B} dX^B + \frac{\partial \tilde{X}^A}{\partial D^K} dD^K = \frac{\partial \tilde{X}^A}{\partial X^B} dX^B, \quad (2.4)$$

$$d\tilde{D}^J = \frac{\partial \tilde{D}^J}{\partial X^B} dX^B + \frac{\partial \tilde{D}^J}{\partial D^K} dD^K = \frac{\partial Q_K^J}{\partial X^B} D^K dX^B + Q_K^J dD^K. \quad (2.5)$$

Given (2.1), $\{\frac{\partial}{\partial \tilde{X}^A}\}$ and $\{dD^K\}$ do not transform as conventional basis vectors on \mathcal{L} . Define [5, 9]

$$\frac{\delta}{\delta \tilde{X}^A} = \frac{\partial}{\partial X^A} - N_A^K \frac{\partial}{\partial D^K}, \quad \delta D^K = dD^K + N_B^K dX^B. \quad (2.6)$$

Non-holonomic basis vectors $\{\frac{\delta}{\delta \tilde{X}^A}\}$ and $\{\delta D^K\}$ obey [10]

$$\frac{\delta}{\delta \tilde{X}^A} = \frac{\partial X^B}{\partial \tilde{X}^A} \frac{\delta}{\delta X^B}, \quad \delta \tilde{D}^J = Q_K^J \delta D^K; \quad \langle \frac{\delta}{\delta \tilde{X}^B}, dX^A \rangle = \delta_B^A, \quad \langle \frac{\partial}{\partial D^K}, \delta D^J \rangle = \delta_K^J. \quad (2.7)$$

The set $\{\frac{\delta}{\delta \tilde{X}^A}, \frac{\partial}{\partial D^K}\}$ are used as a convenient local basis on $T\mathcal{L}$, and the dual set $\{dX^A, \delta D^K\}$ on $T^*\mathcal{L}$ [3, 9]. The $N_B^K(X, D)$ are the nonlinear connection coefficients; N_B^K are presumed differentiable with respect to (X, D) . These do not obey coordinate transformation rules for linear connections nor always correspond to a covariant derivative with the properties of a linear connection. For (2.7) to hold under coordinate transformations $X \rightarrow \tilde{X}$ [3, 5],

$$\tilde{N}_A^J = \left(Q_K^J N_B^K - \frac{\partial Q_K^J}{\partial X^B} D^K \right) \frac{\partial X^B}{\partial \tilde{X}^A}. \quad (2.8)$$

Remark 2.1.2. The geometry of tangent bundle $T\mathcal{L}$ with nonlinear connection admits an orthogonal decomposition $T\mathcal{L} = V\mathcal{L} \oplus H\mathcal{L}$ into a vertical vector bundle $V\mathcal{L}$ with local field of frames $\{\frac{\partial}{\partial D^A}\}$ and a horizontal distribution $H\mathcal{L}$ with local field of frames $\{\frac{\delta}{\delta \tilde{X}^A}\}$ [5].

Fibers of $V\mathcal{L}$ and $H\mathcal{L}$ are of respective dimensions m and n . Henceforth, vertical and horizontal subspaces are of the same dimension: $m = n$. Indices J, K, \dots can thus be replaced with A, B, \dots in the summation convention, which runs from 1 to n . In (2.1), let

$$Q_B^A = \frac{\partial \tilde{D}^A}{\partial D^B} = \frac{\partial \tilde{X}^A}{\partial X^B}. \quad (2.9)$$

A formal way of achieving (2.9) via soldering forms is given by Minguzzi [10]. Coordinate differentiation operations are expressed as follows, with f a differentiable function of arguments (X, D) :

$$\partial_A f(X, D) = \frac{\partial f(X, D)}{\partial X^A}, \quad \bar{\partial}_A f(X, D) = \frac{\partial f(X, D)}{\partial D^A}; \quad \delta_A(\cdot) = \frac{\delta(\cdot)}{\delta X^A} = \partial_A(\cdot) - N_A^B \bar{\partial}_B(\cdot). \quad (2.10)$$

The special cases $f \rightarrow X$ and $f \rightarrow D$ are written [54, 55]

$$\partial_B X^A = \frac{\partial X^A}{\partial X^B} = \delta_B^A, \quad \bar{\partial}_B X^A = 0; \quad \partial_B D^A = \frac{\partial D^A}{\partial X^B}, \quad \bar{\partial}_B D^A = \delta_B^A. \quad (2.11)$$

2.1.2 Length, area, and volume

The Sasaki metric tensor [3, 35, 104] enables a natural inner product of vectors over \mathcal{L} :

$$\mathcal{G}(X, D) = \mathbf{G}(X, D) + \check{\mathbf{G}}(X, D) = G_{AB}(X, D)dX^A \otimes dX^B + \check{G}_{AB}(X, D)\delta D^A \otimes \delta D^B; \quad (2.12)$$

$$\mathcal{G}_{AB} = G_{AB} = \mathbf{G} \left(\frac{\delta}{\delta X^A}, \frac{\delta}{\delta X^B} \right) = \check{\mathbf{G}}_{AB} = \check{\mathbf{G}} \left(\frac{\partial}{\partial D^A}, \frac{\partial}{\partial D^B} \right) = \check{G}_{BA} = G_{BA} = \mathcal{G}_{BA}. \quad (2.13)$$

Components of \mathbf{G} and $\check{\mathbf{G}}$ are equal and simply hereafter referred to as G_{AB} , but their bases span orthogonal subspaces. Components G_{AB} and inverse components G^{AB} lower and raise indices in the usual manner, and G denotes the determinant of the $n \times n$ non-singular matrices of components of \mathbf{G} or $\check{\mathbf{G}}$:

$$G^{AB}G_{BC} = \delta_C^A; \quad G(X, D) = \det[G_{AB}(X, D)] = \det[\check{G}_{AB}(X, D)]. \quad (2.14)$$

Remark 2.1.3. Let $\mathbf{V} = V^A \frac{\delta}{\delta X^A} \in H\mathcal{L}$ be a vector field over \mathcal{L} ; its magnitude at point (X, D) is $|\mathbf{V}| = \langle \mathbf{V}, \mathcal{G}\mathbf{V} \rangle^{1/2} = \langle \mathbf{V}, \mathbf{G}\mathbf{V} \rangle^{1/2} = |\mathbf{V} \cdot \mathbf{V}|^{1/2} = |V^A G_{AB} V^B|^{1/2} = |V^A V_A|^{1/2} \geq 0$, where V^A and G_{AB} are evaluated at (X, D) .

When interpreted as a block diagonal $2n \times 2n$ matrix, the determinant of \mathcal{G} is [49, 50, 52]

$$\mathcal{G}(X, D) = \det[G_{AB}(X, D)] \det[\check{G}_{AB}(X, D)] = |\det[G_{AB}(X, D)]|^2 = |G(X, D)|^2. \quad (2.15)$$

Let $d\mathbf{X}$ denote a differential line element of \mathcal{M} referred to non-holonomic horizontal basis $\{\frac{\delta}{\delta X^A}\}$, and let $d\mathbf{D}$ denote a line element of \mathcal{U} referred to vertical basis $\{\frac{\partial}{\partial D^A}\}$. Squared lengths are

$$|d\mathbf{X}|^2 = \langle d\mathbf{X}, \mathcal{G}d\mathbf{X} \rangle = G_{AB}dX^A dX^B, \quad |d\mathbf{D}|^2 = \langle d\mathbf{D}, \mathcal{G}d\mathbf{D} \rangle = G_{AB}dD^A dD^B. \quad (2.16)$$

The respective volume element dV and volume form $d\Omega$ of the n -dimensional base manifold \mathcal{M} , and the area form Ω for its boundary $\partial\mathcal{M}$, are defined by [37]

$$dV = \sqrt{G}dX^1 dX^2 \dots dX^n, \quad d\Omega = \sqrt{G}dX^1 \wedge dX^2 \wedge \dots \wedge dX^n, \quad (2.17)$$

$$\Omega = \sqrt{B}dU^1 \wedge \dots \wedge dU^{n-1}. \quad (2.18)$$

Local coordinates on the $(n-1)$ -dimensional oriented hypersurface $\partial\mathcal{M}$ are given by parametric equations $X^A = X^A(U^\alpha)$ ($\alpha = 1, \dots, n-1$), $B_\alpha^A = \frac{\partial X^A}{\partial U^\alpha}$, and $B = \det(B_\alpha^A G_{AB} B_\beta^B)$.

2.1.3 Covariant derivatives

Horizontal gradients of basis vectors are determined by generic affine connection coefficients H_{BC}^A and K_{BC}^A , where $\nabla(\cdot)$ is the covariant derivative:

$$\nabla_{\delta/\delta X^B} \frac{\delta}{\delta X^C} = H_{BC}^A \frac{\delta}{\delta X^A}, \quad \nabla_{\delta/\delta X^B} \frac{\partial}{\partial D^C} = K_{BC}^A \frac{\partial}{\partial D^A}. \quad (2.19)$$

Analogously, vertical gradients employ generic connection coefficients V_{BC}^A and Y_{BC}^A :

$$\nabla_{\partial/\partial D^B} \frac{\partial}{\partial D^C} = V_{BC}^A \frac{\partial}{\partial D^A}, \quad \nabla_{\partial/\partial D^B} \frac{\delta}{\delta X^C} = Y_{BC}^A \frac{\delta}{\delta X^A}. \quad (2.20)$$

For example, let $V = V^A \frac{\delta}{\delta X^A} \in H\mathcal{Z}$ be a vector field. Then the (total) covariant derivative of V is

$$\begin{aligned} \nabla V &= \nabla_{\delta/\delta X^B} V \otimes dX^B + \nabla_{\partial/\partial D^B} V \otimes \delta D^B \\ &= (\delta_B V^A + H_{BC}^A V^C) \frac{\delta}{\delta X^A} \otimes dX^B + (\bar{\partial}_B V^A + Y_{BC}^A V^C) \frac{\delta}{\delta X^A} \otimes \delta D^B \\ &= V^A|_B \frac{\delta}{\delta X^A} \otimes dX^B + V^A|_B \frac{\delta}{\delta X^A} \otimes \delta D^B. \end{aligned} \quad (2.21)$$

Denoted by $(\cdot)|_A$ and $(\cdot)|_B$ are horizontal and vertical covariant derivatives with respect to $\{X^A\}$ and $\{D^B\}$.

Remark 2.1.4. The sequence of covariant indices on connections follows some works [4, 22, 31, 98] and is the transpose of others [2, 5, 34]. For symmetric connections, it is inconsequential.

Components of the horizontal covariant derivative of metric tensor $\mathbf{G} = G_{AB} dX^A \otimes dX^B$ (i.e., the horizontal part of \mathcal{G}) are

$$G_{AB|C} = \delta_C G_{AB} - H_{CA}^D G_{DB} - H_{CB}^D G_{AD} = \partial_C G_{AB} - N_C^D \bar{\partial}_D G_{AB} - H_{CA}^D G_{DB} - H_{CB}^D G_{DA}. \quad (2.22)$$

The following identity is also noted for $G = \det(G_{AB})$, a scalar density [37]:

$$(\sqrt{G})|_A = \partial_A(\sqrt{G}) - N_A^B \bar{\partial}_B(\sqrt{G}) - \sqrt{G} H_{AB}^B. \quad (2.23)$$

Christoffel symbols of the second kind for the Levi-Civita connection are γ_{BC}^A , Cartan's tensor is C_{BC}^A , and horizontal coefficients of the Chern-Rund and Cartan connections are Γ_{BC}^A . All are torsion-free (i.e., symmetric):

$$\gamma_{BC}^A = \frac{1}{2} G^{AD} (\partial_C G_{BD} + \partial_B G_{CD} - \partial_D G_{BC}) = G^{AD} \gamma_{BCD}, \quad (2.24)$$

$$C_{BC}^A = \frac{1}{2} G^{AD} (\bar{\partial}_C G_{BD} + \bar{\partial}_B G_{CD} - \bar{\partial}_D G_{BC}) = G^{AD} C_{BCD}, \quad (2.25)$$

$$\Gamma_{BC}^A = \frac{1}{2} G^{AD} (\delta_C G_{BD} + \delta_B G_{CD} - \delta_D G_{BC}) = G^{AD} \Gamma_{BCD}. \quad (2.26)$$

Remark 2.1.5. Chern-Rund-Cartan coefficients are metric-compatible for horizontal covariant differentiation of $\mathbf{G} = G_{AB} dX^A \otimes dX^B$ since $H_{BC}^A = \Gamma_{BC}^A \Rightarrow G_{AB|C} = 0$ in (2.22). Similarly, Cartan's tensor is metric-compatible for vertical covariant differentiation of \mathbf{G} : $Y_{BC}^A = C_{BC}^A \Rightarrow G_{AB|C} = 0$.

From direct calculations with respective (2.24), (2.25), and (2.26), traces of linear connections are related to partial gradients of $G = \det(\mathbf{G})$:

$$\partial_A(\ln \sqrt{G}) = \gamma_{AB}^B, \quad \bar{\partial}_A(\ln \sqrt{G}) = C_{AB}^B, \quad \delta_A(\ln \sqrt{G}) = \frac{1}{2} G^{BC} \delta_A G_{CB} = \Gamma_{AB}^B. \quad (2.27)$$

Remark 2.1.6. $H_{BC}^A = \Gamma_{BC}^A \Rightarrow G|_A = 2G(\ln \sqrt{G})|_A = 0$ and $Y_{BC}^A = C_{BC}^A \Rightarrow G|_A = 2G(\ln \sqrt{G})|_A = 0$.

Nonlinear connection coefficients $N_B^A(X, D)$ admissible under (2.1) and (2.8) can be obtained in several ways. When $T\mathcal{L}$ is restricted to locally flat sections [3, 10], $N_B^A = 0$ in a preferred coordinate chart $\{X, D\}$, but \tilde{N}_B^A in (2.8) do not vanish for heterogeneous transformations under which $\partial_B Q_K^J$ is nonzero. A differentiable real Lagrangian function $L(X, D)$ can be introduced, from which $N_B^A = G_B^A$, where [5]

$$G_B^A = \bar{\partial}_B G^A = \bar{\partial}_B [G^{AE} (D^C \bar{\partial}_E \partial_C L - \partial_E L)]. \quad (2.28)$$

Remark 2.1.7. Let $G_{AB}(X, D)$ be positively homogeneous of degree zero in D . Then G^A below are components of a spray [3, 10], and canonical nonlinear connection coefficients $N_B^A = G_B^A$ that obey (2.8) are

$$G^A = \frac{1}{2} \gamma_{BC}^A D^B D^C, \quad G_B^A = \bar{\partial}_B G^A. \quad (2.29)$$

For classification, let $K_{BC}^A = H_{BC}^A$ and $Y_{BC}^A = V_{BC}^A$. Then a complete generalized Finsler connection is the set $(N_B^A, H_{BC}^A, V_{BC}^A)$. The Chern-Rund connection is $(G_B^A, \Gamma_{BC}^A, 0)$. The Cartan connection is $(G_B^A, \Gamma_{BC}^A, C_{BC}^A)$. The Berwald connection is $(G_B^A, G_{BC}^A, 0)$, where $G_{BC}^A = N_{BC}^A = \bar{\partial}_B N_C^A = \bar{\partial}_B \bar{\partial}_C G^A$.

2.1.4 A divergence theorem

Let \mathcal{M} be a manifold of dimension n having $(n-1)$ -dimensional boundary $\partial\mathcal{M}$ of class C^1 , a positively oriented hypersurface. Stokes' theorem for a C^1 differentiable $(n-1)$ form α on \mathcal{M} is

$$\int_{\mathcal{M}} d\alpha = \int_{\partial\mathcal{M}} \alpha. \quad (2.30)$$

Theorem 2.1.1. *Let \mathcal{M} , $\dim \mathcal{M} = n$, be the base manifold of a generalized Finsler bundle of total space \mathcal{L} with positively oriented boundary $\partial\mathcal{M}$ of class C^1 and $\dim \partial\mathcal{M} = n-1$. Let $\alpha(X, D) = V^A(X, D) N_A(X, D) \Omega(X, D)$ be a differentiable $(n-1)$ -form, and let V^A be contravariant components of vector field $V = V^A \frac{\delta}{\delta X^A} \in H\mathcal{L}$. Denote the field of positive-definite metric tensor components for the horizontal subspace by $G_{AB}(X, D)$ with $G = \det(G_{AB}) > 0$. Assign a symmetric horizontal linear connection $H_{BC}^A = H_{CB}^A$ such that $(\sqrt{G})|_A = 0$, and assume that C^1 functional relations $D = D(X)$ exist for representation of the vertical fiber coordinates at each $X \in \mathcal{M}$. Then in a coordinate chart $\{X^A\}$, (2.30) is explicitly, with volume and area forms given in the second of (2.17) and (2.18),*

$$\int_{\mathcal{M}} [V_{|A}^A + (V^A C_{BC}^C + \bar{\partial}_B V^A) D_{;A}^B] d\Omega = \int_{\partial\mathcal{M}} V^A N_A \Omega, \quad (2.31)$$

where the horizontal covariant derivative is $V_{|A}^A = \delta_A V^A + H_{BA}^B V^A$, the definition $D_{;A}^B = \partial_A D^B + N_A^B$ with $\partial_A D^B = \partial D^B / \partial X^A$, and N_A is the unit outward normal component of $N = N_A dX^A$ to $\partial\mathcal{M}$.

Proof. The proof, not repeated here, is given in the review article [54], implied but not derived explicitly in an earlier work [55]. The proof of (2.31) [54] extends that of Rund [37]—who specified a Finsler space F_n with Cartan connection $(G_B^A, \Gamma_{BC}^A, C_{BC}^A)$ and metric acquired from a Finsler (Lagrangian) function \mathcal{F} (§2.1.5)—to a generalized Finsler space with arbitrary positive-definite metric $G_{AB}(X, D)$ and arbitrary nonlinear connection $N_B^A(X, D)$. \square

Remark 2.1.8. Under the stipulations of Stokes' theorem, (2.31) holds when \mathcal{M} and $\partial\mathcal{M}$ are replaced with any compact region of $\mathcal{M}' \subset \mathcal{M}$ and positively oriented boundary of that region.

Remark 2.1.9. The Chern-Rund-Cartan horizontal connection coefficients, $H_{BC}^A = \Gamma_{BC}^A$, uniquely fulfill symmetry and metric-compatibility requirements.

Remark 2.1.10. A different basis and its dual over \mathcal{M} could be prescribed for \mathbf{V} and \mathbf{N} given certain stipulations [54]. However, geometric interpretation of covariant differentiation on the left side of (2.31) suggests $\{\frac{\delta}{\delta X^A}\}$ should be used for \mathbf{V} , by which dual basis $\{dX^B\}$ should be used for \mathbf{N} to ensure invariance: $\langle \mathbf{V}, \mathbf{N} \rangle \rightarrow V^A N_B \langle \frac{\delta}{\delta X^A}, dX^B \rangle$. If instead \mathbf{V} is referred to the holonomic basis $\{\frac{\partial}{\partial X^A}\}$, then $N_B^A = 0$ should be imposed for invariance with $N_B dX^B$. As noted prior to (2.28), this choice would restrict (2.31) to homogeneous transformations of coordinates $\{X, D\}$.

As assumed in Theorem 2.1.1 [37, 54, 55], C^1 functions $D = D(X)$ must exist over all $X \in \mathcal{M}$. Relations of generalized Finsler geometry [5] still apply, but additional relations emerge naturally when metric G_{AB} is interpreted as an osculating Riemannian metric [2, 44]. Specifically, an alternative representation of (2.31) is newly proven in the following.

Corollary 2.1.1. *Given C^1 functions $D = D(X)$, let $\tilde{G}_{AB}(X) = G_{AB}(X, D(X))$ be components of the osculating Riemannian metric derived from $\mathbf{G} = G_{AB} dX^A \otimes dX^B$. Then (2.31) is equivalent to*

$$\int_{\mathcal{M}} \tilde{V}_{:A}^A d\Omega = \int_{\partial\mathcal{M}} \tilde{V}^A \tilde{N}_A \Omega, \quad (2.32)$$

where the vector $\tilde{V}^A(X) = V^A(X, D(X))$, unit normal $\tilde{N}_A(X) = N_A(X, D(X))$, and covariant derivative $\tilde{V}_{:A}^A = \partial_A \tilde{V}^A + \tilde{\gamma}_{BA}^B \tilde{V}^A$ with connection $\tilde{\gamma}_{BA}^B(X) = \partial_A (\ln \sqrt{\tilde{G}(X)}) = \tilde{\gamma}_{AB}^B(X)$ and $\tilde{G} = \det(\tilde{G}_{AB})$.

Proof. The right of (2.32) is identical to the right of (2.31) given the change of variables. In the left of (2.32), from chain-rule differentiation, vanishing (2.23), and (2.27),

$$\partial_A \tilde{V}^A = \partial_A V^A + \bar{\partial}_B V^A \partial_A D^B, \quad (2.33)$$

$$\begin{aligned} \tilde{V}^A \tilde{\gamma}_{BA}^B &= \tilde{V}^A \partial_A (\ln \sqrt{\tilde{G}}) = V^A [\partial_A (\ln \sqrt{G}) + \bar{\partial}_B (\ln \sqrt{G}) \partial_A D^B] \\ &= V^A [\delta_A (\ln \sqrt{G}) + C_{BC}^C (N_A^B + \partial_A D^B)] = V^A [H_{AB}^B + C_{BC}^C D_{;A}^B] = V^A [H_{BA}^B + C_{BC}^C D_{;A}^B]. \end{aligned} \quad (2.34)$$

Adding (2.33) to (2.34) with canceling $\pm N_A^B \bar{\partial}_B V^A$ terms then produces

$$\begin{aligned} \tilde{V}_{:A}^A &= \{\partial_A V^A + \bar{\partial}_B V^A \partial_A D^B - N_A^B \bar{\partial}_B V^A\} + \{N_A^B \bar{\partial}_B V^A + V^A [H_{BA}^B + C_{BC}^C D_{;A}^B]\} \\ &= \delta_A V^A + V^A H_{BA}^B + \bar{\partial}_B V^A (\partial_A D^B + N_A^B) + V^A C_{BC}^C D_{;A}^B = V_{|A}^A + (\bar{\partial}_B V^A + V^A C_{BC}^C) D_{;A}^B. \end{aligned} \quad (2.35)$$

Integrands on the left sides of (2.31) and (2.32) are thus verified to match, completing the proof. \square

Remark 2.1.11. Coefficients of the Levi-Civita connection of \tilde{G}_{AB} satisfy the symmetry and metric-compatibility requirements used to prove (2.32):

$$\tilde{\gamma}_{BC}^A = \frac{1}{2} \tilde{G}^{AD} (\partial_C \tilde{G}_{BD} + \partial_B \tilde{G}_{CD} - \partial_D \tilde{G}_{BC}) = \tilde{G}^{AD} \tilde{\gamma}_{BCD}. \quad (2.36)$$

Remark 2.1.12. Given (2.36), the form of the divergence theorem in (2.32) appears analogous to that of a Riemannian manifold with boundary. It is not identical, however, since the non-holonomic basis $\{\frac{\delta}{\delta X^A}\}$ is used for \mathbf{V} . As in Remark 2.1.3, the holonomic basis $\{\frac{\partial}{\partial X^A}\}$ could be used in a preferred chart $\{X, D(X)\}$ wherein $N_B^A = 0$; under such special conditions the distinction vanishes.

2.1.5 Pseudo-Finsler and Finsler spaces

Preceding developments hold for generalized Finsler geometry, by which the metric tensor components need not be derived from a Lagrangian [5, 6, 36]. Subclasses of generalized Finsler geometry do require such a Lagrangian function, denoted by \mathcal{L} . Let $\mathcal{Z} = T\mathcal{M} \setminus 0$ (i.e., the tangent bundle of \mathcal{M} excluding zero section $D = 0$). Let $\mathcal{L}(X, D) : \mathcal{Z} \rightarrow \mathbb{R}$ be positive homogeneous of degree two in D , and as many times differentiable as needed with respect to $\{X^A\}$ and $\{D^A\}$ (C^∞ is often assumed [3], but C^5 is usually sufficient [10]). Then $(\mathcal{M}, \mathcal{L})$ is a pseudo-Finsler space when the $n \times n$ matrix of components G_{AB} is both non-singular over \mathcal{Z} and obtained from Lagrangian \mathcal{L} :

$$G_{AB}(X, D) = \bar{\partial}_A \bar{\partial}_B \mathcal{L}(X, D), \quad \mathcal{L} = \frac{1}{2} G_{AB} D^A D^B. \quad (2.37)$$

A Finsler space $(\mathcal{M}, \mathcal{F})$, also denoted by F_n where $n = \dim \mathcal{M}$, is a pseudo-Finsler space for which $G_{AB}(X, D)$ is always positive definite over \mathcal{Z} . For a Finsler space F_n [2, 3], the fundamental scalar Finsler function $\mathcal{F}(X, D)$ is introduced, positive homogeneous of degree one in D :

$$\begin{aligned} \mathcal{F}(X, D) &= \sqrt{2\mathcal{L}(X, D)} = |G_{AB}(X, D) D^A D^B|^{1/2} \\ \leftrightarrow \quad \mathcal{L}(X, D) &= \frac{1}{2} \mathcal{F}^2(X, D); \quad \mathcal{F}(X, D) > 0 \forall D \neq 0. \end{aligned} \quad (2.38)$$

In Finsler geometry [2, 3, 5], it follows that $L = \mathcal{L}$ and $G^A = G^A$ in (2.28) and (2.29), and that

$$G_{AB} = \frac{1}{2} \bar{\partial}_A \bar{\partial}_B (\mathcal{F}^2), \quad G_B^A = \gamma_{BC}^A D^C - C_{BC}^A \gamma_{DE}^C D^D D^E = \Gamma_{BC}^A D^C, \quad C_{ABC} = \frac{1}{4} \bar{\partial}_A \bar{\partial}_B \bar{\partial}_C (\mathcal{F}^2). \quad (2.39)$$

Reductions and embeddings for Finsler spaces are discussed elsewhere [2, 3, 10, 54, 102, 103].

2.2 Spatial configuration

A description on a fiber bundle analogous to that of §2.1 is used for the spatial configuration (i.e., current configuration) of a body. A differential manifold \mathfrak{m} of dimension n represents a (deformed) physical body, with base space embedded in ambient Euclidean space of dimension $N \geq n$.

Remark 2.2.1. Definitions in §2.2 parallel those of §2.1, where lower-case indices and symbols, with the exception of connections, distinguish current-configurational quantities.

Let $x \in \mathfrak{m}$ denote the spatial image of a body particle or point with $\{x^a\} (a = 1, 2, \dots, n)$ being a coordinate chart on \mathfrak{m} . At each spatial point is a vector \mathbf{d} , and chart(s) of secondary coordinates $\{d^k\} (k = 1, 2, \dots, m)$ are assigned over \mathfrak{m} . Define $\mathfrak{z} = (\mathfrak{z}, \pi, \mathfrak{m}, \mathfrak{u})$ as a fiber bundle of total space \mathfrak{z} (dimension $n + m$), where $\pi : \mathfrak{z} \rightarrow \mathfrak{m}$ is the projection and $\mathfrak{u} = \mathfrak{z}_x = \pi^{-1}(x)$ is the fiber at x . A chart covering a region of \mathfrak{z} is $\{x^a, d^k\}$. Each fiber is an m -dimensional vector space, so $(\mathfrak{z}, \pi, \mathfrak{m})$ constitutes a vector bundle.

The global mapping from referential to spatial base manifolds is φ , referred to herein as the motion. The global mapping from referential to current total spaces is the set $\Xi = (\varphi, \theta)$, where in general $\varphi(X, D) : \mathcal{M} \rightarrow \mathfrak{m}$ and $\Xi(X, D) : \mathcal{Z} \rightarrow \mathfrak{z}$. Functional forms of $\varphi(X, D)$ and $\Xi(X, D)$ vary in the literature [54]; details are discussed in §3.1. Mappings and field variables can be made time (t) dependent via introduction of independent parameter t [50, 58, 59]. Explicit time dependence

is excluded from the current theoretical presentation that focuses on equilibrium configurations [55, 62]. The following diagram commutes [5]:

$$\begin{array}{ccc} \mathcal{L} & \xrightarrow{\varepsilon} & \mathfrak{z} \\ \downarrow \Pi & & \downarrow \pi \\ \mathcal{M} & \xrightarrow{\varphi} & \mathfrak{m} \end{array}$$

2.2.1 Basis vectors and nonlinear connections

Coordinate transformations from $\{x, d\}$ to $\{\tilde{x}, \tilde{d}\}$ on \mathfrak{z} are of the general Finsler form

$$\tilde{x}^a = \tilde{x}^a(x), \quad \tilde{d}^j(x, d) = q_k^j(x) d^k, \quad (2.40)$$

where q_k^j is non-singular and differentiable, with inverse obeying $\tilde{q}_k^i q_j^k = \delta_j^i$. The holonomic basis for the tangent bundle $T\mathfrak{z}$ is $\{\frac{\partial}{\partial x^a}, \frac{\partial}{\partial d^k}\}$, and the holonomic basis for the cotangent bundle $T^*\mathfrak{z}$ is $\{dx^a, dd^k\}$. Non-holonomic basis vectors $\{\frac{\delta}{\delta x^a}\}$ and $\{\delta d^k\}$ that transform traditionally under $x \rightarrow \tilde{x}$ are

$$\frac{\delta}{\delta x^a} = \frac{\partial}{\partial x^a} - N_a^k \frac{\partial}{\partial d^k}, \quad \delta d^k = dd^k + N_b^k dx^b. \quad (2.41)$$

The set $\{\frac{\delta}{\delta x^a}, \frac{\partial}{\partial d^k}\}$ is used as a local basis on $T\mathfrak{z}$, and $\{dx^a, \delta d^k\}$ on $T^*\mathfrak{z}$. Tangent bundle $T\mathfrak{z}$ with nonlinear connection admits an orthogonal decomposition into vertical vector bundle and horizontal distribution: $T\mathfrak{z} = V\mathfrak{z} \oplus H\mathfrak{z}$. The transformation law of the spatial nonlinear connection is

$$\tilde{N}_a^j = \left(q_k^j N_b^k - \frac{\partial q_k^j}{\partial x^b} d^k \right) \frac{\partial x^b}{\partial \tilde{x}^a}. \quad (2.42)$$

Subsequently, take $m = n$. Indices $j, k, \dots \rightarrow a, b, \dots$, summation over duplicate indices is from 1 to n , and in (2.40), the d^a transform like components of a contravariant vector field over \mathfrak{m} :

$$q_b^a = \frac{\partial \tilde{d}^a}{\partial d^b} = \frac{\partial \tilde{x}^a}{\partial x^b}. \quad (2.43)$$

Spatial coordinate differentiation is described by the compact notation

$$\partial_a f(x, d) = \frac{\partial f(x, d)}{\partial x^a}, \quad \bar{\partial}_a f(x, d) = \frac{\partial f(x, d)}{\partial d^a}; \quad \delta_a(\cdot) = \frac{\delta(\cdot)}{\delta x^a} = \partial_a(\cdot) - N_a^b \bar{\partial}_b(\cdot); \quad (2.44)$$

$$\partial_b x^a = \frac{\partial x^a}{\partial x^b} = \delta_b^a, \quad \bar{\partial}_b x^a = 0; \quad \partial_b d^a = \frac{\partial d^a}{\partial x^b}, \quad \bar{\partial}_b d^a = \delta_b^a. \quad (2.45)$$

2.2.2 Length, area, and volume

The Sasaki metric tensor that produces an inner product of vectors over \mathfrak{z} is [104]

$$\mathfrak{g}(x, d) = \mathbf{g}(x, d) + \check{\mathbf{g}}(x, d) = g_{ab}(x, d)dx^a \otimes dx^b + \check{g}_{ab}(x, d)\delta d^a \otimes \delta d^b; \quad (2.46)$$

$$\mathfrak{g}_{ab} = g_{ab} = \mathbf{g} \left(\frac{\delta}{\delta x^a}, \frac{\delta}{\delta x^b} \right) = \check{\mathbf{g}}_{ab} = \check{\mathbf{g}} \left(\frac{\partial}{\partial d^a}, \frac{\partial}{\partial d^b} \right) = \check{g}_{ba} = g_{ba} = \mathfrak{g}_{ba}. \quad (2.47)$$

Denote by $d\mathbf{x}$ a differential line element of \mathfrak{m} referred to non-holonomic horizontal basis $\{\frac{\delta}{\delta x^a}\}$ and dd a differentiable line element of \mathfrak{u} referred to vertical basis $\{\frac{\partial}{\partial d^a}\}$. Their squared lengths are

$$|d\mathbf{x}|^2 = \langle d\mathbf{x}, \mathbf{g}d\mathbf{x} \rangle = g_{ab}dx^a dx^b, \quad |dd|^2 = \langle dd, \mathbf{g}dd \rangle = g_{ab}dd^a dd^b. \quad (2.48)$$

The scalar volume element and volume form of \mathfrak{m} , where $\dim \mathfrak{m} = n$, and the area form of $\partial\mathfrak{m}$, the $(n-1)$ -dimensional boundary of a compact region of \mathfrak{m} , are respectively

$$dv = \sqrt{g} dx^1 dx^2 \dots dx^n, \quad d\omega = \sqrt{g} dx^1 \wedge dx^2 \wedge \dots \wedge dx^n, \quad \omega = \sqrt{b} du^1 \wedge \dots \wedge du^{n-1}. \quad (2.49)$$

The surface embedding in \mathfrak{m} is $x^a = x^a(u^\alpha)$ ($\alpha = 1, \dots, n-1$), $b_\alpha^a = \frac{\partial x^a}{\partial u^\alpha}$, and $b = \det(b_\alpha^a g_{ab} b_\beta^b)$.

2.2.3 Covariant derivatives

Denote by ∇ the covariant derivative. Horizontal gradients of basis vectors are determined by coefficients H_{bc}^a and K_{bc}^a , and vertical gradients by V_{bc}^a and Y_{bc}^a :

$$\nabla_{\delta/\delta x^b} \frac{\delta}{\delta x^c} = H_{bc}^a \frac{\delta}{\delta x^a}, \quad \nabla_{\delta/\delta x^b} \frac{\partial}{\partial d^c} = K_{bc}^a \frac{\partial}{\partial d^a}; \quad (2.50)$$

$$\nabla_{\partial/\partial d^b} \frac{\partial}{\partial d^c} = V_{bc}^a \frac{\partial}{\partial d^a}, \quad \nabla_{\partial/\partial d^b} \frac{\delta}{\delta x^c} = Y_{bc}^a \frac{\delta}{\delta x^a}. \quad (2.51)$$

By example, covariant derivative operations over \mathfrak{z} are invoked like (2.21) for $\mathbf{V} = V^a \frac{\delta}{\delta x^a} \in H\mathfrak{z}$:

$$\nabla \mathbf{V} = \nabla_{\delta/\delta x^b} \mathbf{V} \otimes dx^b + \nabla_{\partial/\partial d^b} \mathbf{V} \otimes \delta d^b = V^a|_b \frac{\delta}{\delta x^a} \otimes dx^b + V^a|_b \frac{\delta}{\delta x^a} \otimes \delta d^b. \quad (2.52)$$

Herein $(\cdot)|_a$ and $(\cdot)|_b$ denote horizontal and vertical covariant differentiation with respect to coordinates x^a and d^b . Let γ_{bc}^a be coefficients of the Levi-Civita connection on \mathfrak{z} , C_{bc}^a coefficients of the Cartan tensor on \mathfrak{z} , and Γ_{bc}^a horizontal coefficients of the Chern-Rund and Cartan connections on \mathfrak{z} :

$$\gamma_{bc}^a = \frac{1}{2} g^{ad} (\partial_c g_{bd} + \partial_b g_{cd} - \partial_d g_{bc}) = g^{ad} \gamma_{bcd}, \quad (2.53)$$

$$C_{bc}^a = \frac{1}{2} g^{ad} (\bar{\partial}_c g_{bd} + \bar{\partial}_b g_{cd} - \bar{\partial}_d g_{bc}) = g^{ad} C_{bcd}, \quad (2.54)$$

$$\Gamma_{bc}^a = \frac{1}{2} g^{ad} (\delta_c g_{bd} + \delta_b g_{cd} - \delta_d g_{bc}) = g^{ad} \Gamma_{bcd}. \quad (2.55)$$

2.2.4 A divergence theorem

Let \mathfrak{m} , $\dim \mathfrak{m} = n$, be the base manifold of a generalized Finsler bundle of total space \mathfrak{z} with positively oriented $(n-1)$ -dimensional C^1 boundary $\partial\mathfrak{m}$. Let $\boldsymbol{\alpha}(x, d) = V^a(x, d)n_a(x, d)\boldsymbol{\omega}(x, d)$ be a differentiable $(n-1)$ -form, and let V^a be contravariant components of vector field $\mathbf{V} = V^a \frac{\delta}{\delta x^a} \in H\mathfrak{z}$. Denote the field of components for positive-definite metric tensor on the horizontal subspace by $g_{ab}(x, d)$ with $g = \det(g_{ab}) > 0$. Assign horizontal connection $H_{bc}^a = H_{cb}^a$ such that $(\sqrt{g})_{|a} = 0$ (e.g., $H_{bc}^a = \Gamma_{bc}^a$), and assume that C^1 functional relations $d = d(x)$ exist for representation of the vertical fiber coordinates $\forall x \in \mathfrak{m}$. Then in a chart $\{x^a\}$, with volume and area forms given in (2.49), (2.30) is

$$\int_{\mathfrak{m}} [V_{|a}^a + (V^a C_{bc}^c + \bar{\partial}_b V^a) d_{;a}^b] d\boldsymbol{\omega} = \int_{\partial\mathfrak{m}} V^a n_a \boldsymbol{\omega}, \quad (2.56)$$

with n_a the unit outward normal on $\partial\mathfrak{m}$, $V_{|a}^a = \delta_a V^a + V^a H_{ba}^b$, and $d_{;a}^b = \partial_a d^b + N_a^b$. Proof matches that of Theorem 2.1.1 upon changes of variables; a corollary akin to Corollary 2.1.1 also holds.

3 Finsler-geometric continuum mechanics

The original theory of Finsler-geometric continuum mechanics [55, 56] accounts for finite deformations under conditions of static equilibrium for forces conjugate to material particle motion and state vector evolution. Subtle differences exist among certain assumptions for different instantiations, incrementally revised in successive works. Most differences are explained in a review [54].

3.1 Motion and deformation

Particle motion $\varphi : \mathcal{M} \rightarrow \mathfrak{m}$ and its inverse $\Phi : \mathfrak{m} \rightarrow \mathcal{M}$ are the one-to-one and C^3 -differentiable functions

$$x^a = \varphi^a(X), \quad X^A = \Phi^A(x), \quad (a, A = 1, \dots, n) \quad (3.1)$$

with $(\Phi \circ \varphi)(X) = X$. Total motion is $\Xi : \mathcal{Z} \rightarrow \mathfrak{z}$, where $\Xi = (\varphi, \theta)$. Refer to Fig. 1.

Remark 3.1.1. Vector field \mathbf{D} and its spatial counterpart \mathbf{d} are referred to as internal state vector fields or director vector fields, but neither vector must be of unit length. These are assigned physical interpretations pertinent to the specific class of mechanics problem under consideration [54].

Motions of state vectors are defined as C^3 functions:

$$d^a = \theta^a(X, D), \quad D^A = \Theta^A(x, d), \quad (a, A = 1, \dots, n). \quad (3.2)$$

Remark 3.1.2. Fiber dimensions are $m = \dim \mathcal{U} = \dim \mathfrak{u} = \dim \mathfrak{m} = \dim \mathcal{M} = n$. Extension for $m \neq n$ is conceivable [5, 45]. However, setting $m = n$ enables a more transparent physical interpretation of the vertical vector bundle, and it allows use of (2.9) and (2.43) that simplify notation and calculations. For usual three-dimensional solid bodies, $n = 3$ as implied in parts of prior work [54], but other dimensions are permissible (e.g., two-dimensional membranes ($n = 2$) and one-dimensional rods ($n = 1$)).

From (3.1) and (3.2), transformation formulae for partial differentiation operations between configurations of a differentiable function $h(x, d) : \mathfrak{z} \rightarrow \mathbb{R}$ are

$$\frac{\partial(h \circ \Xi)}{\partial X^A} = \frac{\partial h}{\partial x^a} \frac{\partial \varphi^a}{\partial X^A} + \frac{\partial h}{\partial d^a} \frac{\partial \theta^a}{\partial X^A}, \quad \frac{\partial(h \circ \Xi)}{\partial D^A} = \frac{\partial h}{\partial d^a} \frac{\partial \theta^a}{\partial D^A}. \quad (3.3)$$

Remark 3.1.3. Unlike Chapter 8 of Bejancu [5], basis vectors need not convect from $T\mathcal{Z}$ to $T\mathfrak{z}$ with the motion Ξ . Rather, as in classical continuum field theories of mechanics [20, 105], basis vectors—as well as metric tensors and connection coefficients—can be assigned independently for configuration spaces \mathcal{Z} and \mathfrak{z} . As such, $(\frac{\delta}{\delta x^a}, \frac{\partial}{\partial d^a}, g_{ab}, H_{bc}^a, K_{bc}^a, V_{bc}^a, Y_{bc}^a, N_b^a)$ need not be obtained from $(\frac{\delta}{\delta X^A}, \frac{\partial}{\partial D^A}, G_{AB}, H_{BC}^A, K_{BC}^A, V_{BC}^A, Y_{BC}^A, N_B^A)$ via push-forward operations by Ξ . But choosing N_b^a as the push-forward of N_B^A [5] is beneficial since

$$N_b^a \frac{\partial \varphi^a}{\partial X^A} = N_B^A \frac{\partial \theta^b}{\partial D^B} - \frac{\partial \theta^b}{\partial X^A} \Rightarrow \frac{\delta(h \circ \Xi)}{\delta X^A} = \frac{\delta h}{\delta x^a} \frac{\partial \varphi^a}{\partial X^A} = \frac{\delta h}{\delta x^a} \frac{\delta \varphi^a}{\delta X^A} = \frac{\delta h}{\delta x^a} F_A^a, \quad (3.4)$$

by which $\delta_A(\cdot) = F_A^a \delta_a(\cdot)$ simply relates the delta derivative across configurations.

As implied in (3.4), deformation gradient field $F : H\mathcal{Z} \rightarrow H\mathfrak{z}$ is defined as the two-point tensor field

$$F = \frac{\delta \varphi}{\delta X} = \frac{\delta \varphi^a}{\delta X^A} \frac{\delta}{\delta x^a} \otimes dX^A = \frac{\partial \varphi^a}{\partial X^A} \frac{\delta}{\delta x^a} \otimes dX^A, \quad (3.5)$$

with (3.1) used in the rightmost equality. The inverse deformation gradient $f : H\mathfrak{z} \rightarrow H\mathcal{Z}$ is defined as the following:

$$f = \frac{\delta \Phi}{\delta x} = \frac{\delta \Phi^A}{\delta x^a} \frac{\delta}{\delta X^A} \otimes dx^a = \frac{\partial \Phi^A}{\partial x^a} \frac{\delta}{\delta X^A} \otimes dx^a. \quad (3.6)$$

Remark 3.1.4. Accordingly, $F_A^a(X) f_b^A(x(X)) = \delta_b^a$ and $F_A^a(X) f_a^B(x(X)) = \delta_A^B$. Usual stipulations on regularity [22] of motions (3.1) apply such that $\det(F_A^a) > 0$ and $\det(f_a^A) > 0$.

Transformation equations relating differential line elements of (2.16) and (2.48) follow:

$$dx = dx^a \frac{\delta}{\delta x^a} = F_A^a dX^A \frac{\delta}{\delta x^a} = F dX, \quad dX = dX^A \frac{\delta}{\delta X^A} = f_a^A dx^a \frac{\delta}{\delta X^A} = f dx. \quad (3.7)$$

Advancing (3.7), with definition of the determinant, (2.17), and (2.49), volume elements and forms, respectively, transform between reference and spatial representations on \mathcal{M} and \mathfrak{m} , with $J = \det(F_A^a) \sqrt{g/G} > 0$ and $j = 1/J = J^{-1} > 0$, via (e.g., [22, 98])

$$dv = JdV = [\det(F_A^a) \sqrt{g/G}]dV, \quad dV = jd v = [\det(f_a^A) \sqrt{G/g}]d v, \quad (3.8)$$

$$\varphi^* d\omega = Jd\Omega, \quad \Phi^* d\Omega = j d\omega. \quad (3.9)$$

Strain can be quantified using symmetric Lagrangian deformation tensor $C = C_{AB} dX^A \otimes dX^B$:

$$|dx|^2 = F_A^a g_{ab} F_B^b dX^A dX^B = C_{AB} dX^A dX^B = \langle dX, C dX \rangle, \quad C_{AB} = F_A^a g_{ab} F_B^b = G_{AC} C_B^C = C_{BA}. \quad (3.10)$$

From (3.8), $\det(C_{AB}) = \det(C_A^C G_{CB}) = J^2 G$. Then from the first of (2.50) and (3.4) [56, 62],

$$\nabla_{\delta/\delta X^A} \frac{\delta}{\delta x^c} = \frac{\delta x^a}{\delta X^A} \nabla_{\delta/\delta x^a} \frac{\delta}{\delta x^c} = \delta_A \varphi^a H_{ac}^b \frac{\delta}{\delta x^b} = F_A^a H_{ac}^b \frac{\delta}{\delta x^b}. \quad (3.11)$$

Similarly, the second of (2.50) gives $\nabla_{\delta/\delta X^A} \frac{\partial}{\partial d^c} = F_A^a K_{ac}^b \frac{\partial}{\partial d^b}$, though this is not needed later.

3.2 Particular assumptions

3.2.1 Director fields

The divergence theorem (2.31) is used to derive Euler-Lagrange equations for equilibrium of stress and state vector fields in §3.3.3. Its derivation [37, 54] requires existence of functional relations

$$D^A = D^A(X), \quad d^a = d^a(x), \quad (3.12)$$

where the second of (3.12) is implied by the first under a consistent change of variables per (2.56) and (3.1). Existence of the following functional forms emerges from (3.1), (3.2), and (3.12):

$$d^a = \theta^a(X, D) = \hat{\theta}^a(X, D(X)) = \bar{\theta}^a(X), \quad D^A = \Theta^A(x, d) = \hat{\Theta}^A(x, d(x)) = \bar{\Theta}^A(x). \quad (3.13)$$

Remark 3.2.1. In some prior work [55, 56], alternative representations of particle motions incorporating state vector fields as arguments have been posited. These likely more complex alternatives are admissible but inessential [54]. The current theory, like some others [44, 50, 52], does not always require θ or Θ be specified explicitly, though use of the former is implied later in §5.

The canonical, and pragmatic, choice for $\theta(X, D)$, given field $D^A(X)$, is [62]

$$d = D \circ \Phi \Leftrightarrow d(x) = D(\Phi(x)) \Rightarrow \theta^a(D(X)) = D^A(X) \langle \delta d^a, \frac{\partial}{\partial D^A} \rangle = D^A(X) \delta_A^a, \quad (3.14)$$

where δ_A^a is viewed as a shifter between $V_{\mathfrak{z}}$ and $V_{\mathfrak{Z}}$. Accordingly, $\delta_A^a = 1 \forall a = A$, $\delta_A^a = 0 \forall a \neq A$.

Remark 3.2.2. Invoking (3.14), $\partial_A \theta^a(D(X)) = 0$ by definitions of $\theta^a = \theta^a(D(X))$ and $\partial_A(\cdot) = (\partial(\cdot)/\partial X^A)|_{D=\text{const}}$ in (2.10). Also, $\bar{\partial}_A \theta^a(D(X)) = \delta_A^a$ by (2.11) and (3.14). Then (3.4) reduces to $N_b^a = N_B^A f_b^B \delta_A^a$, and conveniently for the degenerate case: $N_B^A = 0 \Leftrightarrow N_b^a = 0$.

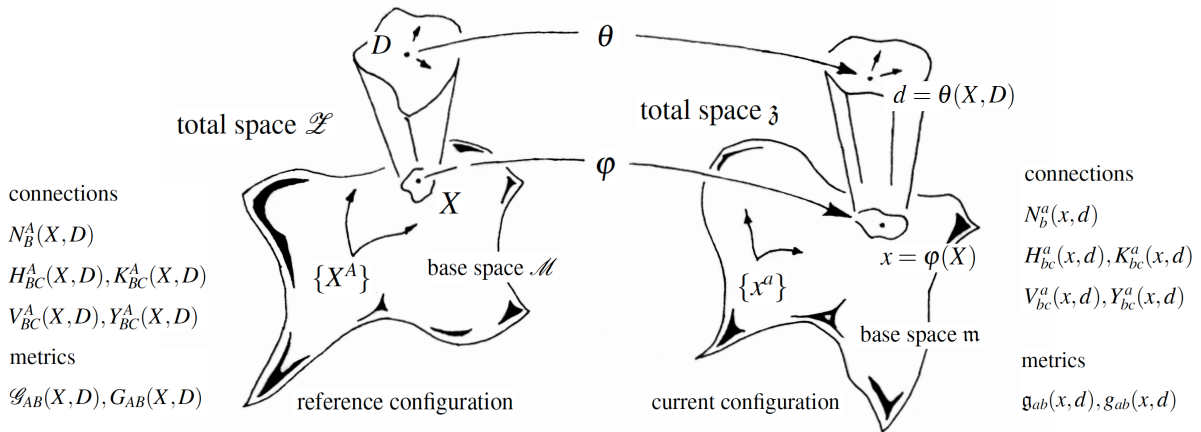


Figure 1 Total deformation $\Xi = (\varphi, \theta) : \mathfrak{Z} \rightarrow \mathfrak{z}$ of material manifold \mathcal{M} ($\dim \mathcal{M} = n = m = 2$) with base-space coordinates $\{X^A\}$ to spatial representation \mathfrak{m} with base-space coordinates $\{x^a\}$. Internal structure fields are (D, d) on total spaces $(\mathfrak{Z}, \mathfrak{z})$; arrows depict local components of state vectors D and d for neighborhoods centered at X and x .

3.2.2 Connections and metrics

Use of (2.31) for any admissible $G_{AB}(X, D)$ necessitates a symmetric linear connection horizontally compatible with G_{AB} , meaning $H_{BC}^A = \Gamma_{BC}^A$, with Γ_{BC}^A Chern-Rund-Cartan coefficients of (2.26). The simplest admissible choice of vertical coefficients is $V_{BC}^A = 0$, corresponding to the Chern-Rund connection [2, 3, 106]. The canonical choice $N_B^A = G_B^A$ of (2.29) also corresponds to the Chern-Rund connection, but it is inessential for generalized Finsler geometry. Choices $K_{BC}^A = H_{BC}^A$ [55, 56] and $Y_{BC}^A = V_{BC}^A$ are logical given (2.9), but these are not mandatory. Setting $K_{BC}^A = 0$, providing compatibility with Cartesian metric δ_{AB} , may also be of utility [54].

Given a Sasaki metric \mathcal{G} of (2.12) with G_{AB} of (2.13), pragmatic connection coefficients over \mathcal{L} are summarized in (3.15); complementary connections over \mathfrak{z} given Sasaki metric \mathfrak{g} with $g_{ab}(x, d)$ of (2.47) follow thereafter:

$$H_{BC}^A = \Gamma_{BC}^A, \quad V_{BC}^A = Y_{BC}^A = 0; \quad H_{bc}^a = \Gamma_{bc}^a, \quad V_{bc}^a = Y_{bc}^a = 0; \quad N_b^a = N_B^A f_b^B \delta_A^a. \quad (3.15)$$

Remark 3.2.3. Note K_{BC}^A and K_{bc}^a are left arbitrary to admit mathematical descriptions of different physics, in contrast to Y_{BC}^A and Y_{bc}^a set equal to their purely vertical counterparts for simplicity. Since nonlinear connection N_B^A is also not explicitly chosen in (3.15) but is left general to admit more physics than considered previously [54], (2.8) is not necessarily ensured for arbitrary changes of coordinates, so transformation properties of N_B^A should be verified. Once the former N_B^A is chosen, N_b^a in (3.15) presumes (3.14) is invoked with (3.4).

Remark 3.2.4. If the fields $G_{AB}(X, D)$ and $g_{ab}(x, d)$ are known, linear connection coefficients in (3.15) can be calculated from definitions in §2.1 and §2.2. Metric G_{AB} need not be homogeneous of degree zero with respect to D , but it can be. Components G_{AB} need not be derived, as in §2.1.5, from a Lagrangian \mathcal{L} or more specifically a fundamental Finsler function \mathcal{F} , but they can be. Dependence of \mathcal{G} on X and D is based on symmetry and physics pertinent to the particular problem of study. Similar statements describe the spatial metric \mathfrak{g} and components g_{ab} .

A decomposition of G_{AB} into a Riemannian part \bar{G}_{AC} and a director-dependent part \hat{G}_B^C is useful for describing fundamental physics and for solving boundary value problems [55–57, 62]:

$$\begin{aligned} \mathbf{G} &= \bar{\mathbf{G}}\hat{\mathbf{G}}; & G_{AB}(X, D) &= \bar{G}_{AC}(X)\hat{G}_B^C(X, D); \\ \bar{\mathbf{G}} &= \bar{G}_{AB}dX^A \otimes dX^B; & \hat{\mathbf{G}} &= \hat{G}_B^A \frac{\delta}{\delta X^A} \otimes dX^B. \end{aligned} \quad (3.16)$$

More specific functional forms in (3.16) are advocated herein, as implied by past applications [54]:

$$\begin{aligned} G_{AB}(X, D) &= \bar{G}_{AC}(X)\hat{G}_B^C(D(X)) = \hat{G}_A^C(D(X))\bar{G}_{CB}(X); \\ \bar{G}_{AB} &= \bar{G}_{BA}, & \hat{G}_A^C G_{BC} &= \hat{G}_B^C G_{CA}. \end{aligned} \quad (3.17)$$

Remark 3.2.5. Components of \bar{G}_{AB} are chosen to best represent symmetry of the physical body; in elasticity, often a Riemannian metric for rectilinear, cylindrical, or spherical coordinates on \mathcal{M} . Components of \hat{G}_B^C are assigned based on how microstructure D affects measured lengths of material elements with respect to an observer in total generalized Finsler space \mathcal{L} (i.e., the space of the physical body enriched with microstructure geometry) [54, 55, 62].

Ideas apply analogously to spatial metric $g_{ab}(x, d)$ with X replaced by x , and with D replaced by d . For example, the spatial analog of (3.17) is

$$g_{ab}(x, d) = \bar{g}_{ac}(x) \hat{g}_b^c(d(x)) = \hat{g}_a^c(d(x)) \bar{g}_{cb}(x); \quad \bar{g}_{ab} = \bar{g}_{ba}, \quad \hat{g}_a^c g_{bc} = \hat{g}_b^c g_{ca}. \quad (3.18)$$

All metrics in (3.17) and (3.18) are assumed invertible with positive determinants. A symmetric tensor \bar{C} [62] and volume ratio $\bar{J} > 0$ are defined to exclude internal state-dependence of strain:

$$\bar{C}(X) = \bar{C}_{AB}(X) dX^A \otimes dX^B, \quad \bar{C}_{AB} = F_A^a \bar{g}_{ab} F_B^b, \quad \bar{C}_B^A = \bar{G}^{AC} \bar{C}_{CB}; \quad (3.19)$$

$$\bar{J}(X) = \sqrt{\det(\bar{C}_B^A(X))}; \quad \bar{J} = J \sqrt{\hat{G}/\hat{g}}, \quad \hat{G} = \det(\hat{G}_B^A), \quad \hat{g} = \det(\hat{g}_b^a). \quad (3.20)$$

3.3 Energy and equilibrium

3.3.1 Variational principle

A variational principle [54–56] is implemented. Let Ψ denote the total energy functional for a compact domain $\mathcal{M}' \subset \mathcal{M}$ with positively oriented boundary $\partial\mathcal{M}'$, and let ψ be the local free energy density per unit reference volume of material:

$$\Psi[\boldsymbol{\varphi}, \mathbf{D}] = \int_{\mathcal{M}'} \psi(F_A^a, D^A, D_{|B}^A, X^A) d\Omega. \quad (3.21)$$

Denote surface forces as $\mathbf{p} = p_a dx^a$, a mechanical load vector (force per unit reference area), and $\mathbf{z} = z_A \delta D^A$, a thermodynamic force conjugate to the internal state vector. Denote a generic local, vector-valued volumetric source term conjugate to structure variations by $\mathbf{R} = R_A \delta D^A$, extending prior theory [54–56] to accommodate more possible physics [30, 107] (Appendix B). A variational principle for Finsler-geometric continuum mechanics, holding X fixed but with $x = \varphi(X)$ and D variable, is

$$\delta\Psi[\boldsymbol{\varphi}, \mathbf{D}] = \oint_{\partial\mathcal{M}'} (\langle \mathbf{p}, \delta\boldsymbol{\varphi} \rangle + \langle \mathbf{z}, \delta\mathbf{D} \rangle) \Omega + \int_{\mathcal{M}'} \langle \mathbf{R}, \delta\mathbf{D} \rangle d\Omega. \quad (3.22)$$

In coordinates, with variation of \mathbf{D} in parentheses to distinguish from non-holonomic basis $\{\delta D^A\}$,

$$\delta \int_{\mathcal{M}'} \psi d\Omega = \oint_{\partial\mathcal{M}'} \{p_a \delta\varphi^a\} \Omega + \oint_{\partial\mathcal{M}'} \{z_C \delta(D^C)\} \Omega + \int_{\mathcal{M}'} \{R_C \delta(D^C)\} d\Omega. \quad (3.23)$$

Results used in §3.3.3 are now noted, with $\alpha = 1$ or $\alpha = 2$ (derived in Appendix A using (3.15)):

$$\delta F_A^a = \delta_A(\delta\varphi^a), \quad \delta D_{|B}^A = [\delta(D^A)]_{|B} - (\bar{\partial}_C N_B^A - \bar{\partial}_C K_{BD}^A D^D) \delta(D^C), \quad (3.24)$$

$$\delta(d\Omega) = \frac{1}{2} \alpha G^{AB} \bar{\partial}_C G_{AB} \delta(D^C) d\Omega = \alpha \bar{\partial}_C (\ln \sqrt{G}) \delta(D^C) d\Omega = \alpha C_{CA}^A \delta(D^C) d\Omega. \quad (3.25)$$

3.3.2 General energy density

As evident in (3.22), independent variables entering total free energy density, per unit reference volume, function ψ are the deformation gradient, the internal state vector, the horizontal gradient of the internal state vector, and the reference position of the material particle:

$$\psi = \psi(\mathbf{F}, \mathbf{D}, \nabla \mathbf{D}, \mathbf{X}) = \psi(F_A^a, D^A, D_{|B}^A, X^A). \quad (3.26)$$

Dependence on \mathbf{F} accounts for bulk elastic strain energy. Dependence on \mathbf{D} generally accounts for effects of microstructure on stored energy. Energy from heterogeneity of microstructure (e.g., internal material surfaces) is captured by dependence on the internal state gradient:

$$\nabla \mathbf{D} = D_{|B}^A \frac{\partial}{\partial D^A} \otimes dX^B + D^A|_B \frac{\partial}{\partial D^A} \otimes \delta D^B; \quad (3.27)$$

$$D_{|B}^A = \delta_B D^A + K_{BC}^A D^C = \partial_B D^A - N_B^A + K_{BC}^A D^C, \quad D^A|_B = \bar{\partial}_B D^A + V_{BC}^A D^C = \delta_B^A. \quad (3.28)$$

Dependence on \mathbf{X} permits heterogeneous properties. Prior work [54, 55] adds motivation for (3.26).

Remark 3.3.1. Vertical gradient $D^A|_B = \delta_B^A$, calculated from $V_{BC}^A = 0$ by (3.15), provides no information, so it is excluded from the arguments of energy density in (3.26).

Expansion of the integrand on the left in (3.23), with $\delta X^A = 0$ by definition, is

$$\begin{aligned} \delta \psi &= \frac{\partial \psi}{\partial F_A^a} \delta F_A^a + \frac{\partial \psi}{\partial D^A} \delta(D^A) + \frac{\partial \psi}{\partial D_{|B}^A} \delta D_{|B}^A = P_a^A \delta F_A^a + Q_A \delta(D^A) + Z_B^A \delta D_{|B}^A; \\ P_a^A &= \frac{\partial \psi}{\partial F_A^a}, \quad Q_A = \frac{\partial \psi}{\partial D^A}, \quad Z_B^A = \frac{\partial \psi}{\partial D_{|B}^A}. \end{aligned} \quad (3.29)$$

Denoted by \mathbf{P} is the mechanical stress tensor (i.e., the first Piola-Kirchhoff stress, a two-point tensor, generally non-symmetric), \mathbf{Q} an internal force vector conjugate to \mathbf{D} , and \mathbf{Z} a micro-stress tensor conjugate to the horizontal gradient of \mathbf{D} .

3.3.3 Euler-Lagrange equations

Connection coefficients in (3.15) are employed along with (3.1), (3.11), (3.12), (3.24), and (3.25). Insertion of (3.29) into the left side of (3.23), followed by integration by parts and use of (2.31) of Theorem 2.1.1, produces

$$\begin{aligned} \delta \int_{\mathcal{M}'} \psi d\Omega &= \int_{\mathcal{M}'} \{P_a^A \delta F_A^a + Q_A \delta(D^A) + Z_B^A \delta D_{|B}^A\} d\Omega + \int_{\mathcal{M}'} \psi \delta(d\Omega) \\ &= - \int_{\mathcal{M}'} \{ \partial_A P_a^A + \bar{\partial}_B P_a^A \partial_A D^B + P_a^B \Gamma_{AB}^A - P_c^A \Gamma_{ba}^c F_A^b + P_a^A C_{BC}^C (\partial_A D^B + N_A^B) \} \delta \varphi^a d\Omega \\ &\quad - \int_{\mathcal{M}'} \{ \partial_A Z_C^A + \bar{\partial}_B Z_C^A \partial_A D^B + Z_C^B \Gamma_{AB}^A - Z_B^A K_{AC}^B - Q_C \\ &\quad \quad + Z_A^B [\bar{\partial}_C N_B^A - \bar{\partial}_C K_{BD}^A D^D + \delta_C^A C_{ED}^D (\partial_B D^E + N_B^E)] - \alpha \psi C_{CA}^A \} \delta(D^C) d\Omega \\ &\quad + \oint_{\partial \mathcal{M}'} \{ P_a^A \delta \varphi^a \} N_A \Omega + \oint_{\partial \mathcal{M}'} \{ Z_C^A \delta(D^C) \} N_A \Omega. \end{aligned} \quad (3.30)$$

Euler-Lagrange equations consistent with any admissible variations $\delta\boldsymbol{\varphi}$ and $\delta\mathbf{D}$ locally at each $X \in \mathcal{M}'$, as well as natural boundary conditions on $\partial\mathcal{M}'$ are obtained as follows. Steps follow those outlined in the original works [55, 56] with minor departures [54].

The first of these culminating Euler-Lagrange equations is the macroscopic balance of linear momentum, derived by setting the first integral on the right-hand side of (3.30) equal to zero, consistent with the right side of (3.23). Localizing the outcome and presuming the result must hold for any admissible variation $\delta\varphi^a$,

$$\partial_A P_a^A + \bar{\partial}_B P_a^A \partial_A D^B + P_a^B \Gamma_{AB}^A - P_c^A \Gamma_{ba}^c F_A^b = -P_a^A C_{BC}^C (\partial_A D^B + N_A^B). \quad (3.31)$$

The second Euler-Lagrange equation is the balance of micro-momentum (i.e., director momentum or internal state equilibrium). It is derived by setting the second integral on the right side of (3.30) equal to the rightmost term in (3.23) and then localizing, giving for any admissible variation $\delta(D^C)$,

$$\begin{aligned} \partial_A Z_C^A + \bar{\partial}_B Z_C^A \partial_A D^B + Z_C^B \Gamma_{AB}^A - Z_B^A K_{AC}^B - (Q_C - R_C) \\ = \alpha \psi C_{CA}^A - Z_A^B [\bar{\partial}_C N_B^A - \bar{\partial}_C K_{BD}^A D^D + \delta_C^A C_{ED}^D (\partial_B D^E + N_B^E)]. \end{aligned} \quad (3.32)$$

Natural boundary conditions on $\partial\mathcal{M}'$ are derived by setting the second-to-last and last boundary integrals in (3.30) equal to the remaining, respective first and second boundary integrals on the right side of (3.23) and localizing the results, yielding for any admissible variations $\delta\varphi^a$ and $\delta(D^C)$,

$$p_a = P_a^A N_A, \quad z_A = Z_A^B N_B. \quad (3.33)$$

Remark 3.3.2. With natural boundary conditions (3.33) or essential boundary conditions (i.e., prescribed $\boldsymbol{\varphi}(X)$ and $\mathbf{D}(X)$ for $X \in \partial\mathcal{M}'$) and local force density vector $\mathbf{R}(X)$ for each $X \in \mathcal{M}'$, (3.31) and (3.32) comprise $2n$ coupled PDEs in $2n$ degrees-of-freedom $x^a = \varphi^a(X)$ and $D^A(X)$ at any $X \in \mathcal{M}'$, and by extension, any $X \in \mathcal{M}$.

Remark 3.3.3. Consider the simplified case when Riemannian metrics are used: no D -dependence of \mathbf{G} and no d -dependence of \mathbf{g} . Then $\Gamma_{BC}^A = \gamma_{BC}^A$, $\Gamma_{bc}^a = \gamma_{bc}^a$, and $C_{BC}^A = 0$. The right side of (3.31) vanishes, and (3.31) is of the form of the static momentum balance of classical continuum mechanics with null body force [22, 23, 33]. Further taking N_B^A and K_{BC}^A independent of D , (3.32) is similar to equilibrium equations for gradient materials [108] as in phase-field mechanics [97, 109].

Remark 3.3.4. In some prior work [55], $G_{AB}(X, D)$ was an argument of ψ , extending (3.26), and D -dependence of the metric manifested in a distinct thermodynamic force, rather than entering implicitly in Q_A . The present approach is favored for brevity [54], but the former is admissible.

Proposition 3.3.1. *Euler-Lagrange equations can be expressed in the following alternative way:*

$$\partial_A P_a^A + \bar{\partial}_B P_a^A \partial_A D^B + P_a^B \gamma_{AB}^A - P_c^A \Gamma_{ba}^c F_A^b = -P_a^A C_{BC}^C \partial_A D^B, \quad (3.34)$$

$$\begin{aligned} \partial_A Z_C^A + \bar{\partial}_B Z_C^A \partial_A D^B + Z_C^B \gamma_{AB}^A - Z_B^A K_{AC}^B - (Q_C - R_C) \\ = \alpha \psi C_{CA}^A - Z_A^B (\bar{\partial}_C N_B^A - \bar{\partial}_C K_{BD}^A D^D + \delta_C^A C_{ED}^D \partial_B D^E). \end{aligned} \quad (3.35)$$

Proof. From (2.10) and (2.27),

$$\Gamma_{AB}^A = \Gamma_{BA}^A = \partial_B(\ln \sqrt{G}) - N_B^A \bar{\partial}_A(\ln \sqrt{G}) = \gamma_{BA}^A - N_B^A C_{AC}^C. \quad (3.36)$$

Substitution of (3.36) with symmetry $\gamma_{BC}^A = \gamma_{CB}^A$ into (3.31) and (3.32) yields (3.34) and (3.35). \square

Remark 3.3.5. Notably, (3.34) and (3.35) show how the nonlinear connection terms N_B^A cancel, simplifying calculations. Nonlinear connection N_B^A still ultimately affects governing equations via influence on $D_{|B}^A = \partial_B D^A - N_B^A + K_{BC}^A D^C$, thus affecting $Z_A^B = \partial \psi / \partial D_{|B}^A$, and through $\bar{\partial}_C N_B^A$ in (3.35). Spatial N_b^a can enter Γ_{bc}^a in (3.34). The linear connection K_{BC}^A and its gradient $\bar{\partial}_D K_{BC}^A$ in (3.35) are somewhat unique to Finsler-geometric continuum mechanics. The trace of Cartan's tensor, C_{BA}^A , in all forms of the Euler-Lagrange equations is also a distinctive feature. This term, of course, vanishes when G_{AB} is independent of D (i.e., a Riemannian rather than Finslerian metric).

3.3.4 Spatial invariance and material symmetry

First consider rotations of the spatial frame of reference, given by orthonormal transformation q_b^a in (2.40) whereby $\det(q_b^a) = 1$ and $\tilde{q}_b^a = g^{ac} q_c^d g_{bd}$ (i.e., $\mathbf{q}^{-1} = \mathbf{q}^T$ [22]). Since $\mathbf{F} \rightarrow \mathbf{qF}$ under such coordinate changes, ψ in (3.26) should obey more restricted forms to maintain proper observer independence. Two possibilities are

$$\psi = \hat{\psi}[\mathbf{C}(\mathbf{F}, \mathbf{g}), \mathbf{D}, \nabla \mathbf{D}, \mathbf{X}] = \hat{\psi}(C_{AB}, D^A, D_{|B}^A, X^A), \quad (3.37)$$

$$\psi = \bar{\psi}[\bar{\mathbf{C}}(\mathbf{F}, \bar{\mathbf{g}}), \mathbf{D}, \nabla \mathbf{D}, \mathbf{X}] = \bar{\psi}(\bar{C}_{AB}, D^A, D_{|B}^A, X^A), \quad (3.38)$$

noting that (3.26) can be consistently expressed from (3.1), (3.2), (3.17), and (3.18) as

$$\psi(\mathbf{F}, \mathbf{D}, \nabla \mathbf{D}, \mathbf{X}) = \check{\psi}(\mathbf{F}, \mathbf{D}, \bar{\mathbf{G}}(\mathbf{X}), \hat{\mathbf{G}}(\mathbf{D}), \hat{\mathbf{g}}(\varphi(\mathbf{X})), \hat{\mathbf{g}}(\theta(\mathbf{X}, \mathbf{D})), \nabla \mathbf{D}, \mathbf{X}). \quad (3.39)$$

From (3.10), (3.19), (3.37) and (3.38), first Piola-Kirchhoff stress P_a^A of (3.29) is calculated using the chain rule:

$$P_a^A = \frac{\partial \psi}{\partial F_A^a} = 2g_{ab} F_B^b \frac{\partial \hat{\psi}}{\partial C_{AB}} = 2\bar{g}_{ab} F_B^b \frac{\partial \bar{\psi}}{\partial \bar{C}_{AB}}. \quad (3.40)$$

The resulting Cauchy stress tensors with spatial components σ^{ab} and $\bar{\sigma}^{ab}$ obey symmetry rules consistent with the classical local balance of angular momentum [20, 22, 33]:

$$\sigma^{ab} = \frac{1}{J} g^{ac} P_c^A F_A^b = \frac{2}{J} F_A^a F_B^b \frac{\partial \hat{\psi}}{\partial C_{AB}} = \sigma^{ba}, \quad \bar{\sigma}^{ab} = \frac{1}{\bar{J}} \bar{g}^{ac} P_c^A F_A^b = \frac{2}{\bar{J}} F_A^a F_B^b \frac{\partial \bar{\psi}}{\partial \bar{C}_{AB}} = \bar{\sigma}^{ba}. \quad (3.41)$$

Now consider changes of the material frame of reference, given by transformation Q_B^A of (2.1) and (2.9) with inverse \tilde{Q}_A^B . Under affine changes of coordinates $X^A \rightarrow Q_A^C X^A$, it follows that $dX^A \rightarrow Q_A^C dX^A$, $F_A^a \rightarrow \tilde{Q}_C^A F_A^a$, $G_{AB} \rightarrow \tilde{Q}_C^A \tilde{Q}_D^B G_{AB}$, $C_{AB} \rightarrow \tilde{Q}_C^A \tilde{Q}_D^B C_{AB}$, $\bar{G}_{AB} \rightarrow \tilde{Q}_C^A \tilde{Q}_D^B \bar{G}_{AB}$, $\bar{C}_{AB} \rightarrow \tilde{Q}_C^A \tilde{Q}_D^B \bar{C}_{AB}$, $D^A \rightarrow Q_A^C D^A$, $\delta D^A \rightarrow Q_A^C \delta D^A$, and $D_{|B}^A \rightarrow Q_A^C \tilde{Q}_D^B D_{|B}^A$. Energy densities ψ , $\hat{\psi}$, and $\bar{\psi}$ should be invariant under all transformations \tilde{Q}_B^A (e.g., rotations, reflections, inversions) belonging to the symmetry group \mathbb{Q} of the material [33, 61, 81, 110] (e.g., $\psi \rightarrow \psi$). The present focus is on

polynomial invariants [81, 110] with basis \mathcal{P} of invariant functions with respect to $\tilde{\mathcal{Q}} \in \mathbb{Q}$ and energy offsets $\hat{\psi}_0 = \text{constant}$, $\bar{\psi}_0 = \text{constant}$:

$$\hat{\mathcal{P}} = \{I_1, I_2, \dots, I_\nu\}; \quad I_\alpha = I_\alpha(\mathbf{C}, \mathbf{D}, \nabla \mathbf{D}), \quad \hat{\psi} = \hat{\psi}(I_1, I_2, \dots, I_\nu, \mathbf{X}) + \hat{\psi}_0; \quad (3.42)$$

$$\bar{\mathcal{P}} = \{\bar{I}_1, \bar{I}_2, \dots, \bar{I}_\zeta\}; \quad \bar{I}_\alpha = \bar{I}_\alpha(\bar{\mathbf{C}}, \mathbf{D}, \nabla \mathbf{D}), \quad \bar{\psi} = \bar{\psi}(\bar{I}_1, \bar{I}_2, \dots, \bar{I}_\zeta, \mathbf{X}) + \bar{\psi}_0. \quad (3.43)$$

The total number of applicable invariants is ν or ζ for (3.37) or (3.38). Stress of (3.40) becomes

$$P_a^A = 2g_{ab}F_B^b \sum_{\alpha=1}^{\nu} \hat{\psi}_\alpha \frac{\partial I_\alpha}{\partial C_{AB}} = 2\bar{g}_{ab}F_B^b \sum_{\alpha=1}^{\zeta} \bar{\psi}_\alpha \frac{\partial \bar{I}_\alpha}{\partial \bar{C}_{AB}}; \quad \hat{\psi}_\alpha = \frac{\partial \hat{\psi}}{\partial I_\alpha}, \quad \bar{\psi}_\alpha = \frac{\partial \bar{\psi}}{\partial \bar{I}_\alpha}. \quad (3.44)$$

Remark 3.3.6. A thorough and modern geometric treatment of material symmetry, uniformity, and homogeneity in continuous media is included in a recent monograph [111].

4 One-dimensional base manifold

The framework of §2 and §3 is applied for $n = 1$: a 1-D base manifold \mathcal{M} . In §4.1, geometry and kinematics are presented, including assumptions that enable tractable solutions to several classes of boundary value problems while at the same time maintaining sufficient generality to address broad physical behaviors. Resulting 1-D governing equations are derived in §4.2. General solutions are obtained for two problem classes in §4.3. Constitutive functions for a soft biological tissue, namely a 1-D strip of skin under axial extension, are given in §4.4. Model parameters and analytical solutions for 1-D skin stretching and tearing are reported in §4.5.

4.1 Geometry and kinematics

Let $X = X^1$. Considered is a reference domain $\{\mathcal{M} : X \in [-L_0, L_0]\}$, where the total length relative to a Euclidean metric is $2L_0$, and boundary $\partial\mathcal{M}$ is the endpoints $X = \pm L_0$. The referential internal state vector reduces to the single component $D = D^1$, which is assumed to have physical units, like X , of length. The spatial coordinate is $x = x^1$, and the spatial state component is $d = d^1$. A normalization constant (i.e., regularization length) l is introduced, and the physically meaningful domain for internal state is assumed as $D \in [0, l]$. The associated order parameter is

$$\xi(X) = \frac{D(X)}{l} = \frac{d(\varphi(X))}{l}, \quad l > 0, \quad (4.1)$$

with meaningful domain $\xi \in [0, 1]$, and where (3.12) and (3.14) are invoked. For generic f and h differentiable in their arguments, let

$$f'(X) = \frac{df(X)}{dX}, \quad f''(X) = \frac{d^2f(X)}{dX^2}; \quad h(\xi) = \frac{dh(\xi)}{d\xi}, \quad \ddot{h}(\xi) = \frac{d^2h(\xi)}{d\xi^2}. \quad (4.2)$$

For 1-D manifolds, the following metrics apply from (3.17) and (3.18):

$$G_{11}(X, D) = G(X, D) = \bar{G}(X)\hat{G}(D) = \hat{G}(D), \quad g_{11}(x, d) = g(x, d) = \bar{g}(x)\hat{g}(d) = \hat{g}(d). \quad (4.3)$$

Since $\bar{g} = \bar{G} = 1$ for isometric 1-D Riemannian spaces, setting

$$\hat{g}(d(\varphi(X))) = \hat{G}(D(X)) \leftrightarrow g(\xi) = G(\xi) \quad (4.4)$$

renders \mathfrak{m} and \mathcal{M} isometric when $\phi(X) = X + c_0 \Leftrightarrow F(X) = 1$, regardless of local values of D , d , or ξ at corresponding points $x = \varphi(X)$.

Remark 4.1.1. This assumption (4.4), used henceforth in §4, may be relaxed in future applications to address residual stress (e.g., from growth [30]; see Appendix B), especially for $n = \dim \mathcal{M} > 1$.

Henceforth in §4, functional dependence on D or d is replaced with that on ξ . Then

$$D' = \frac{\xi'}{l}, \quad \frac{\partial f(X, D)}{\partial D} = \frac{1}{l} \frac{\partial f(X, \xi(D))}{\partial \xi}. \quad (4.5)$$

The following functional forms are assumed for referential nonlinear connection N_B^A and linear connection K_{BC}^A , with $N_0 = \text{constant}$ and $\hat{K}(X)$ both dimensionless:

$$N_B^A \rightarrow N_1^1 = N = -N_0 l \xi', \quad K_{BC}^A \rightarrow K_{11}^1(X, \xi) = K(X, \xi) = \frac{\hat{K}(X)}{l \xi} \Rightarrow \bar{\partial}_1 K_{11}^1 D = -K_{11}^1. \quad (4.6)$$

Spatial coefficients K_{bc}^a do not affect the governing equations and thus are left unspecified. Conditions (3.15) apply in 1-D, leading to, with (4.1)–(4.6),

$$\Gamma_{BC}^A \rightarrow \Gamma_{11}^1 = \frac{1}{2G} \delta_1 G = \frac{1}{2G} (\partial_1 G - N_1^1 \bar{\partial}_1 G) = -N \bar{\partial}_1 (\ln \sqrt{G}) = -N C_{11}^1 = -N \frac{\chi}{l}, \quad (4.7)$$

$$\chi(\xi) = \frac{\dot{G}(\xi)}{2G(\xi)} = \frac{\dot{g}(\xi)}{2g(\xi)} = l C_{11}^1(\xi), \quad (4.8)$$

$$N_b^a \rightarrow \frac{N}{F} = -\frac{N_0 l \xi'}{F} = -N_0 l \frac{d\xi}{dx}, \quad \Gamma_{bc}^a \rightarrow -\frac{N}{F} \frac{\dot{g}}{2g} = -\frac{N}{F} \frac{\chi}{l}. \quad (4.9)$$

The deformation gradient, deformation tensor, Jacobian determinant, and director gradient are

$$F_A^a \rightarrow F_1^1 = F = \frac{d\varphi}{dX} = \varphi', \quad C_B^A \rightarrow C_1^1 = C = G^{11} g_{11} F_1^1 F_1^1 = F^2 = (\varphi')^2, \quad J = F = \sqrt{C}, \quad (4.10)$$

$$D_{|B}^A \rightarrow D_{|1}^1 = \frac{dD}{dX} - N + KD = (1 + N_0) l \xi' + \hat{K}. \quad (4.11)$$

From (4.4), $\bar{C} = \bar{C}_1^1 = C_1^1 = C$ and $\bar{J} = J$ in 1-D reductions of (3.19) and (3.20).

4.2 Governing equations

A generic energy density is assigned and equilibrium equations are derived for the 1-D case given prescriptions of §4.1.

4.2.1 Energy density

In 1-D, C_{AB} consists of a single invariant C , and D^A and $D^A|_B$ likewise. Dependencies in (3.26) are suitably represented by F , ξ , and (ξ', X) with (4.1) and (4.11). Since $\bar{C} = C = F^2$, all energy densities ψ of (3.26) in (3.37) – (3.39) are expressed simply as

$$\psi = \psi(C, \xi, \xi', X). \quad (4.12)$$

Denote by μ_0 a constant, later associated to an elastic modulus, with units of energy density.

Remark 4.2.1. For comparison with data from experiments in ambient Euclidean 3-space, μ_0 can be given units of energy per unit (3-D) volume, such that $\Psi = \int_{\mathcal{M}} \psi d\Omega$ is energy per unit cross-sectional area normal to X . For a 1-D \mathcal{M} , this cross-sectional area is, by definition, constant.

Denote by Υ_0 a constant, related to surface energy, with units of energy per unit (2-D fixed cross-sectional) area. Let W be strain energy density and Λ energy density associated with microstructure. Denote by w a dimensionless strain energy function, y a dimensionless interaction function (e.g., later representing elastic degradation from microstructure changes), λ a dimensionless phase energy function, and ι a dimensionless gradient energy function assigned a quadratic form. Free energy density (4.12) is then prescribed in intermediate functional form as follows:

$$\psi(C, \xi, \xi', X) = W(C, \xi) + \Lambda(\xi, \xi', X) = \frac{\mu_0}{2} w(C) y(\xi) + \frac{\Upsilon_0}{l} [\lambda(\xi) + \iota(\xi', X)], \quad (4.13)$$

$$\iota = |D_{|1}^1|^2 - \hat{K}^2 = D_{|1}^1 G_{11} G^{11} D_{|1}^1 - \hat{K}^2 = [(1 + N_0) l \xi' + \hat{K}]^2 - \hat{K}^2, \quad (N_0 = \text{const}, \hat{K} = \hat{K}(X)). \quad (4.14)$$

Note $\iota(0, X) = 0$. For null ground-state energy and stress, $\psi(1, 0, 0, X) = 0$ and $\frac{\partial \psi}{\partial C}(1, 0, 0, X) = 0$:

$$w(1) = 0, \quad \frac{dw}{dC}(1) = 0, \quad \frac{d^2 w}{dC^2} \geq 0; \quad \lambda(0) = 0. \quad (4.15)$$

The third of (4.15) ensures convexity of w . Thermodynamic forces originating in (3.29) are derived as

$$P = P_1^1 = \frac{\partial \psi}{\partial F} = 2 \frac{g}{G} F \frac{\partial \psi}{\partial C} = 2 \sqrt{C} \frac{\partial \psi}{\partial C} = \mu_0 y \sqrt{C} \frac{dw}{dC}, \quad (4.16)$$

$$Q = Q_1 = \frac{\partial \psi}{\partial D} = \frac{1}{l} \frac{\partial \psi}{\partial \xi} = \frac{\mu_0}{2l} w \frac{dy}{d\xi} + \frac{\Upsilon_0}{l^2} \frac{d\lambda}{d\xi} = \frac{\Upsilon_0}{l^2} (A_0 w y' + \dot{\lambda}), \quad A_0 = \frac{\mu_0 l}{2\Upsilon_0}, \quad (4.17)$$

$$Z = Z_1^1 = \frac{\partial \psi}{\partial D_{|1}^1} = \frac{\Upsilon_0}{l} \frac{\partial \iota}{\partial D_{|1}^1} = 2 \frac{\Upsilon_0}{l} D_{|1}^1 = 2 \frac{\Upsilon_0}{l} [(1 + N_0) l \xi' + \hat{K}]. \quad (4.18)$$

The volumetric source term in (3.22) is prescribed as manifesting from changes in energy density proportional to changes of the local referential volume form (e.g., physically representative of local volume changes from damage/tearing, similar to effects of tissue growth on energy (Appendix B)):

$$R = R_1 = \beta \psi \bar{\partial}_1 (\ln \sqrt{G}) = \frac{\beta}{l} \psi \chi, \quad (\beta = \text{constant}). \quad (4.19)$$

4.2.2 Linear momentum

The macroscopic momentum balance, (3.31) or (3.34) is, upon use of relations in §4.1 and §4.2.1,

$$\frac{dP}{dX} = P(N_0 - 1)\chi \frac{d\xi}{dX} = -(1 - N_0) \frac{P}{2G} \frac{dG}{dX}. \quad (4.20)$$

This is a separable first-order ordinary differential equation (ODE) that can be integrated directly:

$$\int_{P_0}^P d(\ln P) = -(1 - N_0) \int_{G_0}^G d(\ln \sqrt{G}) \quad \Rightarrow \quad P = P_0 \left(\sqrt{G_0/G} \right)^{1-N_0}. \quad (4.21)$$

The integration limit on $G(\xi(X))$ is $G_0 = G(0)$, and P_0 is a constant stress corresponding to $\xi = 0$.

Remark 4.2.2. If G is Riemannian, then $G = G_0$ and $P = P_0 = \text{constant}$. In the Finslerian setting, P can vary with X if ξ varies with X and N_0 differs from unity. However, if P vanishes on $\partial\mathcal{M}$ (i.e., at $X = \pm L_0$), then $P_0 = 0$ necessarily, so $P(X) = 0 \forall X \in \mathcal{M}$, meaning this 1-D domain cannot support residual stress. The same assertion applies when (4.4) is relaxed and N_0 vanishes.

From (4.16) and (4.21), when μ_0 is nonzero,

$$\sqrt{C(X)} \frac{dw(C(X))}{dC} y(\xi(X)) \left[\frac{G(\xi(X))}{G_0} \right]^{(1-N_0)/2} = \frac{P_0}{\mu_0} = \text{constant}, \quad (4.22)$$

where the value of P_0 , constant for a given static problem, depends on the boundary conditions.

4.2.3 Micro-momentum

Define $\bar{K}(X) = l\hat{K}(X)$. Then the microscopic momentum balance, (3.32) or (3.35), is, upon use of relations in §4.1 and §4.2.1 and dividing by $2Y_0(1 + N_0)$,

$$\begin{aligned} & \frac{d^2\xi}{dX^2} + \chi(\xi) \left[1 - \frac{(1 + N_0)(\alpha - \beta)}{2} \right] \left(\frac{d\xi}{dX} \right)^2 + \frac{\bar{K}(X)}{l^2} \chi(\xi) \left[\frac{1}{1 + N_0} - (\alpha - \beta) \right] \frac{d\xi}{dX} \\ & + \frac{d\bar{K}(X)}{dX} \frac{1}{l^2(1 + N_0)} - \frac{1}{2l^2(1 + N_0)} \left[\frac{d\lambda(\xi)}{d\xi} + (\alpha - \beta)\chi(\xi)\lambda(\xi) \right] \\ & = \frac{A_0 w(C(X))}{2l^2(1 + N_0)} \left[\frac{dy(\xi)}{d\xi} + (\alpha - \beta)\chi(\xi)y(\xi) \right]. \end{aligned} \quad (4.23)$$

This is a nonlinear and non-homogeneous second-order ODE with variable coefficients. General analytical solutions are not feasible. However, the following assumption is made henceforth in §4 to reduce the nonlinearity (second term on left side) and render some special solutions possible:

$$\beta = \alpha - 2/(1 + N_0). \quad (4.24)$$

Remark 4.2.3. Assumption (4.24) generalizes, yet is consistent with, physically realistic choices for fracture, shear bands, cavitation, and phase transitions [55, 56, 62]: $\alpha = 2, \beta = 0, N_0 = 0$.

Applying (4.24) with notation of (4.2), (4.23) reduces to the form studied in the remainder of §4:

$$l^2(1+N_0)\xi'' - \frac{\dot{\lambda}}{2} - \frac{\chi\lambda}{1+N_0} - \bar{K}\chi\xi' + \bar{K}' = \frac{A_0w}{2} \left[\dot{y} + \frac{2\chi y}{1+N_0} \right]. \quad (4.25)$$

This is a linear second-order ODE, albeit generally non-homogeneous with variable coefficients. For the special case that $\mathcal{Y}_0(1+N_0) = 0$, terms on the left of (4.23) all vanish, and equilibrium demands

$$\mu_0 w(C(X)) \left[\frac{dy(\xi)}{d\xi} + \frac{2\chi(\xi)y(\xi)}{1+N_0} \right] = 0. \quad (4.26)$$

4.3 General solutions

4.3.1 Homogeneous fields

Consider cases wherein $\xi(X) \rightarrow \xi_H = \text{constant} \forall X \in [-L_0, L_0]$. Assign the notation $f_H(X) = f(X, \xi_H)$. Then stress and momentum conservation in (4.16) and (4.21) combine to

$$P_H = \mu_0 \sqrt{C} \frac{dw}{dC} y_H = P_0 \left(\frac{G_0}{G_H} \right)^{(1-N_0)/2} = \text{constant}. \quad (4.27)$$

If μ_0 , y_H , and dw/dC are nonzero, convexity of w suggests $C = C_H = F_H^2 = \text{constant}$. Accordingly, $\varphi_H(X) = F_H X + c_0$. If $\mu_0 = 0$, $y_H = 0$, or $dw/dC = 0$, then $P_H = 0$ and $\varphi_H(X)$ is arbitrary. Assume now that none of the former are zero, such that $F = F_H$, $C = C_H$, $w = w_H = w(C_H)$ are constants. Then equilibrium equation (4.25) becomes, with $\bar{K}'_H = K'_0$ a dimensionless constant,

$$-\frac{\dot{\lambda}_H}{2} - \frac{\chi_H \lambda_H}{1+N_0} + K'_0 = \frac{A_0 w_H}{2} \left[\dot{y}_H + \frac{2\chi_H y_H}{1+N_0} \right]. \quad (4.28)$$

Remark 4.3.1. If φ_H is imposed by displacement boundary conditions, then C_H is known, as is w_H . In that case, (4.28) is an algebraic equation that can be solved implicitly for ξ_H , the value of which is substituted into (4.27) for stress P_H . If P_H is imposed by traction boundary conditions, then (4.27) and (4.28) are to be solved simultaneously for C_H and ξ_H .

4.3.2 Stress-free states

Now consider cases wherein $P = 0 \forall X \in [-L_0, L_0]$. Relation (4.20) is trivially satisfied. Assume μ_0 is nonzero. Then (4.22) requires, since $C > 0$, $G > 0$,

$$\frac{dw(C(X))}{dC} y(\xi(X)) = 0. \quad (4.29)$$

This is obeyed for any $y(\xi)$ at $C = 1$ (i.e., rigid-body motion) via (4.15). Assume further that $w = 0$, again satisfied at $C = 1$ via (4.15). Then the right side of (4.25) vanishes, leaving

$$\xi'' - \frac{\bar{K}\chi}{l^2(1+N_0)} \xi' - \frac{\dot{\lambda}}{2l^2(1+N_0)} - \frac{\chi\lambda}{l^2(1+N_0)^2} + \frac{\bar{K}'}{l^2(1+N_0)} = 0, \quad (4.30)$$

with functional dependencies $\xi(X)$, $\chi(\xi)$, $\bar{K}(X)$, and $\lambda(\xi)$. The ODE is linear or nonlinear depending on forms of λ and χ ; analytical solutions can be derived for special cases. If $\bar{K} = \text{constant}$, (4.30) is autonomous. If $\bar{K} = 0$, then (4.30) is

$$\frac{d^2\xi}{dX^2} = \zeta \frac{d\zeta}{d\xi} = \frac{1}{2l^2(1+N_0)} \left[\frac{d\lambda}{d\xi} + \frac{2\chi(\xi)\lambda(\xi)}{1+N_0} \right], \quad (4.31)$$

where $\zeta = \xi' \Rightarrow \xi'' = \zeta d\zeta/d\xi$. The right equation can be separated and integrated as

$$\begin{aligned} \frac{1}{2}\zeta^2 &= \frac{1}{2l^2(1+N_0)} \int \left[\frac{d\lambda}{d\xi} + \frac{2\chi(\xi)\lambda(\xi)}{1+N_0} \right] d\xi + c_1 \\ \Rightarrow \frac{d\xi}{dX} &= \pm \frac{1}{l\sqrt{1+N_0}} \left(\int \left[\frac{d\lambda}{d\xi} + \frac{2\chi(\xi)\lambda(\xi)}{1+N_0} \right] d\xi + c_1 \right)^{1/2}. \end{aligned} \quad (4.32)$$

This first-order ODE can be separated and solved for $\xi = \arg[X(\xi)]$, where

$$X(\xi) = \pm l\sqrt{1+N_0} \int \frac{d\xi}{\left\{ \int \left[\frac{d\lambda}{d\xi} + \frac{2\chi(\xi)\lambda(\xi)}{1+N_0} \right] d\xi + c_1 \right\}^{1/2}} + c_2. \quad (4.33)$$

Integration constants are c_1 and c_2 , determined by boundary conditions.

Now allow arbitrary $\bar{K}(X)$ but restrict $\chi = 0$ (e.g., $G = G_0$). Assume $\lambda(\xi)$ is quadratic such that $\dot{\lambda} = 2\omega_0 + 2\omega_1\xi$. Now (4.30) is linear:

$$\frac{d^2\xi}{dX^2} - \frac{\omega_1}{l^2(1+N_0)}\xi = \frac{1}{l^2(1+N_0)} \left(\omega_0 - \frac{d\bar{K}}{dX} \right). \quad (4.34)$$

This ODE is non-homogeneous but has constant coefficients. Assume $\omega_1 > 0$ and $N_0 > -1$. Then

$$\xi(X) = c_1 \exp \left[(X/l) \sqrt{\omega_1/(1+N_0)} \right] + c_2 \exp \left[-(X/l) \sqrt{\omega_1/(1+N_0)} \right] + \xi_p(X), \quad (4.35)$$

where c_1 and c_2 are new constants and ξ_p is the particular solution from ω_0 and $\bar{K}(X) = l\hat{K}(X)$.

4.4 Constitutive model

The framework is applied to a strip of skin loaded in tension along the X -direction.

Remark 4.4.1. A 1-D theory cannot distinguish between uniaxial strain or uniaxial stress conditions, nor can it account for anisotropy. Thus, parameters entering the model (e.g., μ_0 , \mathcal{I}_0) are particular to those loading conditions and material orientations from experiments to which they are calibrated (e.g., uniaxial stress along a preferred fiber direction).

The nonlinear elastic potential of §4.4.2 specializes a 3-D model [71, 82, 83, 92] to 1-D. The internal structure variable $\xi = D/l$ accounts for local rearrangements that lead to softening and degradation under tensile load [72–74, 77]: fiber sliding, pull-out, and breakage of collagen fibers, as well as rupture of the elastin fibers and ground matrix.

Remark 4.4.2. Specifically, D is a representative microscopic sliding or separation distance among microstructure constituents, and l is the value of this distance at which the material can no longer support tensile load. In the context of cohesive theories of fracture [73, 112, 113], D can be interpreted as a crack opening displacement.

Remark 4.4.3. Some physics represented by the present novel theory, not addressed by nonlinear elastic-continuum damage [73, 90] or phase-field [95, 114] approaches, are summarized as follows. The Finslerian metrics $G(\xi) = g(\xi)$ account for local rescaling of material and spatial manifolds \mathcal{M} and \mathfrak{m} due to microstructure changes (e.g, expansion due to tearing or cavitation). Nonlinear connection N_0 rescales the quadratic contribution of the gradient of ξ to surface energy by a constant, and linear connection \hat{K} rescales the linear contribution of the gradient of ξ to surface energy by a continuous and differentiable function of X , enabling a certain material heterogeneity.

4.4.1 Metrics

From (2.16), (2.48), (3.10), (4.3), (4.4), and (4.10), the difference in squared lengths of line elements $d\mathbf{x}$ and $d\mathbf{X}$ is

$$(|d\mathbf{x}|^2 - |d\mathbf{X}|^2)(C, \xi) = G(\xi)(C - 1)dX dX. \quad (4.36)$$

Herein, the metric is assigned an exponential form frequent in generalized Finsler geometry [7, 55] and Riemannian geometry [27, 30]:

$$G(\xi) = \exp\left(\frac{2k}{r}\xi^r\right) \Rightarrow \chi(\xi) = \frac{\dot{G}}{2G} = \frac{\dot{g}}{2g} = k\xi^{r-1}. \quad (4.37)$$

For $\xi \in [0, 1]$, two constants are k , which is positive for expansion, and $r > 0$.

Remark 4.4.4. Local regions of \mathcal{M} at X and \mathfrak{m} at $x = \varphi(X)$ are rescaled isometrically by $G(\xi(X))$. Physically, this rescaling arises from changes in structure associated with degradation, to which measure $\frac{1}{2} \ln G(\xi)$ is interpreted as a contributor to remnant strain. For Riemannian metrics, $G = \bar{G} = \bar{g} = g = 1$, in which case (4.36) is independent of ξ and this remnant strain always vanishes.

The ratio of constants is determined by the remnant strain contribution at failure: $\hat{\epsilon} = \frac{k}{r} = \frac{1}{2} \ln G(1)$. Since $\xi \in [0, 1]$, smaller r at fixed $\frac{k}{r}$ gives a sharper increase in $\frac{1}{2} \ln G$ versus ξ . Values of k and r are calibrated to data in §4.5; choices of N_0 and \bar{K} are explored parametrically therein. Nonlinear connection $N_0 = \text{constant}$ and linear connection $\hat{K}(X) = \bar{K}(X)/l$ affect the contribution of state gradient ξ' to surface energy ι via (4.13) and (4.14). Constraint $N_0 > -1$ is applied to avoid model singularities and encompass trivial choice $N_0 = 0$. The value of N_0 uniformly scales the contribution of $(\xi')^2$ to ι and ψ . Function \hat{K} scales, in a possibly heterogeneous way, the contribution of ξ' to ι and ψ . Even when ξ' vanishes, N_0 and \bar{K} can affect solutions.

4.4.2 Nonlinear elasticity

Strain energy density W in (4.13) is dictated by the normalized (dimensionless) function $w(C)$:

$$w(C) = (\sqrt{C} - 1)^2 + \frac{a_1}{2b_1} [\exp\{b_1(C - 1)^2\} - 1], \quad (4.38)$$

where dimensionless constants are $a_1 \geq 0$ and $b_1 > 0$, and $\mu_0 > 0$ is enforced along with $Y_0 > 0$ in (4.13). This adapts prior models for collagenous tissues [71, 82, 83, 92] to the 1-D case. The first term on the right, linear in C , accounts for the ground matrix and elastin. The second (exponential) term accounts for the collagen fibers, which, in the absence of damage processes, stiffen significantly at large C . Such stiffening is dominated by the parameter b_1 , whereas a_1 controls the fiber stiffness at small stretch $\sqrt{C} \approx 1$ [71].

The elastic degradation function $y(\xi)$ and independent energy contribution $\lambda(\xi)$ in (4.13) are standard from phase-field theories [95, 114], where $\vartheta \in [0, \infty)$ is a constant with $\vartheta = 2$ typical for brittle fracture and $\vartheta = 0 \mapsto y = 1$ for purely elastic response:

$$y(\xi) = (1 - \xi)^\vartheta, \quad \dot{y}(\xi) = -\vartheta(1 - \xi)^{\vartheta-1}; \quad \lambda(\xi) = \xi^2, \quad \dot{\lambda}(\xi) = 2\xi. \quad (4.39)$$

When $\vartheta > 0$, $y(1) = 0$: no strain energy W or tensile load P are supported at X when $D(X) = l$. Verification of (4.15) for prescriptions (4.38) and (4.39) is straightforward [81, 82]. Stress P conjugate to $F = \sqrt{C}$ and force Q conjugate to $D = l\xi$ are, from (4.16), (4.17), (4.38), and (4.39):

$$P(C, \xi) = \mu_0(1 - \xi)^\vartheta \left[(\sqrt{C} - 1) + a_1 \sqrt{C}(C - 1) \exp\{b_1(C - 1)^2\} \right], \quad (4.40)$$

$$Q(C, \xi) = \frac{2Y_0}{l^2} \left[\xi - \frac{A_0 \vartheta}{2} (1 - \xi)^{\vartheta-1} \left((\sqrt{C} - 1)^2 + \frac{a_1}{2b_1} [\exp\{b_1(C - 1)^2\} - 1] \right) \right]. \quad (4.41)$$

Remark 4.4.5. Ideal elasticity (i.e., no structure-mediated metric variation or degradation), is obtained when $k = 0 \Rightarrow G = 1 \Rightarrow \chi = 0$, $\vartheta = 0 \leftrightarrow y = 1 \Rightarrow \dot{y} = 0$, and $\bar{K}' = 0$. In this case, as $\dot{\lambda}(0) = 0$ by (4.39), trivial solutions to (4.21) and (4.23) are $P(X) = P_0 = \text{constant}$, $\xi(X) = 0 \forall X \in \mathcal{M}$.

4.5 Specific solutions

Inputs to the model are nine constants $l > 0$, $k, r > 0$, $N_0 > -1$, $\mu_0 > 0$, $a_1 \geq 0$, $b_1 > 0$, $\vartheta \geq 0$, $Y_0 > 0$, and the function $\bar{K}(X)$. These are evaluated for stretching and tearing of skin [73, 74, 113] by applying the constitutive model of §4.4 to the general solutions derived in §4.3.

4.5.1 Homogeneous fields

Here the skin specimen is assumed to degrade homogeneously in a gauge section of initial length $2L_0$ (i.e., diffuse damage), an idealization fairly characteristic of certain experiments [64, 68, 72, 74, 87]. Per §4.3.1, assume deformation control, with $F = F_H = \sqrt{C_H} \geq 1$ increased incrementally from unity. The analytical solution for $\xi = \xi_H$ is then the implicit solution of (4.28) upon substitution of (4.37), (4.38) and (4.39), here for $\vartheta > 0$:

$$\begin{aligned} \xi_H + [k/(1 + N_0)] \xi_H^{1+r} &= \frac{1}{2} A_0 \vartheta (1 - \xi_H)^{\vartheta-1} \{ (\sqrt{C_H} - 1)^2 + [a_1/(2b_1)] \\ &\times [\exp\{b_1(C_H - 1)^2\} - 1] \} \{ 1 - 2k \xi_H^{r-1} (1 - \xi_H) / [(1 + N_0) \vartheta] \} + K'_0. \end{aligned} \quad (4.42)$$

This dimensionless solution does not depend on μ_0 , Y_0 , or l individually, but only on dimensionless ratio $A_0 = \frac{\mu_0 l}{2Y_0}$. However, stress $P_H = P(C_H, \xi_H)$ is found from (4.40), which does depend on μ_0 .

Stress P is shown in Fig. 2(a), first assuming $N_0 = 0$ and $K'_0 = 0$ for simplicity. The Finsler model, with $A_0 = 8.5 \times 10^{-2}$ corresponding to baseline parameters given in Table 1, successfully matches experimental¹ data [74]. The value of μ_0 is comparable to the low-stretch tensile modulus in some experiments [71, 75], acknowledging significant variability in the literature.

Remark 4.5.1. The ideal elastic solution ($\xi = 0$) is shown for comparison. Excluding structure evolution corresponding to collagen fiber rearrangements, sliding, and breakage, the model is too stiff relative to this data for which such microscopic mechanisms have been observed [74]. The ideal elastic model is unable to replicate the linearizing, softening, and failure mechanisms with increasing stretch \sqrt{C} reported in experiments on skin and other soft tissues [63, 64, 68, 74, 87].

In Fig. 2(b), effects of ϑ on P are revealed for $\hat{\epsilon} = 0.1$, $r = 2$, $N_0 = 0$, and $K'_0 = 0$, noting $\vartheta = 0$ produces the ideal nonlinear elastic solution $\xi_H = 0$ in (4.42). Peak stress increases with decreasing ϑ ; the usual choice from phase-field theory $\vartheta = 2$ provides the close agreement with data in Fig. 2(a). In Fig. 2(c), effects of Finsler metric scaling factors $\hat{\epsilon} = \frac{k}{r}$ and r on stress P are demonstrated, where at fixed r , peak stress increases (decreases) with increasing (decreasing) $\hat{\epsilon}$ and k . Baseline choices $\hat{\epsilon} = 0.1$ and $r = 2$ furnish agreement with experiment in Fig. 2(a). A remnant strain of 0.1 is the same order of magnitude observed in cyclic loading experiments [72, 78]. Complementary effects on evolution of structure versus stretch are shown in Fig. 2(e): modest changes in ξ produce significant changes in P . In Fig. 2(d), effects of connection coefficients N_0 and K'_0 are revealed, holding material parameters at their baseline values of Table 1. For this homogeneous problem, maximum P decreases with increasing N_0 and K'_0 . Corresponding evolution of ξ is shown in Fig. 2(f). When $K'_0 < 0$, a viable solution $\xi_H \in [0, 1]$ exists only for $\sqrt{C} > 1$.

The total energy per unit cross-sectional area of the specimen is $\bar{\Psi}$, found upon integration of $\psi(C_H, \xi_H)$ in (4.13) over \mathcal{M} with local volume element $dV = \sqrt{G(\xi_H)} dX$:

$$\frac{\bar{\Psi}}{L_0} = \mu_0 \left[(1 - \xi_H)^\vartheta \{ (\sqrt{C_H} - 1)^2 + \frac{a_1}{2b_1} [\exp\{b_1(C_H - 1)^2\} - 1] \} + \frac{\xi_H^2}{A_0} \right] \exp\left(\frac{k}{r} \xi_H\right). \quad (4.43)$$

4.5.2 Stress-free states

The stress-free solutions of §4.3.2 are applied to evaluate the remaining unknown parameters l and Y_0 , given μ_0 and A_0 from §4.5.2. Assume the specimen tears completely at its midpoint at $X = 0$, such that $\xi(0) = 1$. No load is supported anywhere, and only rigid body motion is possible at other locations X where $\xi(X) > 0$. Assume the specimen is clamped at its ends where it is gripped, such that $\xi(-L_0) = \xi(L_0) = 0$. Symmetry conditions $\xi(-X) = \xi(X)$ are imposed, with $\xi'(0)$ discontinuous, such that a solution need be calculated only for the half-space $X \in [0, L_0]$.

First take $\bar{K} = l\hat{K} = 0$ so that (4.33) holds. Assume $c_1 = 0$ corresponding to $\xi' = 0$ where $\xi = 0$ since the anti-derivative in (4.32) vanishes at $\xi = 0$ when $\lambda = \xi^2$, $\chi = k\xi^{r-1}$, $r > 0$. It is verified a

¹Stretch corresponding to Fig. 5(e) in experimental work [74] is defined as engineering strain plus 1.2 in Fig. 2(a) of §4.5.1 and Fig. 4(a) of §5.5.1 to account for pre-stress (≈ 0.7 MPa) and pre-strain (≈ 0.2), so $\sqrt{C} = 1$ consistently for stress-free reference states among models and experiments. Stress-free states at null strain are consistent with data in Fig. 3(a) of that work [74]. Alternatively, $2\frac{\sigma_0}{\mu_0}(\sqrt{C} - 1)$, with $\sigma_0 = \text{constant}$, can be added to w of (4.38) giving a pre-stress of $P_{C=1, \xi=0} = \sigma_0$ to fit data with pre-stress; this, however, would require relaxation of the second of (4.15).

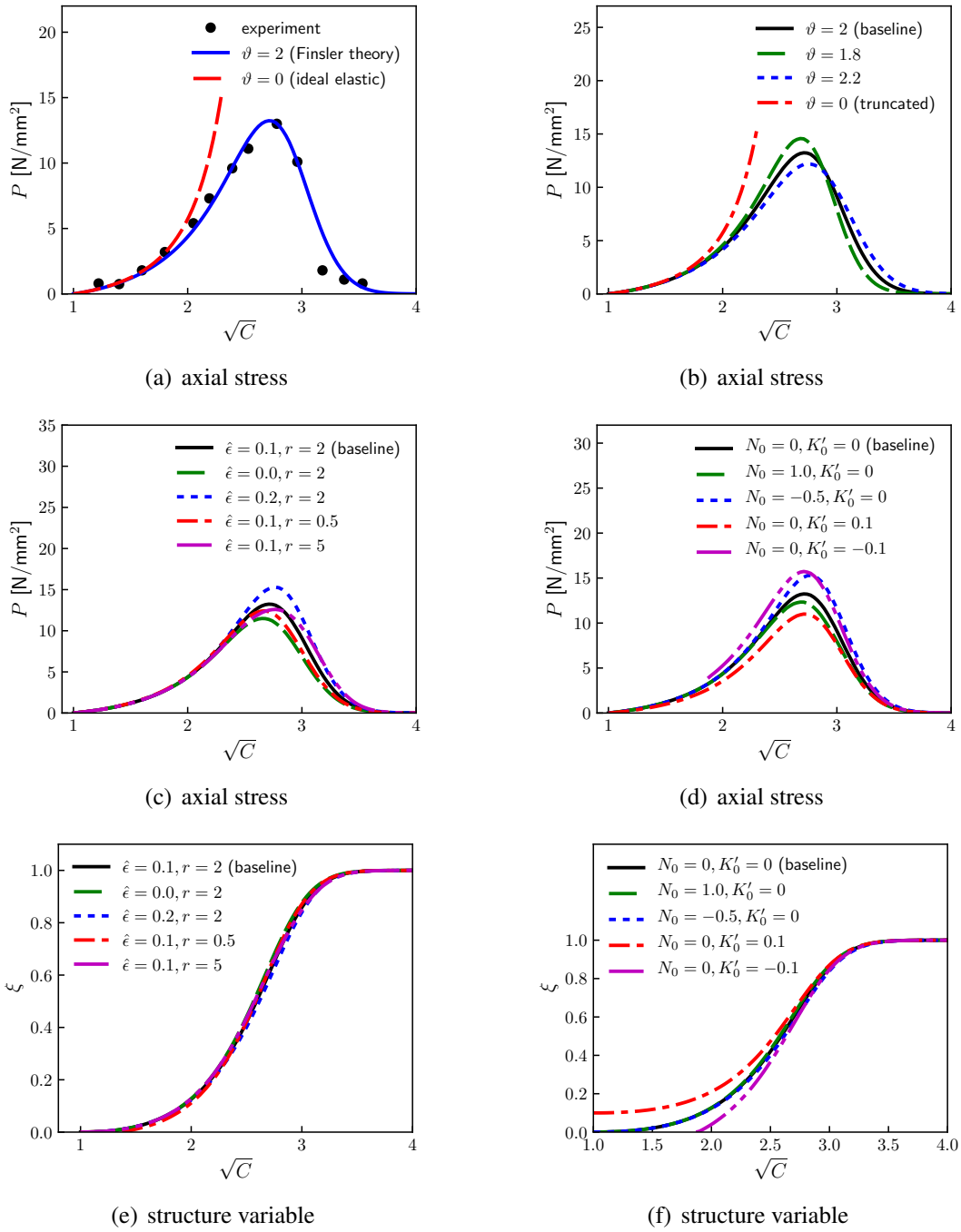


Figure 2 Extension and tearing of skin for imposed axial stretch ratio \sqrt{C} , 1-D model: (a) stress P comparison with data [74] (see text §4.5.1 for definition of experimental stretch ratio) of Finsler model (baseline) and ideal nonlinear elasticity (null structure change) (b) effect on stress P of energy degradation exponent ϑ with $\hat{\epsilon} = 0.1$, $r = 2$, $N_0 = 0$, and $K'_0 = 0$ (c) effect on stress P of Finsler metric scaling $\hat{\epsilon} = \frac{k}{r}$ and r with $\vartheta = 2$, $N_0 = 0$, and $K'_0 = 0$ (d) effect on stress P of nonlinear connection N_0 and linear connection K'_0 with $\vartheta = 2$, $\hat{\epsilon} = 0.1$, and $r = 2$ (e) effect on internal structure $\xi = D/l$ of Finsler metric scaling $\hat{\epsilon} = \frac{k}{r}$ and r with $\vartheta = 2$, $N_0 = 0$, and $K'_0 = 0$ (f) effect on internal structure $\xi = D/l$ of nonlinear connection N_0 and linear connection K'_0 with $\vartheta = 2$, $\hat{\epsilon} = 0.1$, and $r = 2$

Table 1 Baseline model parameters for rabbit skin tissue: 1-D and 2-D theories

Parameter	Units	Definition	Value (1-D)	Value (2-D)
l	mm	length scale	0.04	0.04
k	...	metric scaling factor	0.2	0.2
m	...	metric scaling factor	...	0.3
r	...	metric scaling exponent	2	2
μ_0	N/mm ²	shear modulus (axial 1-D)	0.2	0.2
κ_0	N/mm ²	bulk modulus ($\kappa_0 = k_0\mu_0$)	...	1.2
a_1	...	nonlinear elastic constant	2.8	2.8
a_2	...	nonlinear elastic constant	...	6
b_1	...	nonlinear elastic constant	0.055	0.055
b_2	...	nonlinear elastic constant	...	0.17
ϑ	...	degradation exponent	2	2
ζ	...	degradation exponent	...	2
Υ_0	mJ/mm ²	isotropic surface energy	0.47	0.47
γ_ξ	...	anisotropic energy factor	...	1
γ_η	...	anisotropic energy factor	...	0.84

posteriori [55, 59, 62] that this closely approximates true boundary conditions $\xi(\pm L_0) = 0$ as well as $\xi'(\pm L_0) = 0$ for $L_0 \gg l$. Then the physically valid (negative) root for the half-domain giving $X \geq 0$ in (4.33) becomes, with (4.37) and (4.39),

$$\frac{X(\xi)}{L_0} = -\frac{l}{L_0} \sqrt{1+N_0} \int_{z=1}^{z=\xi} \frac{dz}{z \sqrt{1+2kz^r/[(1+N_0)(2+r)]}}. \quad (4.44)$$

The lower limit follows from $X(1) = 0$, obviating c_2 in (4.33). Analytical solution $\xi = \arg X(\xi)$ is exact, but it is most easily evaluated by quadrature when k is nonzero, decrementing z from 1 to 0 in small negative steps. The profile of $\xi(X)$ depends on X/L_0 and l/L_0 , but not l or L_0 individually.

Remark 4.5.2. This new 1-D solution, (4.44), agrees with more specific solutions derived in past work: $N_0 = 0$ and $r = 1$ [55, 56] with slight correction [59] and $N_0 = 0$ and $r = 2$ [59].

Normalized surface energy per two-sided cross-sectional area, $\bar{\gamma}$, is obtained by integration of $\psi = \Lambda$ in (4.13) over \mathcal{M} :

$$\bar{\gamma} = \frac{1}{2\Upsilon_0} \int_{-L_0}^{L_0} \psi \sqrt{G} dX = \frac{1}{2l} \int_{-L_0}^{L_0} \{\xi^2 + (1+N_0)l\xi'[2\hat{K} + (1+N_0)l\xi']\} \exp[(k/r)\xi^r] dX. \quad (4.45)$$

This energy likewise depends on l/L_0 but not l or L_0 individually. Baseline values of k and r are now taken from Table 1. The solution (4.44) is shown for $N_0 = 0$ and different l/L_0 in Fig. 3(a). The smaller (larger) the regularization length ratio l/L_0 , the sharper (more diffuse) the zone centered at the midpoint of the domain over which prominent structure changes occur.

Normalized energy density (4.45) is shown in Fig. 3(b) versus l/L_0 for several N_0 . Increasing N_0 increases this energy, as might be anticipated from (4.13) with (4.14) when $\hat{K} = 0$. A stress-free

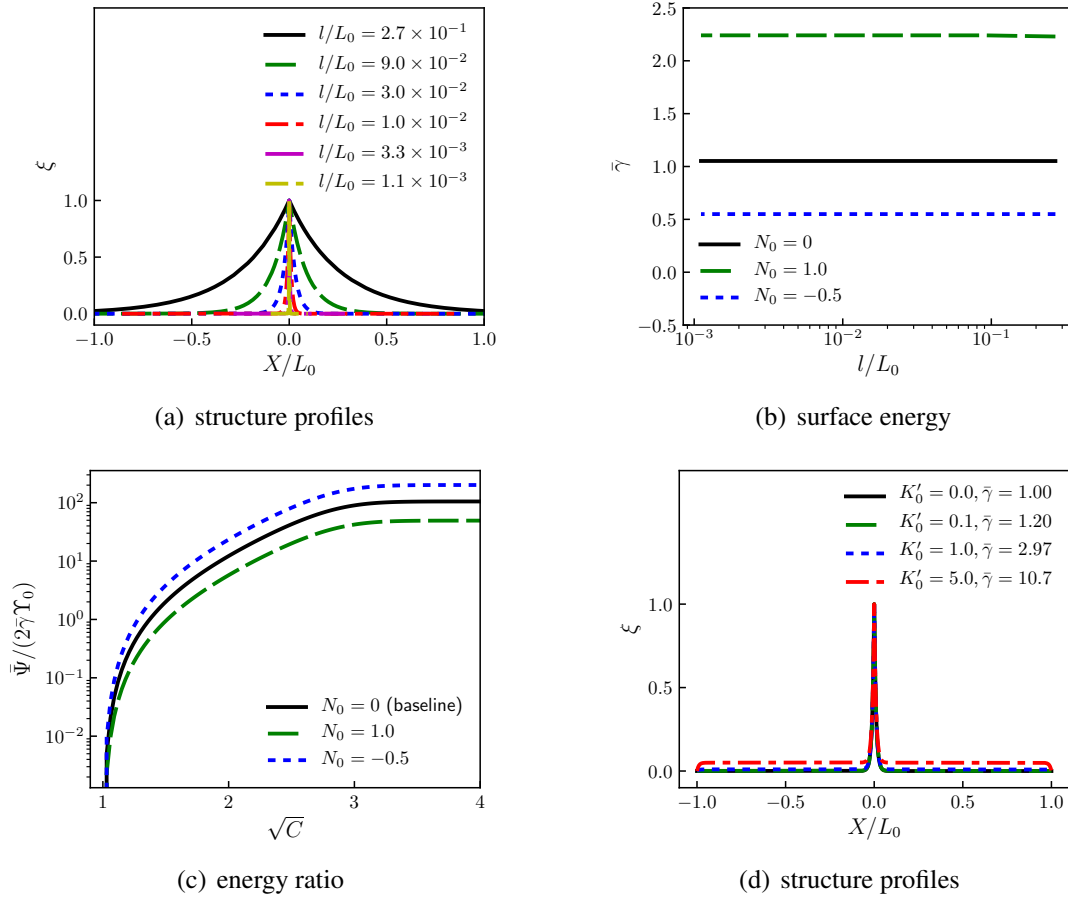


Figure 3 Extension and tearing of skin, 1-D model: (a) stress-free solution for internal state profile (baseline parameters, $N_0 = 0$) (b) normalized surface energy for rupture versus regularization length (c) ratio of homogeneous energy to energy for stress-free localized rupture (d) stress-free solution, $\hat{\epsilon} = 0$, $l/L_0 = 10^{-2}$, heterogeneous connection $\bar{K}(X)$

ruptured state is energetically favorable to a stressed homogeneous state (§4.5.1) from applied deformation C_H when $\bar{\Psi} > 2\bar{\gamma}\Upsilon_0$, with $\bar{\Psi}$ given by (4.43). Ratio $\bar{\Psi}/(2\bar{\gamma}\Upsilon_0)$ is shown in Fig. 3(c) versus $\sqrt{C} = \sqrt{C_H}$ with $l/L_0 = 10^{-2}$ and several N_0 , recalling $K'_0 = 0$. Increasing N_0 increases $\bar{\gamma}$, reducing $\bar{\Psi}/(2\bar{\gamma}\Upsilon_0)$. For cases in Fig. 3(a), Fig. 3(b), and Fig. 3(c), $\xi(\pm L_0) < 10^{-8}$ and $|l\xi'(\pm L_0)| < 10^{-8}$ are observed for $l/L_0 \leq 0.03$, verifying $c_1 = 0$ in (4.33) and (4.44) under this length constraint.

The remaining parameters l and Υ_0 are now quantified. To match the measured energy release rate J_C (i.e., toughness) of skin, $2\bar{\gamma}\Upsilon_0 \approx J_C$. Take $L_0 = 4$ mm, the span of specimens [74] whose data are represented in Fig. 2(a). Then $l/L_0 = 10^{-2} \Rightarrow l = 40 \mu\text{m}$ is more than sufficiently small to adhere to the aforementioned boundary constraints (i.e., $c_1 = 0$) while providing a damage profile of intermediate diffusivity in Fig. 3(a). This value of l then gives $\Upsilon_0 = \frac{\mu_0 l}{2A_0} = 0.47 \text{ kJ/m}^2$ (Table 1).

Remark 4.5.3. Along with the choice $N_0 = 0$, the Finsler model with full set of baseline parameters in Table 1 produces $\bar{\gamma} \approx 1$ in Fig. 3(b) and $2\bar{\gamma}\Upsilon_0 = 1.0 \text{ kJ/m}^2$, in concurrence with experimental data: $0.5 \lesssim J_C \lesssim 2.5 \text{ kJ/m}^2$ [73, 99, 113]. Value $l = 40 \mu\text{m}$ is between $4\times$ and $40\times$ the collagen fiber

diameter [68, 69, 74]. Though not shown in Fig. 3(b), increasing $\hat{\varepsilon} = \frac{k}{r}$ from 0.1 to 0.2 at $\vartheta = r = 2$ with $N'_0 = K'_0 = 0$ and $l/L_0 = 10^{-2}$ increases effective toughness to $2\bar{\gamma}\mathcal{I}_0 = 1.02 \text{ kJ/m}^2$. Under the same conditions, reducing $\hat{\varepsilon}$ to 0 diminishes the predicted toughness to $2\bar{\gamma}\mathcal{I}_0 = 0.94 \text{ kJ/m}^2$.

Finally, take $k = 0$ but permit nonzero $\bar{K}(X) = l\hat{K}(X)$, such that (4.35) applies. As an example, let $\bar{K} = -K'_0 l \cdot (1 - X/L_0)$ for $X \in [0, L_0]$ and $\bar{K} = K'_0 l \cdot (1 + X/L_0)$ for $X \in [-L_0, 0]$. Boundary conditions $\xi(0) = 1$ and $\xi(\pm L_0) = 0$ still apply, as does symmetry relation $\xi(X) = \xi(-X)$. From (4.39), $\omega_1 = 1$ and $\omega_0 = 0$. For the whole domain $X \in [-L_0, L_0]$, $\bar{K}' = K'_0 l/L_0 = \text{constant}$, and simply $\xi_p = K'_0 l/L_0$. Then (4.35) gives

$$\begin{aligned} \xi(X) &= c_1 \exp[X/\{l\sqrt{1+N_0}\}] + c_2 \exp[-X/\{l\sqrt{1+N_0}\}] + K'_0 l/L_0, \\ c_1 = 1 - c_2 - K'_0 l/L_0 &= \frac{-K'_0 l/L_0 - [1 - K'_0 l/L_0] \exp[-L_0/\{l\sqrt{1+N_0}\}]}{\exp[L_0/\{l\sqrt{1+N_0}\}] - \exp[-L_0/\{l\sqrt{1+N_0}\}]} \end{aligned} \quad (4.46)$$

Profiles of $\xi(X)$ are shown in Fig. 3(d) for $K'_0 \geq 0$ with baseline $l/L_0 = 10^{-2}$. Normalized surface energy $\bar{\gamma}$ from (4.45) is reported in Fig. 3(d) for each case, recalling $\hat{\varepsilon} = k = 0$ produces Riemannian (Euclidean) metric $G = 1$. Setting $K'_0 > 0$ increases $\bar{\gamma}$ for this problem. Setting $K'_0 < 0$ reduces $\bar{\gamma}$ and produces a physically invalid solution (not shown in Fig. 3(d)) in (4.46): $\xi < 0$ on part of \mathcal{M} .

5 Two-dimensional base manifold

The framework of §2 and §3 is applied for $n = 2$: a 2-D base manifold \mathcal{M} . In §5.1, geometry and kinematics are presented. Governing equations are derived in §5.2. Solutions are considered for general problem classes in §5.3. Constitutive functions for an orthotropic 2-D patch of skin under planar deformations are assigned in §5.4. Solutions for stretching and tearing follow in §5.5.

5.1 Geometry and kinematics

Reference coordinates are Cartesian (orthogonal): $\{X^1, X^2\}$. Considered is a reference domain $\{\mathcal{M} : X^1 \in [-L_0, L_0], X^2 \in [-W_0, W_0]\}$, where the total area relative to a Euclidean metric is $4L_0W_0$, and boundary $\partial\mathcal{M}$ is the edges $(X^1, X^2) = (\pm L_0, \pm W_0)$. The referential internal state vector has coordinates $\{D^1, D^2\}$, both with physical units of length. Spatial coordinates are Cartesian $\{x^1, x^2\}$ and $\{d^1, d^2\}$. A normalization constant (i.e., regularization length) is l , with physically meaningful domain assumed as $D^A \in [0, l]$ ($A = 1, 2$). With notation $f(X, D) = f(X^A, D^B)$, dimensionless order parameters are, with (3.12) and (3.14) invoked,

$$\xi(X) = \frac{D^1(X)}{l} = \frac{d^1(\varphi(X))}{l}, \quad \eta(X) = \frac{D^2(X)}{l} = \frac{d^2(\varphi(X))}{l}, \quad l > 0. \quad (5.1)$$

Physically meaningful domains are $\xi \in [0, 1]$ and $\eta \in [0, 1]$. For 2-D manifolds with Cartesian base coordinates $\{X^1, X^2\}$ and $\{x^1, x^2\}$, the following metrics apply from (3.17) and (3.18):

$$\bar{G}_{AB} = \delta_{AB}, \quad \bar{g}_{ab} = \delta_{ab}; \quad G_{AB}(X, D) = \hat{G}_{AB}(D), \quad g_{ab}(x, d) = \hat{g}_{ab}(d). \quad (5.2)$$

Herein, the following constraint is imposed:

$$\hat{g}_{ab}(d(\varphi(X))) = \delta_a^A \delta_b^B \hat{G}_{AB}(D(X)) \leftrightarrow g_{ab}(\xi, \eta) = \delta_a^A \delta_b^B G_{AB}(\xi, \eta), \quad (5.3)$$

making \mathfrak{m} and \mathcal{M} isometric when $\phi^a(X) = \delta_A^a X^A + c_0^a \Leftrightarrow F_A^a = \delta_A^a$ regardless of $\{\xi, \eta\}$ at $x = \varphi(X)$.

Remark 5.1.1. Equation (5.3) may be removed in other settings to directly model residual stress (e.g., Appendix B), but all residual stresses are not necessarily eliminated with (5.3) in place.

Though other non-trivial forms are admissible (e.g., §4.1), assume nonlinear N_B^A and linear K_{BC}^A connections vanish:

$$N_B^A = 0 \Rightarrow N_b^a = \delta_A^a N_B^A (F^{-1})_b^B = 0, \quad K_{BC}^A = 0. \quad (5.4)$$

The K_{bc}^a do not affect the governing equations to be solved later, so they are unspecified. Applying (3.15) and (5.1)–(5.4),

$$\delta_A G_{BC} = \partial_A G_{BC} - N_A^D \bar{\partial}_D G_{BC} = 0 \Rightarrow \Gamma_{BC}^A = 0, \quad \delta_a g_{bc} = 0 \Rightarrow \Gamma_{bc}^a = 0, \quad (5.5)$$

$$\chi_A(\xi, \eta) = lC_{AB}^B(\xi, \eta) = l\bar{\partial}_A \{\ln \sqrt{G(\xi, \eta)}\}; \quad l\bar{\partial}_1(\cdot) = \partial(\cdot)/\partial\xi, \quad l\bar{\partial}_2(\cdot) = \partial(\cdot)/\partial\eta. \quad (5.6)$$

The deformation gradient, deformation tensor, Jacobian determinant, and director gradient are

$$F_A^a = \frac{\partial \varphi^a}{\partial X^A}, \quad C_B^A = G^{AC} g_{bc} F_B^b F_C^c = G^{AC} F_C^c \delta_c^F G_{FE} \delta_b^E F_B^b, \quad J = \det(F_A^a) = \sqrt{\det(C_B^A)}, \quad (5.7)$$

$$D_{|B}^A = \delta_B D^A + K_{BC}^A D^C = \partial_B D^A; \quad D_{|A}^1 = l\partial_A \xi, \quad D_{|A}^2 = l\partial_A \eta. \quad (5.8)$$

Unless F_A^a and G_{AB} are diagonal, C and \bar{C} can differ. From (3.19) and (3.20),

$$\bar{C}_B^A = \delta^{AC} \bar{C}_{CB} = \delta^{AC} \delta_{bc} F_B^b F_C^c, \quad \bar{J} = \sqrt{\det(\bar{C}_B^A)} = J. \quad (5.9)$$

5.2 Governing equations

A generic energy density is chosen and equilibrium equations are derived for the 2-D case of §5.1.

5.2.1 Energy density

For the present case, dependencies on D^A and $D_{|B}^A$ are suitably represented by (ξ, η) and $(\partial_A \xi, \partial_A \eta)$ of (5.1) and (5.8). The functional form of (3.38) is invoked without explicit X dependency, whereby

$$\psi = \bar{\Psi}(\bar{C}_{AB}, \xi, \eta, \partial_A \xi, \partial_A \eta). \quad (5.10)$$

Henceforth in §5, the over-bar is dropped from ψ to lighten the notation. Denote by μ_0 a constant, later associated to a shear modulus, with units of energy density.

Remark 5.2.1. For comparison with experiments in ambient 3-space, μ_0 has units of energy per unit 3-D volume, so $\Psi = \int_{\mathcal{M}} \psi d\Omega$ is energy per unit thickness normal to the X^1 and X^2 .

Denote by Υ_0 a constant related to surface energy with units of energy per unit (e.g., 2-D fixed cross-sectional) area, and by γ_ξ and γ_η two dimensionless constants. Let W be strain energy density and Λ energy density associated with microstructure. Denote by w a dimensionless strain energy function (embedding possible degradation), λ and ν dimensionless phase energy functions, ι a dimensionless gradient energy function assigned a sum of quadratic forms, and $\nabla_0(\cdot) = \frac{\partial}{\partial \bar{X}}(\cdot)$ the partial material gradient. Free energy (5.10) is prescribed in intermediate functional form as

$$\begin{aligned}\psi(\bar{C}, \xi, \eta, \nabla_0 \xi, \nabla_0 \eta) &= W(\bar{C}, \xi, \eta) + \Lambda(\xi, \eta, \nabla_0 \xi, \nabla_0 \eta) \\ &= \frac{\mu_0}{2} w(\bar{C}, \xi, \eta) + \frac{\Upsilon_0}{l} [\gamma_\xi \lambda(\xi) + \gamma_\eta \nu(\eta) + \iota(\nabla_0 \xi, \nabla_0 \eta)],\end{aligned}\quad (5.11)$$

$$\iota = \gamma_\xi |l \nabla_0 \xi|^2 + \gamma_\eta l^2 |\nabla_0 \eta|^2 = l^2 \delta^{AB} (\gamma_\xi \partial_A \xi \partial_B \xi + \gamma_\eta \partial_A \eta \partial_B \eta). \quad (5.12)$$

Note $\iota(0, 0) = 0$. Therefore, for null ground-state energy density ψ and stress P_a^A ,

$$w(\delta_{AB}, \xi, \eta) = 0, \quad \frac{\partial w}{\partial \bar{C}_{AB}}(\delta_{AB}, \xi, \eta) = 0; \quad \lambda(0) = \nu(0) = 0. \quad (5.13)$$

Convexity and material symmetry are addressed in §5.4.2. Thermodynamic forces of (3.29) are, applying (3.40),

$$P_a^A = \frac{\partial \psi}{\partial F_A^a} = 2 \delta_{ab} F_B^b \frac{\partial \psi}{\partial \bar{C}_{AB}} = \mu_0 \delta_{ab} F_B^b \frac{\partial w}{\partial \bar{C}_{AB}}, \quad (5.14)$$

$$Q_1 = \frac{1}{l} \frac{\partial \psi}{\partial \xi} = \frac{\Upsilon_0}{l^2} \left(A_0 \frac{\partial w}{\partial \xi} + \gamma_\xi \frac{d\lambda}{d\xi} \right), \quad Q_2 = \frac{1}{l} \frac{\partial \psi}{\partial \eta} = \frac{\Upsilon_0}{l^2} \left(A_0 \frac{\partial w}{\partial \eta} + \gamma_\eta \frac{d\nu}{d\eta} \right); \quad A_0 = \frac{\mu_0 l}{2\Upsilon_0}, \quad (5.15)$$

$$Z_1^A = \frac{\partial \psi}{\partial D_{|A}^1} = \frac{\Upsilon_0}{l^2} \frac{\partial \iota}{\partial (\partial_A \xi)} = 2\Upsilon_0 \gamma_\xi \delta^{AB} \partial_B \xi, \quad Z_2^A = \frac{\partial \psi}{\partial D_{|A}^2} = \frac{\Upsilon_0}{l^2} \frac{\partial \iota}{\partial (\partial_A \eta)} = 2\Upsilon_0 \gamma_\eta \delta^{AB} \partial_B \eta. \quad (5.16)$$

The source term in (3.22) manifests from changes in energy proportional to changes of the local referential volume form (e.g., local volume changes from damage, treated analogously to an energy source from tissue growth (Appendix B)):

$$R_A = \beta \psi \bar{\partial}_A (\ln \sqrt{G}) = \frac{\beta}{l} \psi \chi_A, \quad (\beta = \text{constant}; A = 1, 2). \quad (5.17)$$

5.2.2 Linear momentum

Linear momentum balance (3.31) or (3.34) is, invoking relations in §5.1 and §5.2.1,

$$\begin{aligned}\mu_0 \delta_{ab} \left[\frac{\partial^2 \varphi^b}{\partial X^A \partial X^B} \frac{\partial w}{\partial \bar{C}_{AB}} + \frac{\partial \varphi^b}{\partial X^B} \left(\frac{\partial^2 w}{\partial \bar{C}_{AB} \partial X^A} + \frac{\partial^2 w}{\partial \bar{C}_{AB} \partial \xi} \frac{\partial \xi}{\partial X^A} + \frac{\partial^2 w}{\partial \bar{C}_{AB} \partial \eta} \frac{\partial \eta}{\partial X^A} \right) \right] \\ = -\mu_0 \delta_{ab} \frac{\partial \varphi^b}{\partial X^B} \frac{\partial w}{\partial \bar{C}_{AB}} \left[\frac{\partial}{\partial \xi} (\ln \sqrt{G}) \frac{\partial \xi}{\partial X^A} + \frac{\partial}{\partial \eta} (\ln \sqrt{G}) \frac{\partial \eta}{\partial X^A} \right].\end{aligned}\quad (5.18)$$

Remark 5.2.2. For nonzero μ_0 , (5.18) is two coupled nonlinear PDEs ($a = 1, 2$) in four field variables: $\varphi^1(X)$, $\varphi^2(X)$, $\xi(X)$, and $\eta(X)$.

5.2.3 Micro-momentum

State-space equilibrium (3.32) or (3.35) is, using relations of §5.1 and §5.2.1 and dividing by $2\Upsilon_0$, the two equations

$$\begin{aligned} & \gamma_\xi \delta^{AB} \frac{\partial^2 \xi}{\partial X^A \partial X^B} + \left(1 - \frac{\alpha - \beta}{2}\right) \gamma_\xi \delta^{AB} \frac{\partial}{\partial \xi} \left(\ln \sqrt{G}\right) \frac{\partial \xi}{\partial X^A} \frac{\partial \xi}{\partial X^B} - \frac{\gamma_\xi}{2l^2} \frac{d\lambda}{d\xi} \\ & + \gamma_\xi \delta^{AB} \frac{\partial}{\partial \eta} \left(\ln \sqrt{G}\right) \frac{\partial \xi}{\partial X^A} \frac{\partial \eta}{\partial X^B} - \left(\frac{\alpha - \beta}{2}\right) \gamma_\eta \delta^{AB} \frac{\partial}{\partial \xi} \left(\ln \sqrt{G}\right) \frac{\partial \eta}{\partial X^A} \frac{\partial \eta}{\partial X^B} \\ & - \left(\frac{\alpha - \beta}{2l^2}\right) \frac{\partial}{\partial \xi} \left(\ln \sqrt{G}\right) [\gamma_\xi \lambda + \gamma_\eta \nu] = \frac{A_0}{2l^2} \left[\frac{\partial w}{\partial \xi} + (\alpha - \beta) \frac{\partial}{\partial \xi} \left(\ln \sqrt{G}\right) w \right], \end{aligned} \quad (5.19)$$

$$\begin{aligned} & \gamma_\eta \delta^{AB} \frac{\partial^2 \eta}{\partial X^A \partial X^B} + \left(1 - \frac{\alpha - \beta}{2}\right) \gamma_\eta \delta^{AB} \frac{\partial}{\partial \eta} \left(\ln \sqrt{G}\right) \frac{\partial \eta}{\partial X^A} \frac{\partial \eta}{\partial X^B} - \frac{\gamma_\eta}{2l^2} \frac{d\nu}{d\eta} \\ & + \gamma_\eta \delta^{AB} \frac{\partial}{\partial \xi} \left(\ln \sqrt{G}\right) \frac{\partial \eta}{\partial X^A} \frac{\partial \xi}{\partial X^B} - \left(\frac{\alpha - \beta}{2}\right) \gamma_\xi \delta^{AB} \frac{\partial}{\partial \eta} \left(\ln \sqrt{G}\right) \frac{\partial \xi}{\partial X^A} \frac{\partial \xi}{\partial X^B} \\ & - \left(\frac{\alpha - \beta}{2l^2}\right) \frac{\partial}{\partial \eta} \left(\ln \sqrt{G}\right) [\gamma_\xi \lambda + \gamma_\eta \nu] = \frac{A_0}{2l^2} \left[\frac{\partial w}{\partial \eta} + (\alpha - \beta) \frac{\partial}{\partial \eta} \left(\ln \sqrt{G}\right) w \right]. \end{aligned} \quad (5.20)$$

Remark 5.2.3. For nonzero Υ_0 , (5.19) and (5.20) are two coupled nonlinear PDEs in four field variables: $\varphi^1(X)$, $\varphi^2(X)$, $\xi(X)$, and $\eta(X)$, where derivatives of $\varphi^1(X)$ and $\varphi^2(X)$ enter w on the right sides via $\bar{C}_{AB} = \partial_A \varphi^a \delta_{ab} \partial_B \varphi^b$. For the special case $\Upsilon_0 = 0$, the left sides of (5.19) and (5.20) vanish, whereas for $\mu_0 = 0$, the right sides vanish.

5.3 General solutions

5.3.1 Homogeneous fields

Examine cases for which $\xi(X) \rightarrow \xi_H = \text{constant}$ and $\eta(X) \rightarrow \eta_H = \text{constant}$ at all points $X \in \mathcal{M}$; the constants may differ: $\xi_H \neq \eta_H$ in general. Apply the notation $f_H(X) = f(X, \xi_H, \eta_H)$. Restrict $\mu_0 > 0$. Then (5.14) and (5.18) reduce to

$$\frac{\partial P_a^A}{\partial X^A} = \mu_0 \delta_{ab} \left[\frac{\partial^2 \varphi^b}{\partial X^A \partial X^B} \frac{\partial w}{\partial \bar{C}_{AB}} + \frac{\partial \varphi^b}{\partial X^B} \frac{\partial^2 w}{\partial \bar{C}_{AB} \partial X^A} \right] = 0 \Rightarrow (P_H)_a^A = \frac{\mu_0}{2} \left(\frac{\partial w}{\partial F_A^a} \right)_H = \text{constant}. \quad (5.21)$$

This should be satisfied for any homogeneous $F_A^a = (F_H)_A^a$ for which $\partial^2 \varphi^a / \partial X^A \partial X^B = 0$. Micro-momentum conservation laws (5.19) and (5.20) become

$$-\gamma_\xi \frac{d\lambda}{d\xi} - (\alpha - \beta) \frac{\partial}{\partial \xi} \left(\ln \sqrt{G}\right) [\gamma_\xi \lambda + \gamma_\eta \nu] = A_0 \left[\frac{\partial w}{\partial \xi} + (\alpha - \beta) \frac{\partial}{\partial \xi} \left(\ln \sqrt{G}\right) w \right], \quad (5.22)$$

$$-\gamma_\eta \frac{d\nu}{d\eta} - (\alpha - \beta) \frac{\partial}{\partial \eta} \left(\ln \sqrt{G}\right) [\gamma_\xi \lambda + \gamma_\eta \nu] = A_0 \left[\frac{\partial w}{\partial \eta} + (\alpha - \beta) \frac{\partial}{\partial \eta} \left(\ln \sqrt{G}\right) w \right], \quad (5.23)$$

wherein $\lambda = \lambda_H$, $\nu = \nu_H$, $(\frac{\partial}{\partial \xi} \ln \sqrt{G})_H$, and $(\frac{\partial}{\partial \eta} \ln \sqrt{G})_H$ are all algebraic functions of (ξ_H, η_H) , while $w = w_H$, $(\frac{\partial}{\partial \xi} w)_H$, and $(\frac{\partial}{\partial \eta} w)_H$ are algebraic functions of $(\xi_H, \eta_H, (F_H)_A^a)$.

Remark 5.3.1. Homogeneous equilibrium is satisfied by the six algebraic equations (5.21) ($a, A = 1, 2$), (5.22), and (5.23) in ten unknowns $(P_H)_a^A, (F_H)_A^a, \xi_H, \eta_H$. Given $(P_H)_a^A$ or $(F_H)_A^a$ as mechanical loading, the remaining six unknowns can be obtained from a simultaneous solution. If $(F_H)_A^a$ is imposed, (5.22) and (5.23) are two equations in ξ_H, η_H . Then (5.21) yields the remaining $(P_H)_a^A$.

Remark 5.3.2. Essential boundary conditions for homogeneous states are $\xi = \xi_H$ and $\eta = \eta_H$, both $\forall X \in \partial \mathcal{M}$. Since ξ and η are constants, $Z_A^B = 0$ by (5.16), so corresponding natural boundary conditions for forces conjugate to internal structure parameters in (3.33) are $z_A = Z_A^B N_B = 0$.

5.3.2 Stress-free states

Consider cases whereby $P_a^A = 0 \forall X \in \mathcal{M}$. Linear momentum conservation laws (3.31), (3.34), and (5.18) are trivially satisfied. Restrict $\mu_0 > 0$. Since F_A^a is non-singular, (5.14) requires $\partial w / \partial \bar{C}_{AB} = 0$. This is obeyed at $\bar{C}_{AB} = \delta_{AB}$ via (5.13); thus assume rigid body motion (i.e., $\varphi^a = Q_A^a X^A + c_0^a$, with Q_A^a constant and proper orthogonal and c_0^a constant) whereby $w = 0$ vanishes as well by (5.13).

Remark 5.3.3. General analytical solutions for stress-free states are not apparent without particular forms of functions $w(\bar{C}_{AB}, \xi, \eta)$, $G(\xi, \eta)$, $\lambda(\xi)$, $\nu(\eta)$, and values of $\gamma_\xi, \gamma_\eta, \alpha, \beta$, and l .

Remark 5.3.4. If $\partial w / \partial \xi = \partial w / \partial \eta = 0$ for $\bar{C}_{AB} = \delta_{AB}$, then right sides of (5.19) and (5.20) vanish. Whether or not stress-free deformation states with $\bar{C}_{AB} \neq \delta_{AB}$ (e.g., locally) exist depends on w .

5.4 Constitutive model

The framework is applied to a rectangular patch of skin loaded in the X^1 - X^2 plane. A 2-D theory (i.e., membrane theory) cannot distinguish between plane stress and plane strain conditions [115], nor can it account for out-of-plane anisotropy. Nonetheless, 2-D nonlinear elastic models are widely used to represent soft tissues, including skin [68, 89]. Thus, parameters entering the model (e.g., μ_0, γ_0) are particular to loading conditions and material orientations from experiments to which they are calibrated (e.g., here, plane stress).

Remark 5.4.1. In a purely 2-D theory, incompressibility often used for 3-D modeling of biological tissues [68, 71, 80, 82], cannot be assumed since contraction under biaxial stretch is not quantified in a 2-D theory. Incompressibility is also inappropriate if the material dilates due to damage.

The skin is treated as having orthotropic symmetry, with two constant orthogonal directions in the reference configuration denoted by unit vectors \mathbf{n}_1 and \mathbf{n}_2 :

$$\mathbf{n}_1 = n_1^A \frac{\delta}{\delta X^A}, \quad \mathbf{n}_2 = n_2^A \frac{\delta}{\delta X^A}; \quad n_i^A \delta_{AB} n_j^B = \delta_{ij} \quad (i, j = 1, 2). \quad (5.24)$$

Remark 5.4.2. The collagen fibers in the plane of the skin need not all align with \mathbf{n}_1 or \mathbf{n}_2 , so long as orthotropic symmetry is respected. For example, each \mathbf{n}_i can bisect the alignments of two equivalent primary families of fibers in the skin whose directions are not necessarily orthogonal [71, 92]. In such a case, \mathbf{n}_1 is still a unit vector orthogonal to \mathbf{n}_2 ; planar orthotropy is maintained with respect to reflections about both unit vectors \mathbf{n}_i .

Remark 5.4.3. The internal structure variables $\xi = D^1/l$ and $\eta = D^2/l$ account for mechanisms that lead to softening and degradation under tensile load: fiber sliding, pull-out, and breakage of collagen fibers, and rupture of the elastin fibers and ground matrix. Each D^A ($A = 1, 2$) is a representative microscopic sliding or separation distance in the $\mathbf{n}_i\delta_A^i$ direction, with l the distance at which the material can no longer support tensile load along that direction.

Remark 5.4.4. In the cohesive zone interpretation, each D^A is viewed as a crack opening displacement for separation on a material surface (line in 2-D) normal to $\mathbf{n}_i\delta_A^i$.

Finslerian metrics $G_{AB}(\xi, \eta) = \delta_A^a \delta_B^b g_{ab}(\xi, \eta)$ of §5.4.1 anisotropically rescale material and spatial manifolds \mathcal{M} and \mathfrak{m} due to microstructure changes in different directions. In the absence of damage, the nonlinear elastic potential of §5.4.2 specializes a 3-D model [71, 82, 83, 92] to 2-D.

5.4.1 Metrics

From (2.16), (2.48), (5.2), (5.3), and (5.7), the difference in squared lengths of line elements $d\mathbf{x}$ and $d\mathbf{X}$ is

$$(|d\mathbf{x}|^2 - |d\mathbf{X}|^2)(\mathbf{F}, \xi, \eta) = [\delta_a^E \delta_b^F G_{EF}(\xi, \eta) F_A^a F_B^b - G_{AB}(\xi, \eta)] dX^A dX^B. \quad (5.25)$$

Remark 5.4.5. Local regions of \mathcal{M} at X and \mathfrak{m} at $x = \varphi(X)$ are rescaled isometrically by components $G_{AB}(\xi(X), \eta(X))$. When $F_A^a = \delta_A^a$, $|d\mathbf{x}| = |d\mathbf{X}|$ regardless of G_{AB} , ξ , or η . For degenerate Riemannian metrics $G_{AB} = \bar{G}_{AB} = \delta_{AB}$ and $g_{ab} = \bar{g}_{ab} = \delta_{ab}$, (5.25) becomes independent of (ξ, η) .

The Cartesian coordinate chart $\{X^A\}$ is prescribed such that $n_i^A = \delta_i^A$ in (5.24); thus \mathbf{n}_1 and \mathbf{n}_2 are parallel to respective X^1 - and X^2 -directions on \mathcal{M} . Rescaling arises from changes in structure associated with degradation and damage in orthogonal directions, to which remnant strain contributions $\frac{1}{2} \ln[G_{11}(\xi)]$ and $\frac{1}{2} \ln[G_{22}(\eta)]$ can be linked. The metric tensor G_{AB} is hereafter assigned specific exponential terms, generalizing the 1-D form of §4.4.1 to an anisotropic 2-D form appropriate for orthotropic symmetry:

$$[G_{AB}(\xi, \eta)] = \begin{bmatrix} \exp\left(\frac{2k}{r}\xi^r\right) & 0 \\ 0 & \exp\left(\frac{2m}{r}\eta^r\right) \end{bmatrix} \Rightarrow G(\xi, \eta) = \det[G_{AB}(\xi, \eta)] = \exp\left(\frac{2}{r}[k\xi^r + m\eta^r]\right). \quad (5.26)$$

For $\xi \in [0, 1]$ and $\eta \in [0, 1]$, two constants in (5.26) are k and m , positive for expansion. A third constant $r > 0$ modulates rates of change of $G_{11}(\xi)$ and $G_{22}(\eta)$ with respect to their arguments. Ratios are determined by remnant strain contributions at failure: $\hat{\epsilon}_\xi = \frac{k}{r}$ and $\hat{\epsilon}_\eta = \frac{m}{r}$. Values of k , m , and r are calibrated to data in §5.5.1. Isotropy arises in (5.26) when $\eta = \xi$ and $m = k$.

Remark 5.4.6. More general forms of $G_{AB}(\xi, \eta)$, likely with more parameters, are possible; (5.26) is a simple form sufficient to address experimental observations for extension and tearing of skin.

From (5.26), non-vanishing components of Cartan's tensor in (2.25) and (5.6) are

$$lC_{11}^1 = \chi_1 = \frac{\partial}{\partial \xi}(\ln \sqrt{G}) = k\xi^{r-1}, \quad lC_{22}^2 = \chi_2 = \frac{\partial}{\partial \eta}(\ln \sqrt{G}) = m\eta^{r-1}. \quad (5.27)$$

5.4.2 Nonlinear elasticity

The nonlinear elasticity model generalizes that of §4.4.2 to a 2-D base space \mathcal{M} with anisotropic Finsler metric depending on two structure variable components, ξ and η in normalized dimensionless form. For the 2-D case, material symmetry of §3.3.4 requires careful consideration. Here, the skin is treated as a planar orthotropic solid [68, 75, 89].

Viewing the D^A as components of a material vector field, orthotropic symmetry suggests invariants ξ^2 and η^2 . For physically admissible ranges $\xi \in [0, 1]$ and $\eta \in [0, 1]$, these can be replaced with ξ and η . Viewing the $D_{|B}^A$ similarly, orthotropic symmetry permits a more general functional dependence than the sum of quadratic forms in ι of (5.11) and (5.12). However, the chosen form of ι in (5.12) allows for partial anisotropy, not inconsistent with orthotropy, when γ_ξ and γ_η differ. Thus, the structure-dependent contribution to ψ , $\Lambda l = \Upsilon_0(\gamma_\xi \lambda + \gamma_\eta \nu + \iota)$, more specifically here

$$\lambda(\xi) = \xi^2, \quad \nu(\eta) = \eta^2; \quad \iota(\nabla_0 \xi, \nabla_0 \eta) = l^2 \delta^{AB} (\gamma_\xi \partial_A \xi \partial_B \xi + \gamma_\eta \partial_A \eta \partial_B \eta), \quad (5.28)$$

is consistent with material symmetry requirements. Strain energy density W in (5.11) is dictated by dimensionless function $w(\bar{C}_{AB}, \xi, \eta)$. Per the above discussion, ξ and η are treated as scalar invariant arguments. A partial list of remaining invariants [82, 91] of (3.43) for orthotropic symmetry of a 2-D material entering w (and thus $\psi = \bar{\psi}$) is then, applying $n_i^A = \delta_i^A$ in (5.24),

$$\bar{I}_1 = \text{tr} \bar{C} = \delta^{AB} \bar{C}_{AB}, \quad \bar{I}_2 = J^2 = \det \bar{C}, \quad \bar{I}_3 = \bar{C}_{AB} n_1^A n_1^B = \bar{C}_{11}, \quad \bar{I}_4 = \bar{C}_{AB} n_2^A n_2^B = \bar{C}_{22}. \quad (5.29)$$

Remark 5.4.7. As \mathbf{n}_1 and \mathbf{n}_2 are orthonormal, $\bar{I}_1 = \bar{I}_3 + \bar{I}_4$, so one of $\bar{I}_1, \bar{I}_3, \bar{I}_4$ in (5.29) is redundant. Since $J \geq 1$, dependence on $\bar{I}_2 = \bar{C}_{11} \bar{C}_{22} - (\bar{C}_{12})^2$ can be replaced by J (or by $(\bar{C}_{12})^2$ given \bar{I}_3, \bar{I}_4).

The Euclidean metric $\bar{G}^{AB} = \delta^{AB}$, rather than Finsler metric G^{AB} , is used for scalar products in (5.28) and (5.29), consistent with (5.9). In 2-space, \bar{I}_1 and \bar{I}_2 are the complete set of isotropic invariants of \bar{C} . Two orthotropic invariants are \bar{I}_3 and \bar{I}_4 ; several higher-order invariants are admissible [82, 91] but excluded here since (5.29) is sufficient for the present application. The dimensionless strain energy function entering (5.11) is prescribed specifically as

$$\begin{aligned} w(\bar{C}_{AB}, \xi, \eta) = & \left[\frac{1}{J} (\bar{C}_{11} + \bar{C}_{22}) + k_0 (J - 1)^2 - 2 \right] y_\mu(\xi, \eta) \\ & + \left[\frac{a_1}{2b_1} (\exp\{b_1 (\bar{C}_{11} - 1)^2\} - 1) \right] \text{H}(\bar{C}_{11} - 1) y_\xi(\xi) \\ & + \left[\frac{a_2}{2b_2} (\exp\{b_2 (\bar{C}_{22} - 1)^2\} - 1) \right] \text{H}(\bar{C}_{22} - 1) y_\eta(\eta). \end{aligned} \quad (5.30)$$

Dimensionless constants are $k_0 > 0$, $a_1 \geq 0$, $b_1 > 0$, $a_2 \geq 0$, and $b_2 > 0$. Right-continuous Heaviside functions $H(f) = 1 \forall f \geq 0$, $H(f) = 0 \forall f < 0$. Also, $\mu_0 > 0$ and $\Upsilon_0 > 0$ are enforced in (5.11).

Remark 5.4.8. Potential w in (5.30) extends prior models for collagenous tissues [71, 82, 83, 92] to include anisotropic structure changes. The first term on the right, linear in \bar{I}_1/J and independent of volume change, accounts for isotropic shearing resistance of ground matrix and elastin. The second term on the right accounts for resistance to volume (area) change, k_0 being a dimensionless bulk (area) modulus finite for a 2-D model; the dimensional bulk modulus $\kappa_0 = k_0\mu_0$. Exponential terms account for stiffening from collagen fibers in orthogonal directions \mathbf{n}_i . Heaviside functions prevent fibers from supporting compressive load [82, 116] since they would likely buckle.

Degradation functions are $y_\mu(\xi, \eta)$, $y_\xi(\xi)$, and $y_\eta(\eta)$, where for the anisotropic theory,

$$y_\mu = (1 - \xi)^\vartheta (1 - \eta)^\varsigma = y_\xi y_\eta, \quad y_\xi = (1 - \xi)^\vartheta, \quad y_\eta = (1 - \eta)^\varsigma. \quad (5.31)$$

Corresponding material constants are $\vartheta \in [0, \infty)$ and $\varsigma \in [0, \infty)$. Notice that matrix strain energy degrades equivalently with increasing ξ and η via y_μ , maintaining isotropy of the first term in (5.30). As collagen fibers debond, the ground matrix and elastin simultaneously weaken.

Remark 5.4.9. Choices $\vartheta = \varsigma = 2$ are typical for phase-field fracture [98], though other values are possible for soft biologic tissues [95]. Setting $\vartheta = \varsigma = 0$ implies null degradation (i.e., ideal elastic stress-stretch response).

Remark 5.4.10. When $\xi = \eta = 0$, w of (5.30) is polyconvex [81, 90], facilitating existence and uniqueness of solutions. Also, ψ with (5.28), (5.30), and (5.31) obeys (5.13).

Stress components P_a^A conjugate to $F_A^a = \partial_A \varphi^a$ are found from (3.44), (5.14), (5.30), and (5.31), while forces $Q_{1,2}$ conjugate to ξ, η are found from (5.15), (5.28), (5.30), and (5.31):

$$\begin{aligned} P_a^A / \mu_0 &= J^{-1} [\delta_{ab} \delta^{AB} F_B^b - \frac{1}{2} \bar{C}_{BC} \delta^{BC} (F^{-1})_a^A + k_0 J^2 (J - 1) (F^{-1})_a^A] (1 - \xi)^\vartheta (1 - \eta)^\varsigma \\ &\quad + [a_1 (\bar{C}_{11} - 1) \exp\{b_1 (\bar{C}_{11} - 1)^2\} \delta_{ab} \delta_1^A F_1^b] (1 - \xi)^\vartheta H(\bar{C}_{11} - 1) \\ &\quad + [a_2 (\bar{C}_{22} - 1) \exp\{b_2 (\bar{C}_{22} - 1)^2\} \delta_{ab} \delta_2^A F_2^b] (1 - \eta)^\varsigma H(\bar{C}_{22} - 1), \end{aligned} \quad (5.32)$$

$$\begin{aligned} Q_1 l^2 / (2\Upsilon_0) &= \gamma_\xi \xi - A_0 \vartheta \left[(1 - \xi)^{\vartheta-1} (1 - \eta)^\varsigma \{J^{-1} (\bar{C}_{11} + \bar{C}_{22}) + k_0 (J - 1)^2 - 2\} \right] \\ &\quad - A_0 \vartheta (1 - \xi)^{\vartheta-1} \left[\frac{1}{2} (a_1 / b_1) (\exp\{b_1 (\bar{C}_{11} - 1)^2\} - 1) \right] H(\bar{C}_{11} - 1), \end{aligned} \quad (5.33)$$

$$\begin{aligned} Q_2 l^2 / (2\Upsilon_0) &= \gamma_\eta \eta - A_0 \varsigma \left[(1 - \eta)^{\varsigma-1} (1 - \xi)^\vartheta \{J^{-1} (\bar{C}_{11} + \bar{C}_{22}) + k_0 (J - 1)^2 - 2\} \right] \\ &\quad - A_0 \varsigma (1 - \eta)^{\varsigma-1} \left[\frac{1}{2} (a_2 / b_2) (\exp\{b_2 (\bar{C}_{22} - 1)^2\} - 1) \right] H(\bar{C}_{22} - 1). \end{aligned} \quad (5.34)$$

Remark 5.4.11. An ideal elastic response is obtained when $k = m = 0 \Rightarrow G_{AB} = \delta_{AB} \Rightarrow \chi_A = 0$, and $\vartheta = \varsigma = 0 \Rightarrow \frac{\partial w}{\partial \xi} = \frac{\partial w}{\partial \eta} = 0$. Then since $\frac{d\lambda}{d\xi}(0) = 0$ and $\frac{d\nu}{d\eta}(0) = 0$ by (5.28), the right side of (5.18) vanishes identically, and the (trivial) solutions to (5.19) and (5.20) are $\xi(X) = \eta(X) = 0 \forall X \in \mathcal{M}$.

Remark 5.4.12. An isotropic version of the theory can be obtained, if along with $m = k$ in (5.26), the following choices are made instead of (5.31):

$$y_\mu = \frac{1}{2}[(1 - \xi)^\vartheta + (1 - \eta)^\vartheta], \quad \varsigma = \vartheta, \quad y_\xi = y_\eta = 0; \quad \gamma_\xi = \gamma_\eta = \frac{1}{2}\gamma_\mu \geq 0. \quad (5.35)$$

Collagen fiber contributions to strain energy are removed such that w now only depends on isotropic invariants of $\bar{\mathbf{C}}$. Equilibrium equations (5.18), (5.19), and (5.20) are identical under the change of variables $\xi \leftrightarrow \eta$, implying $\eta(X) = \xi(X)$ if identical boundary conditions on D^A or z_A are applied for each field on $\partial\mathcal{M}$. In this case, one of (5.19), and (5.20) is redundant and replaced with $\eta = \xi$.

5.5 Specific solutions

Possible inputs to the 2-D model are seventeen constants $l > 0, k, m, r > 0, \mu_0 > 0, k_0 > 0, a_1 \geq 0, b_1 > 0, a_2 \geq 0, b_2 > 0, \vartheta \geq 0, \varsigma \geq 0, \Upsilon_0 > 0, \gamma_\xi, \gamma_\eta, \alpha$, and β . Values of l and Υ_0 are taken from the analysis in §4.5.2 of complete tearing of a 1-D specimen of skin to a stress-free state. This is appropriate given that 1-D and 2-D theories are applied to describe surface energy and material length scale pertinent to the same experiments [73, 74, 99, 113], and since stress-free solutions in §5.5.3 perfectly parallel those of §4.5.2. The remaining parameters are evaluated, in §5.5.1, by applying the constitutive model of §5.4 to the general solutions for homogeneous fields derived in §5.3.1 to uniaxial-stress extension of 2-D skin specimens along the material X^1 - and X^2 -directions, respectively aligned perpendicular and parallel to Langer's lines.

Remark 5.5.1. Collagen fibers of the microstructure in the dermis are aligned predominantly along Langer's lines and are more often pre-stretched in vivo along these directions [75]. In vivo or in vitro, elastic stiffness at finite stretch tends to be larger in directions along Langer's lines (i.e., parallel to X^2 and \mathbf{n}_2) than in orthogonal directions (e.g., parallel to \mathbf{n}_1). Degradation and failure behaviors are also anisotropic: rupture stress tends to be larger, and failure elongation lower, for stretching in the stiffer \mathbf{n}_2 -direction [74, 75, 87].

In §5.5.2, model outcomes are reported for planar biaxial extension [68, 70, 115] of 2-D specimens, highlighting simultaneous microstructure degradation perpendicular and parallel to Langer's lines. Lastly, in §5.5.3, stress-free states analogous to those modeled in a 1-D context in §4.5.2 are evaluated for the 2-D theory.

In §5.5.1 and §5.5.2, equilibrium solutions of §5.3.1 hold. Invoking (5.27), (5.28), (5.30), (5.31), and (5.32), and dropping $(\cdot)_H$ notation for brevity, (5.21), (5.22), and (5.23) comprise the algebraic system

$$\begin{aligned} P_a^A &= \mu_0 J^{-1} [\delta_{ab} \delta^{AB} F_B^b - \frac{1}{2} \bar{C}_{BC} \delta^{BC} (F^{-1})_a^A + k_0 J^2 (J - 1) (F^{-1})_a^A] (1 - \xi)^\vartheta (1 - \eta)^\varsigma \\ &\quad + [a_1 (\bar{C}_{11} - 1) \exp\{b_1 (\bar{C}_{11} - 1)^2\} \delta_{ab} \delta_1^A F_1^b] (1 - \xi)^\vartheta H(\bar{C}_{11} - 1) \\ &\quad + [a_2 (\bar{C}_{22} - 1) \exp\{b_2 (\bar{C}_{22} - 1)^2\} \delta_{ab} \delta_2^A F_2^b] (1 - \eta)^\varsigma H(\bar{C}_{22} - 1) \\ &= \text{constant}, \end{aligned} \quad (5.36)$$

$$\gamma_\xi \xi + k \xi^{r-1} [\gamma_\xi \xi^2 + \gamma_\eta \eta^2] = -\frac{A_0}{2} \left[\frac{\partial w(\bar{C}_{AB}, \xi, \eta)}{\partial \xi} + 2k \xi^{r-1} w(\bar{C}_{AB}, \xi, \eta) \right], \quad (5.37)$$

$$\gamma_\eta \eta + m\eta^{r-1}[\gamma_\xi \xi^2 + \gamma_\eta \eta^2] = -\frac{A_0}{2} \left[\frac{\partial w(\bar{C}_{AB}, \xi, \eta)}{\partial \eta} + 2m\eta^{r-1} w(\bar{C}_{AB}, \xi, \eta) \right]. \quad (5.38)$$

Consistent with (4.24) for $N_0 = 0$ [55, 56, 62], $\beta = \alpha - 2$ is assumed in (5.37) and (5.38), reducing the number of requisite parameters to fifteen; α and β enter the governing equations only through their difference. Boundary conditions on internal state, are, for homogeneous conditions,

$$\xi(X^1 = \pm L_0, X^2 = \pm W_0) = \xi_H, \quad \eta(X^1 = \pm L_0, X^2 = \pm W_0) = \eta_H. \quad (5.39)$$

Alternative conditions to (5.36)–(5.39) are considered for heterogeneous stress-free states in §5.5.3.

5.5.1 Uniaxial extension

First consider homogeneous uniaxial-stress extension in either the X^1 - or X^2 -direction. From symmetry of the loading mode and material model, shear stresses vanish identically: $P_2^1 = 0$, $P_1^2 = 0$. Similarly, $F_2^1 = 0$, $F_1^2 = 0$, and $\bar{C}_{12} = \bar{C}_{21} = 0$. The homogeneous deformation fields are

$$\varphi^1 = \lambda_1 X^1, \quad \varphi^2 = \lambda_2 X^2; \quad F_1^1 = \lambda_1, \quad F_2^2 = \lambda_2; \quad \bar{C}_{11} = (\lambda_1)^2, \quad \bar{C}_{22} = (\lambda_2)^2; \quad J = \lambda_1 \lambda_2. \quad (5.40)$$

At any single given load increment, stretch ratios are the constants $\lambda_1 > 0$ and $\lambda_2 > 0$.

Mechanical boundary conditions are, for extension along X^1 with $\lambda_1 \geq 1$,

$$\varphi^1(X^1 = \pm L_0) = \pm \lambda_1 L_0, \quad p_2(X^2 = \pm W_0) = P_2^2(X^2 = \pm W_0) = 0. \quad (5.41)$$

In this case, $P_2^2 = 0 \forall X \in \mathcal{M}$, and the sole non-vanishing stress component in (5.36) is P_1^1 . Note that λ_2 is unknown a priori. Given λ_1 from the first of (5.41), values consistent with (5.39) are obtained by solving (5.36) for $a = A = 2$ with $P_2^2 = 0$, (5.37), and (5.38) simultaneously for λ_2 , ξ , and η as functions of λ_1 . Axial stress P_1^1 is then found afterwards using (5.36) with $a = A = 1$.

For axial loading along X^2 with $\lambda_2 \geq 1$,

$$\varphi^2(X^2 = \pm W_0) = \pm \lambda_2 W_0, \quad p_1(X^1 = \pm L_0) = P_1^1(X^1 = \pm L_0) = 0. \quad (5.42)$$

Now $P_1^1 = 0 \forall X \in \mathcal{M}$, and the sole non-vanishing stress component in (5.36) is P_2^2 . Given λ_2 from the first of (5.42), values consistent with (5.39) are obtained by solving (5.36) for $a = A = 1$ with $P_1^1 = 0$, (5.37), and (5.38) simultaneously for λ_1 , ξ , and η as functions of λ_2 . Axial stress P_2^2 is found afterwards using (5.36) with $a = A = 2$.

Values of all baseline parameters are listed in Table 1. Identical values of those constants shared among 1-D and 2-D theories are found to aptly describe the experimental data for stretching along \mathbf{n}_1 , in conjunction with natural choice $\gamma_\xi = 1$. The 2-D theory features additional parameters to account for orthotropic anisotropy (e.g., stiffer response along \mathbf{n}_2 , with peak stress occurring at lower stretch) as well as an areal bulk modulus κ_0 absent in the 1-D theory.

Remark 5.5.2. Adherence to physical observations dictates $a_2 > a_1$, $b_2 > b_1$, and $\kappa_0 > \mu_0$. Since degradation is more severe, and toughness lower for stretching along \mathbf{n}_2 , $m > k$ and $\gamma_\eta < \gamma_\xi$. The standard choice [95, 98] $\zeta = \vartheta = 2$ in (5.31) was found sufficient to describe test data.

Model outcomes for non-vanishing stress components and internal state vector components are presented in respective Fig. 4(a) and Fig. 4(b). Experimental P_1^1 versus λ_1 data for loading along \mathbf{n}_1 , with $\lambda_1 \geq 0$ prescribed in the corresponding model calculations, are identical to P versus \sqrt{C} data depicted using the 1-D theory in §4.5.1. These data [74] are for relatively high-rate extension of rabbit skin along a longitudinal direction, parallel to the backbone of the torso and perpendicular to Langer's lines. Nonlinear elastic parameters should be viewed as instantaneous dynamic moduli in a pseudo elastic representation [68, 84, 85], since loading times are brief relative to stress relaxation times [74]. Single-experiment data of similar fidelity for transverse extension, parallel to Langer's lines, to complete load drop were not reported, but a range of maximum stress and strain were given for extension along \mathbf{n}_2 [74]. A representative peak stress P_2^2 and corresponding stretch λ_2 based on such data [74] are included in Fig. 4(a). According to such data [74], the material is stiffer, and ruptures at a higher stress ($\approx \frac{4}{3} \times$) but lower strain ($\approx \frac{2}{3} \times$), in the transverse \mathbf{n}_2 -direction.

Remark 5.5.3. For loading along \mathbf{n}_1 , $\xi \rightarrow 1$ and $\eta \rightarrow 0$ for $\lambda_1 \gtrsim 3.5$, meaning most internal structure evolution correlates with degradation in this direction, with small transverse effects of η . Analogously, loading along \mathbf{n}_2 gives $\eta \rightarrow 1$ and $\xi \rightarrow 0$ for $\lambda_2 \gtrsim 3$. The rate of increase of η with $\lambda_2 > 1$ is more rapid than the rate of increase of ξ with $\lambda_1 > 1$, since the skin degrades sooner and fails at a lower strain for stretching parallel to Langer's lines. The present diffuse model is an idealization characteristic of experiments when there is no sharp pre-crack [64, 68, 72, 74, 87].

Shown in Fig. 4(c) and Fig. 4(d) are predictions at modest stretch along \mathbf{n}_1 or \mathbf{n}_2 under uniaxial stress conditions identical to those of Fig. 4(a) as well as uniaxial strain, whereby $\lambda_2 = 1$ or $\lambda_1 = 1$ is enforced using the scheme of §5.5.2 rather than respective $P_2^2 = 0$ or $P_1^1 = 0$. Predictions for the ideal elastic case ($\vartheta = \zeta = 0 \Rightarrow \xi = \eta = 0$) are shown for comparison. Results are stiffer for the ideal elastic case since degradation commensurate with structure change is omitted. In agreement with other data [70], skin is elastically stiffer in uniaxial strain relative to uniaxial stress. Choosing a higher value of $k_0 = \kappa_0/\mu_0 > 1$ in (5.30) would further increase this difference if merited

5.5.2 Biaxial extension

Now consider homogeneous biaxial-stress extension in the X^1 - and X^2 -directions. From symmetry, $P_2^1 = 0$, $P_1^2 = 0$, $F_2^1 = 0$, $F_1^2 = 0$, and $\bar{C}_{12} = \bar{C}_{21} = 0$. The homogeneous deformation fields are

$$\varphi^1 = \lambda_1 X^1, \quad \varphi^2 = \lambda_2 X^2; \quad F_1^1 = \lambda_1, \quad F_2^2 = \lambda_2; \quad \bar{C}_{11} = (\lambda_1)^2, \quad \bar{C}_{22} = (\lambda_2)^2; \quad J = \lambda_1 \lambda_2. \quad (5.43)$$

Stretch ratios are $\lambda_1 > 0$ and $\lambda_2 > 0$, constants over \mathcal{M} . Mechanical boundary conditions are

$$\varphi^1(X^1 = \pm L_0) = \pm \lambda_1 L_0, \quad \varphi^2(X^2 = \pm W_0) = \pm \lambda_2 W_0. \quad (5.44)$$

With λ_1 and λ_2 prescribed by (5.44), equilibrium equations (5.37) and (5.38) are solved simultaneously for ξ and η as functions of λ_1, λ_2 , giving homogeneous values of fields consistent with (5.39). Then P_1^1 and P_2^2 are obtained afterwards with (5.36) for $a = A = 1$ and $a = A = 2$.

Model predictions for equi-biaxial stretching, $\lambda_1 = \lambda_2$, are produced using the baseline material parameters of Table 1, obtained for the 2-D theory in §5.5.1. In Fig. 5(a), stresses also include those

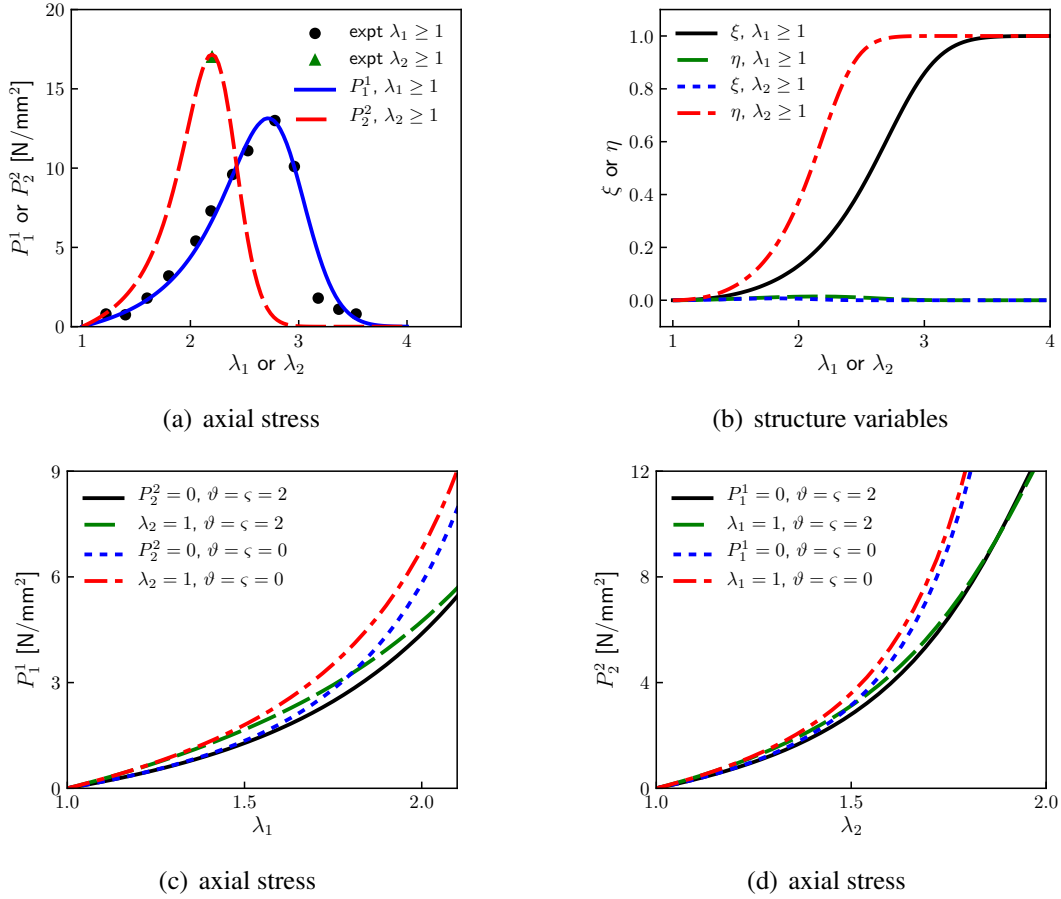


Figure 4 Uniaxial extension and tearing of skin for imposed axial stretch $\lambda_1 \geq 1$ or $\lambda_2 \geq 1$, 2-D model: (a) stress P_1^1 or P_2^2 (baseline parameters, Table 1) with representative experimental data [74] (see text §4.5.1 for consistent definition of experimental stretch accounting for pre-stress) for straining perpendicular or parallel to Langer's lines (b) normalized internal structure components ξ and η (baseline parameters) (c) stress P_1^1 for moderate extension $\lambda_1 \leq 2.1$ under uniaxial stress ($P_2^2 = 0$) or uniaxial strain ($\lambda_2 = 1$) conditions for Finsler model (baseline parameters) and ideal elastic model ($\vartheta = \zeta = 0$) (d) stress P_2^2 for moderate extension $\lambda_2 \leq 2.0$ under uniaxial stress ($P_1^1 = 0$) or uniaxial strain ($\lambda_1 = 1$) conditions for Finsler model (baseline) and ideal elastic model ($\vartheta = \zeta = 0$)

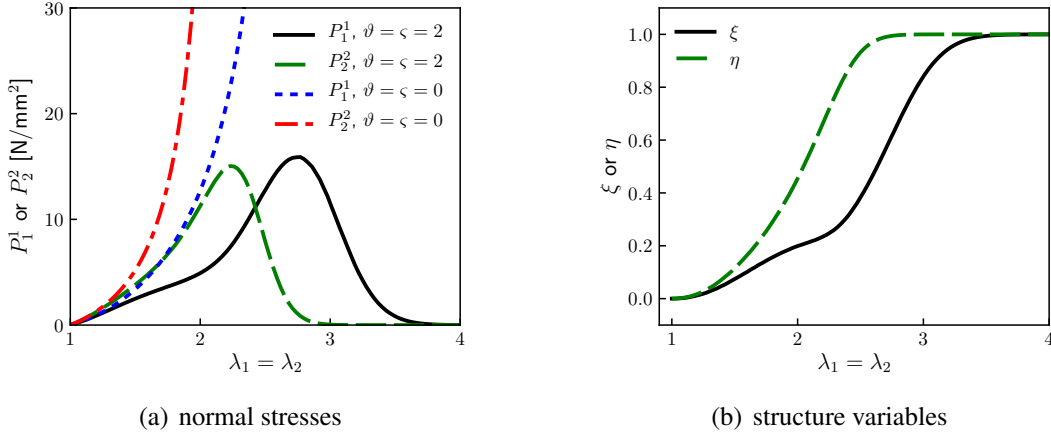


Figure 5 Equi-biaxial extension and tearing of skin, 2-D model: (a) stress components from Finsler model (baseline parameters, $\vartheta = \varsigma = 2$) and ideal elastic model ($\vartheta = \varsigma = 0$) (b) normalized internal structure components ξ and η

for the ideal elastic case ($\vartheta = \varsigma = 0 \Rightarrow \xi = \eta = 0$) that are noticeably higher for $\lambda_1 > 1.5$ and increase monotonically with stretch. For the Finsler theory, under this loading protocol ($\lambda_1 = \lambda_2$), P_2^2 increases more rapidly than P_1^1 with increasing λ_1 , reaching a slightly lower peak value at significantly lower stretch. Elastic stiffness during the lower-stretch loading phase is higher in the n_2 -direction due to the preponderance of aligned collagen fibers, but degradation associated with internal structure evolution is more rapid due to the lower toughness of skin when torn in this direction. The latter phenomenon is evident in Fig. 5(b), wherein $\eta(\lambda_1) > \xi(\lambda_1)$ for $\lambda_1 \in [1.1, 3.9]$.

Remark 5.5.4. Experimental data on failure of skin focus on uniaxial extension [74, 75]. Known biaxial data (e.g, [68, 70]) do not report stretch magnitudes sufficient to cause tearing, so direct validation does not appear possible. Should skin prove to be more stiff and damage tolerant in equi-biaxial stretch experiments, w of (5.30) can be modified so the tangent bulk modulus proportional to k_0 increases more strongly with J and does not degrade so severely with structure evolution.

5.5.3 Stress-free states

Protocols of §5.3.2 now apply. Two boundary value problems are addressed that parallel the 1-D analysis of §4.5.2. External boundary conditions are $\xi = 0$ and $\eta = 0$ everywhere along $\partial\mathcal{M}$. Stress $P_a^A = 0$ everywhere in \mathcal{M} , so mechanical traction $p_a = P_a^A N_A = 0$ over $\partial\mathcal{M}$. For the generalized Finsler metric in (5.26), restrict $r > 1 \Rightarrow \chi_1(\xi = 0) = \chi_2(\eta = 0) = 0$ in (5.27).

In the first problem, assume the specimen is stretched uniaxially along the n_1 -direction (i.e., along X^1 , perpendicular to Langer's lines) until localized failure occurs. The skin ruptures completely across the midspan at $X^1 = 0$, such that $\xi(0, X^2) = 1$. In this ruptured state, $\bar{C}_{AB} = \delta_{AB}$ everywhere on \mathcal{M} for all components except \bar{C}_{11} , which can differ from δ_{AB} only along the line $X^1 = 0$. The solution for $\eta(X^1, X^2)$ is $\eta(X^1, X^2) = 0$, for which (5.20) is trivially satisfied. From symmetry, the remaining unknown field ξ depends only on $X = X^1$, and $\xi(-X) = \xi(X)$. With this partial solution, the remaining governing equation (5.19) has vanishing right side and reduces to

the generally nonlinear but autonomous second-order ODE

$$\gamma_\xi \frac{d^2 \xi}{dX^2} = \frac{\gamma_\xi \xi}{l^2} (1 + k\xi^r). \quad (5.45)$$

Dividing by $\gamma_\xi > 0$, (5.45) is identical to (4.31) with $N_0 = 0$, $\lambda = \xi^2$, and $\chi = \chi_1 = k\xi^{r-1}$. Solutions (4.33) and (4.44) hold verbatim. Normalized energy per unit area normal to the X^1 -direction is

$$\bar{\gamma}_1 = \frac{1}{2Y_0} \int_{-L_0}^{L_0} \psi \sqrt{G} dX = \frac{\gamma_\xi}{2l} \int_{-L_0}^{L_0} \{\xi^2 + l^2 (d\xi/dX)^2\} \exp[(k/r)\xi^r] dX, \quad (5.46)$$

identical to (4.45) when $\gamma_\xi = 1$ and $N_0 = 0$. Given $\gamma_\xi = 1$, $k = 0.2$, $r = 2$, and $Y_0 = 0.47 \text{ kJ/m}^2$ (Table 1), outcomes of the 2-D theory here match those of the 1-D theory in Fig. 3(a) and Fig. 3(b) with $N_0 = 0$ and $\bar{\gamma}_1 = \bar{\gamma}$. Toughness $2\bar{\gamma}_1 Y_0 = 1.0 \text{ kJ/m}^2$ is consistent with experiment [73, 99, 113].

In the second problem, assume the specimen is stretched along \mathbf{n}_2 (i.e., along X^2 , parallel to Langer's lines). The skin ruptures completely across the midspan at $X^2 = 0$, with $\eta(X^1, 0) = 1$. Now, $\bar{C}_{AB} = \delta_{AB}$ everywhere for all components except \bar{C}_{22} , which can differ from δ_{AB} only along $X^2 = 0$. The solution for $\xi(X^1, X^2)$ is $\xi = 0$, for which (5.19) is trivially obeyed. From symmetry, η depends only on $X = X^2$, and $\eta(-X) = \eta(X)$. Balance law (5.20) reduces to

$$\gamma_\eta \frac{d^2 \eta}{dX^2} = \frac{\gamma_\eta \eta}{l^2} (1 + m\eta^r). \quad (5.47)$$

Dividing by $\gamma_\eta > 0$, (5.47) matches (4.31) with $N_0 = 0$, $\nu = \eta^2$, $\chi = \chi_2 = m\eta^{r-1}$, and the obvious change of variables. Solutions (4.33) and (4.44) hold. Normalized energy per unit area is

$$\bar{\gamma}_2 = \frac{1}{2Y_0} \int_{-L_0}^{L_0} \psi \sqrt{G} dX = \frac{\gamma_\eta}{2l} \int_{-L_0}^{L_0} \{\eta^2 + l^2 (d\eta/dX)^2\} \exp[(m/r)\eta^r] dX \quad (5.48)$$

for free surfaces normal to the X^2 -direction, matching (4.45) if $\gamma_\eta = 1$ and $N_0 = 0$. Given $\gamma_\eta = 0.84$, $m = 0.3$, $r = 2$, and $Y_0 = 0.47 \text{ kJ/m}^2$ (Table 1), profiles of $\eta(X)$ for this problem are very similar to those of $\xi(X)$ from the 1-D theory in Fig. 3(a). Energy for $N_0 = 0$ in Fig. 3(b) transforms as $\bar{\gamma}_2 \approx \gamma_\eta \bar{\gamma}$, and $2\bar{\gamma}_2 Y_0 = 0.85 \text{ kJ/m}^2$ is within experimental ranges of 0.5 to 2.5 kJ/m^2 [73, 99, 113].

Remark 5.5.5. Since $2\bar{\gamma}_2 Y_0 < 2\bar{\gamma}_1 Y_0$, the model predicts that skin is more brittle in directions parallel to Langer's lines than perpendicular to Langer's lines, in concurrence with experiment [74, 87]. Collagen fibers are less coiled initially in directions parallel to Langer's lines [75], giving the skin lower compliance and less potential strain accommodation at rupture in those directions.

Remark 5.5.6. All parameters in Table 1 have clear physical or geometric origins; none are ad hoc. Constant l is the critical fiber sliding distance or crack opening displacement for rupture. Ratios $\frac{k}{r}$ and $\frac{m}{r}$ are associated with remnant strain contributions in orthogonal \mathbf{n}_1 - and \mathbf{n}_2 -directions along primary initial fiber directions (e.g., perpendicular and parallel to Langer's lines). The isotropic shear modulus and bulk modulus for the matrix, consisting of ground substance and elastin, are μ_0 and κ_0 . Nonlinear elastic constants a_1 and b_1 control stiffening due to collagen fiber elongation in the \mathbf{n}_1 -direction, while a_2 and b_2 control stiffening due to fiber elongation in the \mathbf{n}_2 -direction. Loss of elastic stiffness due to fiber rearrangements and damage processes in matrix, fibers, and their interfaces, in respective \mathbf{n}_1 - and \mathbf{n}_2 -directions, is modulated by ϑ and ζ . Isotropic surface energy is Y_0 , with factors γ_ξ and γ_η scaling the fracture toughness in respective \mathbf{n}_1 - and \mathbf{n}_2 -directions.

6 Conclusion

A theory of finite-deformation continuum mechanics with a basis in generalized Finsler geometry has been developed and refined. Elements of an internal state vector represent evolving microstructure features and can be interpreted as order parameters. Dependence of the material metric on internal state affects how distances are measured in the material manifold and how gradients (i.e., covariant derivatives) are resolved. A new application of the theory to anisotropic soft-tissue mechanics has been presented, whereby the internal state is primarily associated with collagen fiber rearrangements and breakages. The material metric contains explicit contributions from sliding or opening modes in different material directions. Solutions to boundary value problems for tensile extension with tearing in different directions agree with experimental data and microscopic observations on skin tissue, providing physical and geometric insight into effects of microstructure.

Funding: This research received no external funding.

Conflicts of interest: The author declares no conflicts of interest.

Data availability statement: Not applicable; this research produced no data.

7 Appendix A: Variational derivatives

The variational derivative $\delta(\cdot)$ of §3.3.1 invokes (φ^a, D^A) with $a, A = 1, \dots, n$ as the total set of $2n$ varied independent parameters or degrees-of-freedom.

A.1 Deformation gradient and director gradient

The first of (3.24) follows from (3.1), (3.5), and commutation of $\delta(\cdot)$ and $\partial_A(\cdot)$ operators since the variation is performed at fixed X^A :

$$\delta F_A^a(\varphi(X), X) = \delta(\partial_A \varphi^a(X)) = \partial_A(\delta \varphi^a(X)) = \delta_A(\delta \varphi^a(X)) = (\delta \varphi^a(X))|_A, \quad (\text{A.1})$$

with F treated as a two-point tensor.

Remark A.1.1. The third equality in (A.1) follows from $N_A^B(X, D) \bar{\partial}_B \varphi^a(X) = 0$. The leftmost and rightmost equalities interpret $\varphi^a(X)$ and $\delta \varphi^a(X)$, respectively, as point functions rather than vector fields [20, 22].

Denote by $f(X, D)$ a generic differentiable function of arguments $\{X^A, D^A\}$ in a coordinate chart on \mathcal{L} . The variation of $f(X, D)$ is defined by the first of the following:

$$\delta f(X, D) = f(X, D)|_A \delta(D^A) = \bar{\partial}_A f(X, D) \delta(D^A), \quad (\text{A.2})$$

where $(\cdot)|_A$ is the vertical covariant derivative (e.g., as in (2.21)). For the choices $V_{BC}^A = 0$ and $Y_{BC}^A = 0$ of (3.15), $f(X, D)|_A = \bar{\partial}_A f(X, D)$ and the rightmost form is obtained, consistent with prior

definitions [54, 55]. This is used with (3.28) to obtain the second of (3.24):

$$\begin{aligned}
\delta D^A|_B &= \delta(\partial_B D^A) - \delta N_B^A + \delta(K_{BC}^A)D^C + K_{BC}^A \delta(D^C) \\
&= [\partial_B \delta(D^A) - N_B^C \bar{\partial}_C \delta(D^A) + K_{BC}^A \delta(D^C)] - \bar{\partial}_C N_B^A \delta(D^C) + \bar{\partial}_D K_{BC}^A D^C \delta(D^D) \\
&= [\delta(D^A)]|_B - (\bar{\partial}_C N_B^A - \bar{\partial}_C K_{BD}^A D^D) \delta(D^C),
\end{aligned} \tag{A.3}$$

where it is assumed per (3.12) that $\bar{\partial}_C \delta[D^A(X)] = \bar{\partial}_C [\delta(D^A)(X)] = 0$ on \mathcal{M} and \mathcal{Z} .

A.2 Volume form

Two definitions have been set forth in prior work for the variation of the volume form $d\Omega(X, D)$. The first quoted here sets [54]

$$\begin{aligned}
\delta(d\Omega) &= [\delta\sqrt{G}/\sqrt{G}]d\Omega = (\ln\sqrt{G})|_A \delta(D^A)d\Omega = \frac{1}{2}G^{BC}G_{CB}|_A \delta(D^A)d\Omega \\
&= (C_{AB}^B - Y_{AB}^B)\delta(D^A)d\Omega = C_{AB}^B \delta(D^A)d\Omega,
\end{aligned} \tag{A.4}$$

where the first equality is a definition and (2.27) and (A.2) have been used subsequently.

Remark A.2.1. According to (A.4), the magnitude of the volume form is varied locally over n -dimensional base space in (3.25) with $\alpha = 1$ prior to application of the divergence theorem (2.31) used to procure (3.31) and (3.32) from (3.30) of §3.3.3. The choice (A.4) was used in the most recent theory [54] and implied in a prior numerical implementation [59].

The second definition quoted here was used in the original theoretical derivations [55, 56]:

$$\begin{aligned}
\delta(d\Omega) &= [\delta\sqrt{\mathcal{G}}/\sqrt{\mathcal{G}}]d\Omega = (\ln\sqrt{\mathcal{G}})|_A \delta(D^A)d\Omega = (\ln\sqrt{G^2})|_A \delta(D^A)d\Omega \\
&= G^{BC}G_{CB}|_A \delta(D^A)d\Omega = 2(C_{AB}^B - Y_{AB}^B)\delta(D^A)d\Omega = 2C_{AB}^B \delta(D^A)d\Omega.
\end{aligned} \tag{A.5}$$

In derivation of (A.5), the determinant of the Sasaki metric as defined in (2.15) has been used along with (2.27) and (A.2).

Remark A.2.2. The definition given by the first equality in (A.5) is notionally consistent with other earlier theory [49, 50, 52]. In the present viewpoint with (A.5), the magnitude of the volume form is varied locally in $2n$ -dimensional total space \mathcal{Z} via (3.25) with $\alpha = 2$ before integrating over base n -dimensional space \mathcal{M} in (3.30) of §3.3.3.

Remark A.2.3. Definition (A.4) corresponds to $\alpha = 1$ and definition (A.5) to $\alpha = 2$ in (3.25). The only ramification in the governing Euler-Lagrange equations is scaling of local free energy density by a factor of one or two through $\alpha\psi C_{CA}^A$ in the micro-momentum balance, in either form (3.32) or (3.35). Macroscopic momentum is unaffected by the definition of $\delta(d\Omega)$.

8 Appendix B: Toward residual stress and growth

B.1 Macroscopic momentum

Consideration of residual stress begins with examination of the balance of linear momentum in the form (3.34), repeated and reorganized for convenience:

$$\partial_A P_a^A + P_a^B \gamma_{AB}^A - P_c^A \gamma_{ba}^c F_A^b = -\{[\bar{\partial}_B P_a^A + P_a^A \bar{\partial}_B(\ln \sqrt{G})]\partial_A D^B + P_c^A (\gamma_{ba}^c - \Gamma_{ba}^c) F_A^b\}. \quad (\text{B.1})$$

Remark B.1.1. Terms on the left side of (B.1) are standard for nonlinear elasticity theory [22]. If the free energy ψ does not depend on D^A or $D_{|B}^A$, then the stress $P_a^A = \partial\psi/\partial F_A^a$ is also conventional, presuming ψ is such that in the undeformed state, $C_{AB} = G_{AB} \Rightarrow P_a^A = 0$. In that case, when the right side of (B.1) vanishes, the body manifold \mathcal{M} should not contain residual stresses when $F_A^a = \partial_A \varphi^a$ for regular motions $\varphi^a(X)$ (e.g., in the absence of topological changes).

Remark B.1.2. Departures from classical nonlinear elasticity arise when (i) ψ has dependencies on D^A or $D_{|B}^A$, (ii) when P_a^A or G depends on D^A along with heterogeneous state field $\partial_A D^B \neq 0$, or (iii) when a different connection than the Levi-Civita connection is used for Γ_{ba}^c (i.e., $\Gamma_{ba}^c \neq \gamma_{ba}^c$ due to d -dependence of spatial metric g_{ab}). Each of these departures could potentially induce stresses $P_a^A \neq 0$ in a simply connected body externally unloaded via $p_a = P_a^A N_A = 0$ everywhere on its oriented boundary $\partial\mathcal{M}$ (i.e., residual stresses).

Analysis of a particular version of the general theory offers more insight. First assume in (3.18) that $\hat{g}_b^a \rightarrow \delta_b^a$ such that $g_{ab}(x, d) \rightarrow g_{ab}(x) = \bar{g}_{ab}(x)$: the spatial metric tensor \mathbf{g} is Riemannian rather than Finslerian. Then $\gamma_{bc}^a = \Gamma_{bc}^a$. Now use the osculating Riemannian interpretation of the Finslerian material metric \mathbf{G} offered by Corollary 2.1.1 manifesting from (3.12):

$$\tilde{G}_{AB}(X) = G_{AB}(X, D(X)), \quad \tilde{G}(X) = \det(\tilde{G}_{AB}(X)), \quad (\text{B.2})$$

$$\tilde{\gamma}_{BA}^A = \partial_B(\ln \sqrt{\tilde{G}}) = \partial_B(\ln \sqrt{G}) + \bar{\partial}_A(\ln \sqrt{G})\partial_B D^A = \gamma_{BA}^A + \bar{\partial}_A(\ln \sqrt{G})\partial_B D^A, \quad (\text{B.3})$$

$$\tilde{P}_a^A(X) = P_a^A(X, D(X)), \quad \partial_B \tilde{P}_a^A = \partial_B P_a^A + \bar{\partial}_C P_a^A \partial_B D^C. \quad (\text{B.4})$$

Substituting (B.3) and (B.4) into (B.1) gives, with $\gamma_{ba}^c = \Gamma_{ba}^c$,

$$\partial_A \tilde{P}_a^A + \tilde{P}_a^B \tilde{\gamma}_{AB}^A - \tilde{P}_c^A \gamma_{ba}^c F_A^b = 0. \quad (\text{B.5})$$

Remark B.1.3. Expression (B.5) has the standard appearance for static equilibrium in classical continuum mechanics, but stress \tilde{P}_a^A and connection $\tilde{\gamma}_{BC}^A$ both implicitly depend on internal state D^A . The former, \tilde{P}_a^A , possibly depends on $D_{|B}^A$ in addition to D^A if state gradient $D_{|B}^A$ appears in the arguments of ψ . Coefficients $\tilde{\gamma}_{BC}^A$ are those of the Levi-Civita connection of \tilde{G}_{AB} via (2.36).

Now neglect dependence on internal state gradient in the energy density, require D -dependence to arise only through G_{AB} , and assume the body is homogeneous (with mild abuse of notation):

$$\psi = \psi(F_A^a, D^A) = \psi(F_A^a, G_{AB}(X, D)) = \tilde{\psi}(F_A^a, \tilde{G}_{AB}(X)) = \tilde{\psi}(C_{AB}(F_A^a, g_{ab}), \tilde{G}_{AB}(X)). \quad (\text{B.6})$$

Recall from (3.10) that $C_{AB} = F_A^a g_{ab} F_B^b$. As a simple example, take, where $n = \dim \mathcal{M}$,

$$\tilde{\psi} = \frac{\mu_0}{2} (C_{AB} \tilde{G}^{AB} - n) \Rightarrow \tilde{P}_a^A = \frac{\partial \tilde{\psi}}{\partial F_A^a} = \mu_0 g_{ab} \tilde{G}^{AB} F_B^b, \quad \frac{\partial \tilde{\psi}}{\partial \tilde{G}_{AB}} = -\frac{\mu_0}{2} \tilde{G}^{AC} \tilde{G}^{BD} C_{CD}, \quad (\text{B.7})$$

and where $\mu_0 > 0$ is a constant (e.g., an elastic shear modulus). Now assume that spatial manifold \mathfrak{m} is Euclidean [27, 30] such that the Riemann-Christoffel curvature tensor from γ_{bc}^a (and thus derived from g_{ab}) vanishes identically.

Remark B.1.4. In this case, (B.5), the last of (B.6), and the example (B.7) are consistent with the geometric theory of growth mechanics of Yavari [30] in the setting of quasi-statics. Incompressibility can be addressed by appending linear momentum to include contribution from an indeterminate pressure to be determined by boundary conditions under isochoric constraint $J = 1$ [22]. Otherwise, $\tilde{\psi}$ can be augmented with term(s) to ensure $C_B^A \rightarrow \delta_B^A \Rightarrow \tilde{P}_a^A = 0$ (e.g., (4.38) for $n = 1$).

The Riemann-Christoffel curvature tensor from $\tilde{\gamma}_{BC}^A$ (and thus \tilde{G}_{AB}) need not vanish in general:

$$\tilde{\mathcal{R}}_{BCD}^A = \partial_B \tilde{\gamma}_{CD}^A - \partial_C \tilde{\gamma}_{BD}^A + \tilde{\gamma}_{BE}^A \tilde{\gamma}_{CD}^E - \tilde{\gamma}_{CE}^A \tilde{\gamma}_{BD}^E. \quad (\text{B.8})$$

Remark B.1.5. In Riemannian geometry, $\tilde{\gamma}_{BC}^A$ are symmetric, differentiable, and obey (2.36); (B.8) has $\frac{1}{12}n^2(n^2 - 1)$ independent components [31]. For $n = 3$, $\tilde{\mathcal{R}}_{BCD}^A$ contains six independent components, determined completely by the metric and Ricci curvature $\tilde{\mathcal{R}}_{ABC}^A$ [30, 98]. For $n = 2$, $\tilde{\mathcal{R}}_{BCD}^A$ contains only one independent component, determined completely by the scalar curvature $\tilde{\kappa} = \frac{1}{2}\mathcal{R}_{AB}\tilde{G}^{AB}$. For $n = 1$, $\tilde{\mathcal{R}}_{BCD}^A$ always vanishes (i.e., a 1-D manifold is always flat in this sense).

When $\tilde{\mathcal{R}}_{BCD}^A$ is nonzero over a region of \mathcal{M} , then no compatible deformation $\tilde{F}_a^A(X)$ exists that can push-forward \tilde{G}_{AB} to match the Euclidean metric $g_{ab}(\phi(X))$ that would render corresponding regions of \mathcal{M} and \mathfrak{m} isometric. In other words, the push-forward $g_{ab} = \tilde{F}_a^A \tilde{G}_{AB} \tilde{F}_b^B$ where $\tilde{F}_a^A = \partial_a \zeta^A$ does not exist, ζ^A being (nonexistent) Euclidean coordinates on \mathcal{M} . In such cases, \mathcal{M} would always have to be deformed (e.g., strained) to achieve its spatial representation \mathfrak{m} , since no isometry exists between the two configurations.

Remark B.1.6. If an intrinsically curved body manifold in the reference state \mathcal{M} is stress-free per the constitutive prescription (e.g., (B.7) augmented per Remark B.1.4 or another standard elasticity model), then the intrinsically flat body in the current state \mathfrak{m} would be necessarily strained and stressed, even if external traction p_a vanishes along its boundary. Thus, this particular rendition of the generalized Finsler theory supplies residual stress from a non-Euclidean material metric tensor \tilde{G}_{AB} in a manner matching other works that use Riemannian geometry [27, 30].

In the full version of the generalized Finsler theory [54, 55], as discussed following (B.1), residual stresses could emerge from additional sources to those discussed under the foregoing assumptions of a Euclidean spatial metric, a conventional hyperelastic energy potential, and an osculating Riemannian material metric with non-vanishing curvature. A number of different curvature forms can be constructed from the various connections and derivatives of Finsler geometry and its generalizations [3, 5]. Further analysis, beyond the present scope, is needed to relate these geometric objects to physics in the continuum mechanical setting, including residual stresses.

Remark B.1.7. Deformation gradient F_A^a could be decomposed into a product of two mappings [62]: $F_A^a(X) = \partial_A \varphi^a(X) = (F^E)_\alpha^a(X)(F^D)_A^\alpha(D(X))$. In this case, the strain energy potential is written to emphasize the elastic deformation F^E , with the state-dependent deformation F^D accounting explicitly for inelastic deformation mechanisms, including growth [29, 107]. In this setting, residual stresses can arise if $(F^E)^{-1}$ and thus F^D do not fulfill certain integrability conditions: neither two-point tensor $(F^E)^{-1}$ nor F^D is always integrable to a vector field [98].

B.2 Micro-momentum and growth

Now consider the internal state-space equilibrium equation, (3.35), first under the foregoing assumptions used to derive (B.5). Furthermore, take $N_B^A = N_B^A(X)$, $K_{BC}^A = \gamma_{BC}^A(X)$, and $\alpha = 1$. Then, with these assumptions, in the osculating Riemannian interpretation of Corollary 2.1.1, (3.35) is

$$\partial_A \tilde{Z}_C^A + \tilde{Z}_C^B \tilde{\gamma}_{AB}^A - \tilde{Z}_B^A \gamma_{AC}^B - Q_C = \psi \bar{\partial}_C (\ln \sqrt{G}) - R_C, \quad (\text{B.9})$$

$$\tilde{Z}_B^A(X) = Z_B^A(X, D(X)) = \frac{\partial \psi}{\partial D_B^A}(X, D(X)), \quad Q_A(X, D(X)) = \frac{\partial \psi}{\partial D^A}(X, D(X)), \quad (\text{B.10})$$

where (B.10) follows from (3.29). Use energy density ψ of (B.6), so $\tilde{Z}_B^A = 0$ identically. Choose the volumetric source term $R_C = \psi \bar{\partial}_C (\ln \sqrt{G})$, which here represents the local change in energy density per unit reference volume due to effects of growth on the local volume form $d\Omega(X, D)$, since now, per (A.4) of Appendix A, $\psi \delta(d\Omega) = \psi [\bar{\partial}_C (\ln \sqrt{G}) \delta(D^C)] d\Omega = R_C \delta(D^C) d\Omega$.

Remark B.2.1. Physical justification exists in the context of growth mechanics for biological systems: R_C can account for the affect on energy density from changes in mass due to tissue growth [30, 107]. Thus (B.9) further reduces to, with (B.6), to a form very similar to the equilibrium case of Yavari [30] (e.g., matching equation (2.73) of ref. [30] with vanishing time derivative, if here $\bar{\partial}_A G_{BC}$ is arbitrary):

$$Q_A = \frac{\partial \psi}{\partial D^A} = \frac{\partial \psi}{\partial G_{BC}} \frac{\partial G_{BC}}{\partial D^A} = \frac{\partial \tilde{\psi}}{\partial \tilde{G}_{BC}} \frac{\partial G_{BC}}{\partial D^A} = 0. \quad (\text{B.11})$$

To see how internal state components $\{D^A\}$ can represent growth, consider the case $n = 2$ (i.e., 2-D \mathcal{M} such as a biological membrane), by which $\{D^A\} \rightarrow (D^1, D^2) = (l_1 \xi^1, l_2 \xi^2)$, where $l_{1,2} > 0$ are normalization constants that render the ξ^A dimensionless. Choose a polar (i.e., cylindrical $\{X^A\} \rightarrow (R, \Theta)$) coordinate system on a region of \mathcal{M} with (3.17) applying, such that $\tilde{G} = \text{diag}(1, R^2)$. Assume a generalized Finslerian contribution $\tilde{G} = \text{diag}(\exp(h_1(\xi^1)), \exp(h_2(\xi^2)))$, where $h_1(D(X)) = h_1(D^1(R, \Theta)/l_1)$ and $h_2(D(X)) = h_2(D^2(R, \Theta)/l_2)$ are differentiable functions of their arguments. In matrix form, the second of (3.17) becomes, in this example of anisotropic growth,

$$[G_{AB}] = \begin{bmatrix} G_{RR} & 0 \\ 0 & G_{\Theta\Theta} \end{bmatrix} = [\hat{G}_A^C][\bar{G}_{CB}] = \begin{bmatrix} \exp(h_1(\xi^1)) & 0 \\ 0 & R^2 \exp(h_2(\xi^2)) \end{bmatrix}. \quad (\text{B.12})$$

A more specific case is now studied in detail. Denote by $\chi(R)$ a radial growth function. Then set

$$\xi = \xi^1 = \frac{D^1}{l_1} = \frac{D^2}{l_2} = \xi^2, \quad \xi = \xi(R); \quad h = h_1 = -h_2 = 2\chi, \quad h = h(\xi(R)) = 2\chi(R). \quad (\text{B.13})$$

This produces metric $\tilde{G}_{AB}(X)$ of Yavari (ref. [30], eq. (2.101)) for anisotropic growth of an annulus:

$$\begin{aligned} [G_{AB}(R, \xi)] &= \begin{bmatrix} \exp(h(\xi(R))) & 0 \\ 0 & R^2 \exp(-h(\xi(R))) \end{bmatrix} \\ \Rightarrow [\tilde{G}_{AB}(R)] &= \begin{bmatrix} \exp(2\chi(R)) & 0 \\ 0 & R^2 \exp(-2\chi(R)) \end{bmatrix}. \end{aligned} \quad (\text{B.14})$$

Remark B.2.2. In this special case given by (B.14), internal state changes preserve volume via $\det(G_{AB}(X, D)) = R^2$ being independent of χ , ξ , and D , so $C_{AB}^B = 0$.

Now apply the energy potential (B.7), such that for internal state equilibrium, (B.11) becomes, defining $\dot{h}(\xi) = dh(\xi)/d\xi$,

$$Q_A = -\frac{\mu_0}{2} \tilde{G}^{BD} \tilde{G}^{CE} C_{DE} \bar{\partial}_A G_{BC} = 0 \Rightarrow \begin{cases} 2l_1 Q_1(\xi, R) = -\mu_0 \exp(-h(\xi)) C_{RR} \dot{h}(\xi) = 0, \\ 2l_2 Q_2(\xi, R) = \mu_0 R^{-2} \exp(h(\xi)) C_{\Theta\Theta} \dot{h}(\xi) = 0. \end{cases} \quad (\text{B.15})$$

Thus, equilibrium of internal state is only ensured for this particular strain energy function and material metric when $\dot{h} = 0$. A sample function with three equilibrium states at $\xi = 0, \frac{1}{2}, 1$ is the double well:

$$h = \xi^2(1 - \xi)^2, \quad \dot{h} = 2\xi(1 - \xi)(1 - 2\xi). \quad (\text{B.16})$$

Now revisit the Levi-Civita connection and curvature for the metric \tilde{G} in (B.14). Denote $h'(\xi(R)) = [dh(\xi(R))/d\xi][d\xi(R)/dR] = \dot{h}(\xi)\xi'(R)$. From (2.36), the $\tilde{\gamma}_{BC}^A$, have the non-vanishing components

$$\tilde{\gamma}_{RR}^R = \frac{h'}{2}, \quad \tilde{\gamma}_{\Theta\Theta}^R = \exp(-2h) \left(\frac{R^2 h'}{2} - R \right), \quad \tilde{\gamma}_{R\Theta}^\Theta = \tilde{\gamma}_{\Theta R}^\Theta = \frac{1}{R} - \frac{h'}{2}. \quad (\text{B.17})$$

Recalling $\tilde{\kappa}$ is the scalar curvature, the non-vanishing covariant components of $\tilde{\mathcal{R}}_{BCDE} = \tilde{\mathcal{R}}_{BCD}^A \tilde{G}_{AE}$ are, from (B.8),

$$\begin{aligned} \tilde{\mathcal{R}}_{R\Theta R\Theta} &= \tilde{\mathcal{R}}_{\Theta R \Theta R} = -\tilde{\mathcal{R}}_{R\Theta \Theta R} = -\tilde{\mathcal{R}}_{\Theta R R\Theta} = -R^2 \tilde{\kappa} = -[\partial_R \tilde{\gamma}_{\Theta\Theta}^R + \tilde{\gamma}_{\Theta\Theta}^R (\tilde{\gamma}_{RR}^R - \tilde{\gamma}_{R\Theta}^\Theta)] \tilde{G}_{RR} \\ &= -\frac{d}{dR} \left[\exp(-2h) \left(\frac{R^2 h'}{2} - R \right) \right] \exp(h) + \left(\frac{R^2 h'}{2} - R \right) \left(\frac{1}{R} - h' \right) \exp(-h) \\ &= -\frac{R}{2} \exp(-h) [R\{h'' - (h')^2\} + 4h'] \\ &= -\frac{R}{2} \exp(-h) \left[R \left(\frac{d^2 \xi}{dR^2} + \frac{d\xi}{dR} \frac{d}{dR} \right) \frac{dh}{d\xi} - R \left(\frac{dh}{d\xi} \frac{d\xi}{dR} \right)^2 + 4 \frac{dh}{d\xi} \frac{d\xi}{dR} \right]. \end{aligned} \quad (\text{B.18})$$

Take the annular material manifold $\{\mathcal{M} : R \in [R_0, R_1], \Theta \in [0, \Theta_1]\}$, $R_1 > R_0 > 0$, $\Theta_1 < 2\pi$. Since $R > 0$ and for bounded h , the local flatness condition from (B.18) is

$$R\{h'' - (h')^2\} + 4h' = 0 \quad \Leftrightarrow \quad R \left(\frac{d^2 \xi}{dR^2} + \frac{d\xi}{dR} \frac{d}{dR} \right) \frac{dh}{d\xi} - R \left(\frac{dh}{d\xi} \frac{d\xi}{dR} \right)^2 + 4 \frac{dh}{d\xi} \frac{d\xi}{dR} = 0. \quad (\text{B.19})$$

Remark B.2.3. The first of (B.19) is a second-order nonlinear ODE for radial distribution of the generic function $h = h(R)$. The second is a second-order nonlinear ODE for $\xi = \xi(R)$ that could be solved if intermediate functional form $h(\xi)$ is known a priori (e.g., (B.16)). Trivial solutions are $h(R) = \text{constant}$ and $\xi(R) = \text{constant}$. General non-trivial analytical solutions are not obvious. Given appropriate boundary conditions, determination of particular non-trivial solutions for flatness, if they exist, would appear to require numerical methods.

References

- [1] P. Finsler. *Uber Kurven und Flachen in allgemeiner Raumen*. Dissertation, Gottingen, 1918.
- [2] H. Rund. *The Differential Geometry of Finsler Spaces*. Springer-Verlag, Berlin, 1959.
- [3] D. Bao, S.-S. Chern, and Z. Shen. *An Introduction to Riemann-Finsler Geometry*. Springer-Verlag, New York, 2000.
- [4] A.C. Eringen. Tensor Analysis. In A.C. Eringen, editor, *Continuum Physics*, volume I, pages 1–155. Academic Press, New York, 1971.
- [5] A. Bejancu. *Finsler Geometry and Applications*. Ellis Horwood, New York, 1990.
- [6] R. Miron. Metrical Finsler structures and metrical Finsler connections. *Journal of Mathematics of Kyoto University*, 23:219–224, 1983.
- [7] S. Watanabe, S. Ikeda and F. Ikeda. On a metrical Finsler connection of a generalized Finsler metric $g_{ij} = e^{2\sigma(x,y)} \gamma_{ij}(x)$. *Tensor, N.S.*, 39:97–102, 1983.
- [8] M. Matsumoto. *Foundations of Finsler Geometry and Special Finsler Spaces*. Kaiseisha Press, Shigaken (Japan), 1986.
- [9] A. Bejancu and H.R. Farran. *Geometry of Pseudo-Finsler Submanifolds*. Kluwer, Dordrecht, 2000.
- [10] E. Minguzzi. The connections of pseudo-Finsler spaces. *International Journal of Geometric Methods in Modern Physics*, 11:1460025, 2014.
- [11] P.L. Antonelli, R.S. Ingarden, and M. Matsumoto. *The Theory of Sprays and Finsler Spaces with Applications in Physics and Biology*. Kluwer, Dordrecht, 1993.
- [12] S. Vacaru, P. Stavrinos, E Gaburov, and D. Gonța. *Clifford and Riemann-Finsler Structures in Geometric Mechanics and Gravity*. Geometry Balkan Press, 2005.
- [13] H.E. Brandt. Differential geometry of spacetime tangent bundle. *International Journal of Theoretical Physics*, 31:575–580, 1992.
- [14] N. Voicu. New considerations on Einstein equations in pseudo-Finsler spaces. *AIP Conference Proceedings*, 1283:249–257, 2010.

- [15] V. Balan, G.Y. Bogoslovsky, S.S. Kokarev, D.G. Pavlov, S.V. Siparov, and N. Voicu. Geometrical models of the locally anisotropic space-time. *arXiv preprint*, arXiv:1111.4346, 2011.
- [16] T. Ma, V.S. Matveev, and I. Pavlyukevich. Geodesic random walks, diffusion processes and Brownian motion on Finsler manifolds. *Journal of Geometric Analysis*, 31:12446–12484, 2021.
- [17] M. Hohmann, C. Pfeifer, and N. Voicu. Mathematical foundations for field theories on Finsler spacetimes. *Journal of Mathematical Physics*, 63:032503, 2022.
- [18] N. Popov and I. Matveev. Six-dimensional manifold with symmetric signature in a unified theory of gravity and electromagnetism. *Symmetry*, 14:1163, 2022.
- [19] A. Abbondandolo, G. Benedetti, and L. Polterovich. Lorentz-Finsler metrics on symplectic and contact transformation groups. *arXiv preprint*, arXiv:2210.02387, 2022.
- [20] C.A. Truesdell and R.A. Toupin. The Classical Field Theories. In S. Flugge, editor, *Handbuch der Physik*, volume III/1, pages 226–793. Springer-Verlag, Berlin, 1960.
- [21] E. Kröner. Allgemeine kontinuumstheorie der versetzungen und eigenspannungen. *Archive for Rational Mechanics and Analysis*, 4:273–334, 1960.
- [22] J.E. Marsden and T.J.R. Hughes. *Mathematical Foundations of Elasticity*. Prentice-Hall, Englewood Cliffs NJ, 1983.
- [23] R.A. Toupin and R.S. Rivlin. Dimensional changes in crystals caused by dislocations. *Journal of Mathematical Physics*, 1:8–15, 1960.
- [24] A. Yavari and A. Goriely. Riemann-Cartan geometry of nonlinear dislocation mechanics. *Archive for Rational Mechanics and Analysis*, 205:59–118, 2012.
- [25] J.D. Clayton. Defects in nonlinear elastic crystals: differential geometry, finite kinematics, and second-order analytical solutions. *Zeitschrift für Angewandte Mathematik und Mechanik (ZAMM)*, 95:476–510, 2015.
- [26] R. Stojanovitch. On the stress relation in non-linear thermoelasticity. *International Journal of Non-Linear Mechanics*, 4:217–233, 1969.
- [27] A. Ozakin and A. Yavari. A geometric theory of thermal stresses. *Journal of Mathematical Physics*, 51, 2010.
- [28] K. Takamizawa. Stress-free configuration of a thick-walled cylindrical model of the artery: An application of Riemann geometry to the biomechanics of soft tissues. *Journal of Applied Mechanics*, 58:840–842, 1991.
- [29] E.K. Rodriguez, A. Hoger, and A.D. McCulloch. Stress-dependent finite growth in soft elastic tissues. *Journal of Biomechanics*, 27:455–467, 1994.

- [30] A. Yavari. A geometric theory of growth mechanics. *Journal of Nonlinear Science*, 20: 781–830, 2010.
- [31] J.A. Schouten. *Ricci Calculus*. Springer-Verlag, Berlin, 1954.
- [32] J.D. Clayton. On anholonomic deformation, geometry, and differentiation. *Mathematics and Mechanics of Solids*, 17:702–735, 2012.
- [33] J.D. Clayton. *Nonlinear Mechanics of Crystals*. Springer, Dordrecht, 2011.
- [34] P. Steinmann. *Geometrical Foundations of Continuum Mechanics*. Springer, Berlin, 2015.
- [35] A.B. Hushmandi and M.M. Rezaii. On the curvature of warped product Finsler spaces and the Laplacian of the Sasaki-Finsler metrics. *Journal of Geometry and Physics*, 62:2077–2098, 2012.
- [36] S. Watanabe and F. Ikeda. On metrical Finsler connections of a metrical Finsler structure. *Tensor, N.S.*, 39:37–41, 1982.
- [37] H. Rund. A divergence theorem for Finsler metrics. *Monatshefte für Mathematik*, 79:233–252, 1975.
- [38] R.A. Toupin. Theories of elasticity with couple stress. *Archive for Rational Mechanics and Analysis*, 17:85–112, 1964.
- [39] R.D. Mindlin. Microstructure in linear elasticity. *Archive for Rational Mechanics and Analysis*, 16:51–78, 1964.
- [40] A.C. Eringen. Mechanics of micromorphic continua. In E. Kröner, editor, *Mechanics of Generalized Continua*, pages 18–35. Springer, Berlin, 1968.
- [41] R.A. Regueiro. On finite strain micromorphic elastoplasticity. *International Journal of Solids and Structures*, 47:786–800, 2010.
- [42] V.A. Eremeyev, L.P. Lebedev, and H. Altenbach. *Foundations of Micropolar Mechanics*. Springer, Heidelberg, 2013.
- [43] V.A. Eremeyev and V. Konopińska-Zmysłowska. On dynamic extension of a local material symmetry group for micropolar media. *Symmetry*, 12:1632, 2020.
- [44] S. Amari. A theory of deformations and stresses of ferromagnetic substances by Finsler geometry. In K. Kondo, editor, *RAAG Memoirs*, volume 3, pages 257–278. Gakujutsu Bunken Fukyu-Kai, Tokyo, 1962.
- [45] S. Ikeda. A physico-geometrical consideration on the theory of directors in the continuum mechanics of oriented media. *Tensor, N.S.*, 27:361–368, 1973.

- [46] S. Ikeda. On the conservation laws in the theory of fields in Finsler spaces. *Journal of Mathematical Physics*, 22:1211–1214, 1981.
- [47] S. Ikeda. On the theory of fields in Finsler spaces. *Journal of Mathematical Physics*, 22:1215–1218, 1981.
- [48] S. Ikeda. On the covariant differential of spin direction in the Finslerian deformation theory of ferromagnetic substances. *Journal of Mathematical Physics*, 22:2831–2834, 1981.
- [49] J. Saczuk. On the role of the Finsler geometry in the theory of elasto-plasticity. *Reports on Mathematical Physics*, 39:1–17, 1997.
- [50] H. Stumpf and J. Saczuk. A generalized model of oriented continuum with defects. *Zeitschrift für Angewandte Mathematik und Mechanik (ZAMM)*, 80:147–169, 2000.
- [51] H. Stumpf and J. Saczuk. On nonlocal gradient model of inelastic heterogeneous media. *Journal of Theoretical and Applied Mechanics*, 40:205–234, 2002.
- [52] J. Saczuk. *Finslerian Foundations of Solid Mechanics*. Polskiej Akademii Nauk, Gdansk (Poland), 1996.
- [53] T. Yajima and H. Nagahama. Connection structures of topological singularity in micromechanics from a viewpoint of generalized Finsler space. *Annalen der Physik*, 532:2000306, 2020.
- [54] J.D. Clayton. Finsler differential geometry in continuum mechanics: fundamental concepts, history, and renewed application to ferromagnetic solids. *Mathematics and Mechanics of Solids*, 27:910–949, 2022.
- [55] J.D. Clayton. Finsler geometry of nonlinear elastic solids with internal structure. *Journal of Geometry and Physics*, 112:118–146, 2017.
- [56] J.D. Clayton. Finsler-geometric continuum mechanics. Technical Report ARL-TR-7694, DEVCOM Army Research Laboratory, Aberdeen Proving Ground MD, May 2016.
- [57] J.D. Clayton. Generalized pseudo-Finsler geometry applied to the nonlinear mechanics of torsion of crystalline solids. *International Journal of Geometric Methods in Modern Physics*, 15:1850113, 2018.
- [58] J.D. Clayton. Finsler-geometric continuum dynamics and shock compression. *International Journal of Fracture*, 208:53–78, 2017.
- [59] J.D. Clayton and J. Knap. Continuum modeling of twinning, amorphization, and fracture: theory and numerical simulations. *Continuum Mechanics and Thermodynamics*, 30:421–455, 2018.
- [60] G.A. Maugin and A.C. Eringen. Deformable magnetically saturated media. I. Field equations. *Journal of Mathematical Physics*, 13:143–155, 1972.

- [61] G.A. Maugin and A.C. Eringen. Deformable magnetically saturated media. II. Constitutive theory. *Journal of Mathematical Physics*, 13:1334–1347, 1972.
- [62] J.D. Clayton. Generalized Finsler geometric continuum physics with applications in fracture and phase transformations. *Zeitschrift für Angewandte Mathematik und Physik (ZAMP)*, 68:9, 2017.
- [63] Y. Takano and H. Koibuchi. J-shaped stress-strain diagram of collagen fibers: Frame tension of triangulated surfaces with fixed boundaries. *Physical Review E*, 95:042411, 2017.
- [64] K. Mitsunashi, S. Ghosh, and H. Koibuchi. Mathematical modeling and simulations for large-strain J-shaped diagrams of soft biological materials. *Polymers*, 10:715, 2018.
- [65] H. Koibuchi and H. Sekino. Monte Carlo studies of a Finsler geometric surface model. *Physica A*, 393:37–50, 2014.
- [66] H. Koibuchi and A. Shobukhov. Internal phase transition induced by external forces in Finsler geometric model for membranes. *International Journal of Modern Physics C*, 27:1650042, 2016.
- [67] H. Koibuchi, C. Bernard, J.-M. Chenal, G. Diguët, G. Sebald, J.-Y. Cavaille, T. Takagi, and L. Chazeau. Monte Carlo study of rubber elasticity on the basis of Finsler geometry modeling. *Symmetry*, 11:1124, 2019.
- [68] Y.-C. Fung. *Biomechanics: Mechanical Properties of Living Tissues*. Springer, New York (NY), second edition, 1993.
- [69] S.C. Cowin and S.B. Doty. *Tissue Mechanics*. Springer, New York, 2007.
- [70] Y. Lanir and Y.C. Fung. Two-dimensional mechanical properties of rabbit skin—II. Experimental results. *Journal of Biomechanics*, 7:171–182, 1974.
- [71] A.N. Annaidh, K. Bruyère, M. Destrade, M.D. Gilchrist, C. Maurini, M. Otténio, and G. Saccomandi. Automated estimation of collagen fibre dispersion in the dermis and its contribution to the anisotropic behaviour of skin. *Annals of Biomedical Engineering*, 40:1666–1678, 2012.
- [72] M.J. Munoz, J.A. Bea, J.F. Rodríguez, I. Ochoa, J. Grasa, A.P. del Palomar, P. Zaragoza, R. Osta, and M. Doblaré. An experimental study of the mouse skin behaviour: damage and inelastic aspects. *Journal of Biomechanics*, 41:93–99, 2008.
- [73] O. Tubon, J.D.T. Moreno-Flores, V.D. Sree, and A.B. Tepole. Anisotropic damage model for collagenous tissues and its application to model fracture and needle insertion mechanics. *Biomechanics and Modeling in Mechanobiology*, 21:1857–1872, 2022.
- [74] W. Yang, V.R. Sherman, B. Gludovatz, E. Schaible, P. Stewart, R.O. Ritchie, and M.A. Meyers. On the tear resistance of skin. *Nature Communications*, 6:6649, 2015.

- [75] H. Joodaki and M.B. Panzer. Skin mechanical properties and modeling: a review. *Proceedings of the Institution of Mechanical Engineers, Part H: Journal of Engineering in Medicine*, 232:323–343, 2018.
- [76] R. Oftadeh, B.K. Connizzo, H.T. Nia, C. Ortiz, and A.J. Grodzinsky. Biological connective tissues exhibit viscoelastic and poroelastic behavior at different frequency regimes: application to tendon and skin biophysics. *Acta Biomaterialia*, 70:249–259, 2018.
- [77] T.C. Gasser. An irreversible constitutive model for fibrous soft biological tissue: a 3-D microfiber approach with demonstrative application to abdominal aortic aneurysms. *Acta Biomaterialia*, 7:2457–2466, 2011.
- [78] M.B. Rubin and S.R. Bodner. A three-dimensional nonlinear model for dissipative response of soft tissue. *International Journal of Solids and Structures*, 39:5081–5099, 2002.
- [79] Y. Lanir. The rheological behavior of the skin: experimental results and a structural model. *Biorheology*, 16:191–202, 1979.
- [80] G.A. Holzapfel, T.C. Gasser, and R.W. Ogden. A new constitutive framework for arterial wall mechanics and a comparative study of material models. *Journal of Elasticity*, 61:1–48, 2000.
- [81] D. Balzani, P. Neff, J. Schröder, and G.A. Holzapfel. A polyconvex framework for soft biological tissues. adjustment to experimental data. *International Journal of Solids and Structures*, 43:6052–6070, 2006.
- [82] G.A. Holzapfel and R.W. Ogden. Constitutive modelling of passive myocardium: a structurally based framework for material characterization. *Philosophical Transactions of the Royal Society A*, 367:3445–3475, 2009.
- [83] D.R. Nolan, A.L. Gower, M. Destrade, R.W. Ogden, and J.P. McGarry. A robust anisotropic hyperelastic formulation for the modelling of soft tissue. *Journal of the Mechanical Behavior of Biomedical Materials*, 39:48–60, 2014.
- [84] J. Lim, J. Hong, W.W. Chen, and T. Weerasooriya. Mechanical response of pig skin under dynamic tensile loading. *International Journal of Impact Engineering*, 38:130–135, 2011.
- [85] J.D. Clayton and A.D. Freed. A constitutive model for lung mechanics and injury applicable to static, dynamic, and shock loading. *Mechanics of Soft Materials*, 2:3, 2020.
- [86] G.A. Holzapfel and J.C. Simo. A new viscoelastic constitutive model for continuous media at finite thermomechanical changes. *International Journal of Solids and Structures*, 33: 3019–3034, 1996.
- [87] A.N. Annaihd, K. Bruyère, M. Destrade, M.D. Gilchrist, and M. Otténio. Characterization of the anisotropic mechanical properties of excised human skin. *Journal of the Mechanical Behavior of Biomedical Materials*, 5:139–148, 2012.

- [88] R. Skalak, S. Zargaryan, R.K. Jain, P.A. Netti, and A. Hoger. Compatibility and the genesis of residual stress by volumetric growth. *Journal of Mathematical Biology*, 34:889–914, 1996.
- [89] P. Tong and Y.C. Fung. The stress-strain relationship for the skin. *Journal of Biomechanics*, 9:649–657, 1976.
- [90] D. Balzani, S. Brinkhues, and G.A. Holzapfel. Constitutive framework for the modeling of damage in collagenous soft tissues with application to arterial walls. *Computer Methods in Applied Mechanics and Engineering*, 213:139–151, 2012.
- [91] O. Gültekin, G. Sommer, and G.A. Holzapfel. An orthotropic viscoelastic model for the passive myocardium: continuum basis and numerical treatment. *Computer Methods in Biomechanics and Biomedical Engineering*, 19:1647–1664, 2016.
- [92] T.C. Gasser, R.W. Ogden, and G.A. Holzapfel. Hyperelastic modelling of arterial layers with distributed collagen fibre orientations. *Journal of the Royal Society Interface*, 3:15–35, 2006.
- [93] J.F. Rodríguez, F. Cacho, J.A. Bea, and M. Doblaré. A stochastic-structurally based three dimensional finite-strain damage model for fibrous soft tissue. *Journal of the Mechanics and Physics of Solids*, 54:864–886, 2006.
- [94] J.C. Simo. On a fully three-dimensional finite-strain viscoelastic damage model: formulation and computational aspects. *Computer Methods in Applied Mechanics and Engineering*, 60:153–173, 1987.
- [95] O. Gültekin, S.P. Hager, H. Dal, and G.A. Holzapfel. Computational modeling of progressive damage and rupture in fibrous biological tissues: application to aortic dissection. *Biomechanics and Modeling in Mechanobiology*, 18:1607–1628, 2019.
- [96] S.N. Chittajallu, A. Richhariya, K.M. Tse, and V. Chinthapenta. A review on damage and rupture modelling for soft tissues. *Bioengineering*, 9:26, 2022.
- [97] M.E. Gurtin. Generalized Ginzburg-Landau and Cahn-Hilliard equations based on a microforce balance. *Physica D*, 92:178–192, 1996.
- [98] J.D. Clayton. *Differential Geometry and Kinematics of Continua*. World Scientific, Singapore, 2014.
- [99] B.P. Pereira, P.W. Lucas, and T. Swee-Hin. Ranking the fracture toughness of thin mammalian soft tissues using the scissors cutting test. *Journal of Biomechanics*, 30:91–94, 1997.
- [100] W. Li. Damage models for soft tissues: a survey. *Journal of Medical and Biological Engineering*, 36:285–307, 2016.

- [101] J.D. Clayton. Modeling lung tissue dynamics and injury under pressure and impact loading. *Biomechanics and Modeling in Mechanobiology*, 19:2603–2626, 2020.
- [102] A. Deicke. Finsler spaces as non-holonomic subspaces of Riemannian spaces. *Journal of the London Mathematical Society*, 30:53–58, 1955.
- [103] K. Yano and E.T. Davies. On the connection in Finsler space as an induced connection. *Rendiconti del Circolo Matematico di Palermo*, 3:409–417, 1954.
- [104] K. Yano and S. Ishihara. *Tangent and Cotangent Bundles: Differential Geometry*. Marcel Dekker, New York, 1973.
- [105] J.L. Ericksen. Tensor Fields. In S. Flugge, editor, *Handbuch der Physik*, volume III/1, pages 794–858. Springer-Verlag, Berlin, 1960.
- [106] S.-S. Chern. Local equivalence and Euclidean connections in Finsler spaces. *Scientific Reports of National Tsing Hua University Series A*, 5:95–121, 1948.
- [107] V.A. Lubarda and A. Hoger. On the mechanics of solids with a growing mass. *International Journal of Solids and Structures*, 39:4627–4664, 2002.
- [108] G. Capriz. *Continua with Microstructure*. Springer, New York, 1989.
- [109] J.D. Clayton and J. Knap. A phase field model of deformation twinning: nonlinear theory and numerical simulations. *Physica D: Nonlinear Phenomena*, 240:841–858, 2011.
- [110] A.J.M. Spencer. Theory of invariants. In A.C. Eringen, editor, *Continuum Physics*, volume I, pages 239–353. Academic Press, New York, 1971.
- [111] M. de León, M. Epstein, and V. Jiménez. *Material Geometry: Groupoids in Continuum Mechanics*. World Scientific, Singapore, 2021.
- [112] J.D. Clayton. Dynamic plasticity and fracture in high density polycrystals: constitutive modeling and numerical simulation. *Journal of the Mechanics and Physics of Solids*, 53: 261–301, 2005.
- [113] V.D. Sree, A. Ardekani, P. Vlachos, and A.B. Tepole. The biomechanics of autoinjector-skin interactions during dynamic needle insertion. *Journal of Biomechanics*, 134:110995, 2022.
- [114] J.D. Clayton and J. Knap. A geometrically nonlinear phase field theory of brittle fracture. *International Journal of Fracture*, 189:139–148, 2014.
- [115] G.A. Holzapfel and R.W. Ogden. On planar biaxial tests for anisotropic nonlinearly elastic solids. A continuum mechanical framework. *Mathematics and Mechanics of Solids*, 14: 474–489, 2009.
- [116] M. Latorre and F.J. Montáns. On the tension-compression switch of the Gasser-Ogden-Holzapfel model: Analysis and a new pre-integrated proposal. *Journal of the Mechanical Behavior of Biomedical Materials*, 57:175–189, 2016.